

Sensor and Simulation Notes

Note 266

July 1980

A Distributed Source-Region EMP Simulator

F.C. Yang

The Dikewood Corporation
Santa Monica, California 90405

CLEARED
FOR PUBLIC RELEASE
AFRL/DEOB-FA
24 JUL 98

Abstract

A source-region EMP simulator with a source sheet at a distance h above the ground and a conducting medium in between is investigated. The simulated magnetic field and the total current density (conduction plus displacement currents) are explicitly calculated for two cases of simulator media: (a) only one uniform medium below the source surface, and (b) a perfectly conducting ground; and for two special simulator electric source fields: (a) $V_0 \delta(ct - x) \exp(-x/x_0)$, and (b) $E_0 U(t - x/c) \times \exp(-x/x_0)$.

ACKNOWLEDGEMENT

The author would like to thank Dr. K.S.H. Lee for his guidance during the work and to thank Mr. V. Tatoian for generating the curves of this report.

AFRL/DE 98-545

CONTENTS

<u>Section</u>		<u>Page</u>
I	INTRODUCTION AND SUMMARY	3
II	GENERAL FORMULATION	8
III	IMPULSE SOURCE FIELD	11
IV	UNIT-STEP SOURCE FIELD	40
	REFERENCES	60

I. INTRODUCTION AND SUMMARY

The EMP environment of a nuclear source region is different from that outside such a source region. In the source region, there is a Compton current source throughout and the air has a nonlinear time-varying conductivity. These additional features make the EMP simulation for the source region considerably more difficult. In Reference 1, several simulators have been suggested for producing some, but not all, of the desired source-region features. One such simulator is to use a distributed source sheet at a distance h above the ground and to fill up the region in between with a medium of constant conductivity. At the source sheet, one may specify a tangential magnetic field (Reference 2) or a tangential electric field. The latter source specification is exclusively treated in the present report. From the engineering point of view, the electric source field can be realized by an array of slats excited by a set of pulsers triggered in an appropriate sequence (Reference 3).

The theoretical model of the simulator and the coordinate system are shown in Figure 1. The idealized model assumes the simulator to have an infinite extent in both the x - and z -directions. This is a reasonable assumption if the region to be simulated is at some distance away from the edges of a finite-sized simulator. The medium permittivities and conductivities are assumed constants, and the tangential electric field is specified at the source surface $y = h$.

In the following sections, the relationship between the source field (distributed or discrete) and the simulated field will first be formulated in terms of Fourier integrals. Based on this relationship, the simulated field will be explicitly calculated for two special simulator media: (a) only one uniform medium below the source surface, and (b) the lower medium is perfectly conducting; and for two special simulator source fields: (a) $V_0 \delta(ct - x) \exp(-x/x_0)$, and (b) $E_0 U(t - x/c) \exp(-x/x_0)$. The factor

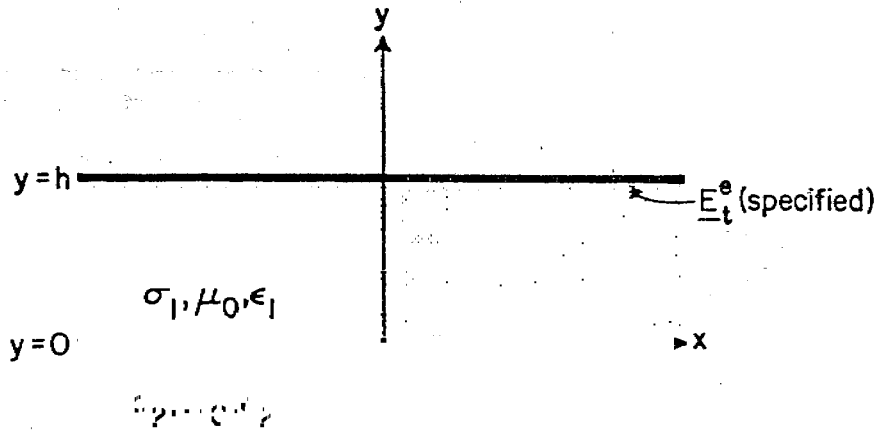


Figure 1. The theoretical model and the coordinate system.

$\exp(-x/x_0)$ and the $(ct - x)$ -variation in the source field are introduced to simulate the decaying and propagating properties of the Compton source current propagating away from the blast. The impulse response can also be used to calculate the response of an excitation field of the form $f(t - x/c)\exp(-x/x_0)$ by convolution. The case with $f(t - x/c) = U(t - x/c)$ given in this report is an example. The solutions of a single-medium simulator can also be used to construct the solutions of a two-medium simulator by a superposition of the direct illumination and subsequent reflections at the medium interface and the source surface, an example of which is the simulator with a perfectly conducting lower medium considered in this report.

The results of this report are expressed in terms of formulas, figures and tables of the normalized H_z , $(\sigma + \epsilon \frac{\partial}{\partial t}) E_x$ and $(\sigma + \epsilon \frac{\partial}{\partial t}) E_y$. These three quantities are the driving terms in determining the effects of the EMP on a test object (Reference 4) and thus are generally the quantities to be simulated.

From the results, it can be concluded that

- (a) $\exp(-x/x_0)$ appears as an overall factor times the result for the case where $x_0 = \infty$, under most practical situations,
- (b) for a single-medium simulator with $\epsilon = \epsilon_0$, the responses are determined by diffusion,
- (c) when $\epsilon > \epsilon_0$, Cerenkov phenomenon is important, and
- (d) at late times, the responses are independent of the medium permittivity.

The simulated H_z that can be generated by the type of simulator discussed in this report are summarized in the following two tables. The detailed descriptions of H_z , and other quantities such as $(\sigma + \epsilon \frac{\partial}{\partial t}) E_x$ and $(\sigma + \epsilon \frac{\partial}{\partial t}) E_y$ can be easily found in the text.

H_z/H_0 AT $y=0$ FOR SIMULATORS WITH $V_0 \delta(ct-x) \exp(-x/x_0)$ SOURCE FIELD[†]

Medium Parameters	Approximate Behaviors
$\epsilon_1 = \epsilon_2 = \epsilon_0$ $\sigma_1 = \sigma_2 = \sigma$	<ul style="list-style-type: none"> • rise time \approx tenths of t_d • fall time \approx several times of rise time • peak value $\leq 3 t_r/t_d$ • late time value ≈ 0
$\epsilon_1 = \epsilon_2 = \epsilon_r$ $\epsilon_r \epsilon_0 \geq 10 \epsilon_0$ $\sigma_1 = \sigma_2 = \sigma$	<ul style="list-style-type: none"> • switched on at t'_t • peak value ≤ 0.5 (at τ between t'_t and $t'_t + 0.3t_d$) • late time ($\tau > 10t_d, 10t'_r$) value ≈ 0
$\sigma_2 \rightarrow \infty$ $\epsilon_1 = \epsilon_0, \sigma_1 = \sigma$	<ul style="list-style-type: none"> • rise time \approx tenths of t_d • peak value ≈ 1, or $6 t_r/t_d$, whichever is larger • late time ($\tau > t_d$) value ≈ 1
$\sigma_2 \rightarrow \infty$ $\epsilon_1 = \epsilon_r \epsilon_0 \geq 10 \epsilon_0$ $\sigma_1 = \sigma$	<ul style="list-style-type: none"> • initial value at $t'_t \leq 0.5$ • sudden jumps at $\tau = (2n+1)t'_t, n=0,1,2\dots$ • late time ($\tau > 10t'_r, 10t_d$) value ≈ 1

$$^\dagger H_0 = V_0 \exp(-x/x_0) / (hZ_0), \quad t_r = \epsilon_0 / \sigma, \quad t_d = \mu_0 \sigma h^2,$$

$$t'_t = h\sqrt{\epsilon_r - 1}/c, \quad t'_r = \epsilon_0(\epsilon_r - 1)/\sigma, \quad \tau = t - x/c$$

H_z/H'_0 AT $y=0$ FOR SIMULATORS WITH $E_0 U(t-x/c)\exp(-x/x_0)$ SOURCE FIELD[†]

Medium Parameters	Approximate Behaviors
$\epsilon_1 = \epsilon_2 = \epsilon_0$ $\sigma_1 = \sigma_2 = \sigma$	<ul style="list-style-type: none"> • monotonically increasing when $t_r/t_d < 4$ • pass a local maximum $\approx 0.5(t_r/t_d)^{1/2}$ at $\tau \approx t_d$, and a local minimum $\lesssim 1.5$ at $\tau \approx 0.5 t_r$, then become monotonically increasing, when $t_r/t_d \geq 4$ • late time value $\approx \sqrt{4\tau/(\pi t_r)}$
$\epsilon_1 = \epsilon_2 = \epsilon$ $= \epsilon_r \epsilon_0 \geq 10 \epsilon_0$ $\sigma_1 = \sigma_2 = \sigma$	<ul style="list-style-type: none"> • jump from 0 to $\approx \sqrt{\epsilon_r} \exp(-0.5t'_t/t'_r)$ at $\tau = t'_t$ • monotonically increasing • late time value $\approx \sqrt{4\tau/(\pi t_r)}$
$\sigma_2 \rightarrow \infty$ $\epsilon_1 = \epsilon_2 = \epsilon_0$ $\sigma_1 = \sigma$	<ul style="list-style-type: none"> • monotonically increasing from 0 at $\tau = 0$ • late time value $\approx \tau/(t_r/t_d)^{1/2}$
$\sigma_2 \rightarrow \infty$ $\epsilon_1 = \epsilon_2 = \epsilon_0 \epsilon_r$ $\sigma_1 = \sigma$ $\epsilon_r \geq 10$	<ul style="list-style-type: none"> • jump from 0 to $\approx \sqrt{\epsilon_r} \exp(-0.5t'_t/t'_r)$ at $\tau = t'_t$ • monotonically increasing • sudden jumps at $\tau = (2n+1)t'_t$, $n=0,1,2,\dots$ • late time value $\approx \tau/(t_r t_d)^{1/2}$

$$^\dagger H'_0 = E_0 \exp(-x/x_0)/Z_0, \quad t_r = \epsilon_0/\sigma, \quad t_d = \mu_0 \sigma h^2, \quad t'_t = h\sqrt{\epsilon_r - 1}/c,$$

$$t'_r = \epsilon_0(\epsilon_r - 1)/\sigma.$$

II. GENERAL FORMULATION

The model of the simulator under consideration is shown in Figure 1, in which the x-axis is the propagation direction and $y=h$ is the source plane with a specified tangential electric field. The space below the source plane is divided into two regions: region 2 is the ground with conductivity σ_2 and permittivity ϵ_2 , and region 1 is filled with material with conductivity σ_1 and permittivity ϵ_1 . Both σ_1 , ϵ_1 and σ_2 , ϵ_2 are assumed to be constant.

To find the field distributions in regions 1 and 2, one may use the Fourier-transform technique. The transform pair is defined as follows:

$$\begin{aligned}\tilde{F}(\omega, k) &= \frac{1}{2\pi} \int_{C_1} \int_{C_2} F(t, x) e^{-j\omega t} e^{jkx} dt dx \\ F(t, x) &= \frac{1}{2\pi} \int_{\tilde{C}_1} \int_{\tilde{C}_2} \tilde{F}(\omega, k) e^{j\omega t} e^{-jkx} d\omega dk\end{aligned}\tag{1}$$

Here, " ~ " is used to indicate the quantity in the transformed (ω, k) domain and C_1 , C_2 , \tilde{C}_1 , \tilde{C}_2 are the appropriate contours for the transform integrals.

Since all quantities are z-independent, only \tilde{E}_x , \tilde{E}_y and \tilde{H}_z are the non-vanishing field components, which can be calculated by solving the following differential equations derived from Maxwell's equations:

$$\begin{aligned}(\sigma_i + j\omega\epsilon_i)\tilde{E}_x &= \frac{\partial \tilde{H}_z}{\partial y} \\ (\sigma_i + j\omega\epsilon_i)\tilde{E}_y &= jk\tilde{H}_z \\ \frac{d^2}{dy^2} \tilde{H}_z + (\omega^2 \mu_o \epsilon_i - k^2 - j\omega \mu_o \sigma_i) \tilde{H}_z &= 0\end{aligned}\tag{2}$$

($i = 1, 2$), with the boundary conditions that

- (a) \tilde{E}_x, \tilde{H}_z are continuous at $y=0$,
- (b) \tilde{E}_x equals the known field distribution \tilde{E}_x^e at $y=h$,
- (c) All field components become vanishingly small as $y \rightarrow -\infty$.

In the above equations, the subscript $i=1,2$ denotes quantities respectively in regions 1,2; μ_0 is the permeability for both regions; and \tilde{E}_x^e is the Fourier transform of specified E_x^e at the source plane.

Equations 2 are solved in a straightforward manner and the following (ω,k) -domain quantities are obtained.

- (a) In region 1 ($h \geq y \geq 0$):

$$\begin{aligned}\tilde{H}_z &= A_1 \cosh(\zeta_1 y) + B_1 \sinh(\zeta_1 y) \\ (\sigma_1 + j\omega\epsilon_1)\tilde{E}_x &= \zeta_1 A_1 \sinh(\zeta_1 y) + \zeta_1 B_1 \cosh(\zeta_1 y) \\ (\sigma_1 + j\omega\epsilon_1)\tilde{E}_y &= jkA_1 \cosh(\zeta_1 y) + jkB_1 \sinh(\zeta_1 y)\end{aligned}\tag{3}$$

- (b) In region 2 ($y \leq 0$):

$$\begin{aligned}\tilde{H}_z &= A_2 e^{\zeta_2 y} \\ (\sigma_2 + j\omega\epsilon_2)\tilde{E}_x &= \zeta_2 A_2 e^{\zeta_2 y} \\ (\sigma_2 + j\omega\epsilon_2)\tilde{E}_y &= jkA_2 e^{\zeta_2 y}\end{aligned}\tag{4}$$

Here,

$$A_1 = A_2 = \frac{(\sigma_1 + j\omega\epsilon_1)(\sigma_2 + j\omega\epsilon_2)}{\zeta_1(\sigma_2 + j\omega\epsilon_2)\sinh(\zeta_1 h) + \zeta_2(\sigma_1 + j\omega\epsilon_1)\cosh(\zeta_1 h)} \tilde{E}_x^e$$

$$B_1 = \frac{\zeta_2(\sigma_1 + j\omega\epsilon_1)}{\zeta_1(\sigma_2 + j\omega\epsilon_2)} A_1$$

$$\zeta_i^2 = k^2 - \omega^2 \mu_0 \epsilon_i + j\omega \mu_0 \sigma_i, \quad (i = 1, 2)$$

with $\text{Re}(\zeta_2) \geq 0$.

From the (ω, k) -domain solutions 3 and 4 one can obtain the desired (t, x) -domain solutions by evaluating the appropriate inverse Fourier-transform integrals. In the next sections, several special cases will be considered.

III. IMPULSE SOURCE FIELD

In this section the consideration is restricted to the following special cases:

$$(a) \quad \sigma_1 = \sigma_2 = \sigma, \quad \epsilon_1 = \epsilon_2 = \epsilon, \quad E_x^e = V_0 \delta(ct - x) \exp(-x/x_0)$$

$$(b) \quad \sigma_2 \rightarrow \infty, \quad E_x^e = V_0 \delta(ct - x) \exp(-x/x_0)$$

Case (a) can be realized by applying an impulse source field immediately above the ground, while case (b) assumes that the ground is perfectly conducting. The impulse response due to the source of the form $\delta(ct - x) \exp(-x/x_0)$ can be used to calculate the response of any excitation field of the form $f(ct - x) \times \exp(-x/x_0)$ by convolution. The case of unit step source field will be considered in the next section.

The solutions for the above two cases in the (ω, k) -domain can be easily obtained from Equations 3 and 4, namely

$$A. \quad \text{for } \sigma_1 = \sigma_2 = \sigma, \quad \epsilon_1 = \epsilon_2 = \epsilon, \quad E_x^e = V_0 \delta(ct - x) \exp(-x/x_0), \quad y \leq h$$

$$\tilde{H}_z = \tilde{E}_x^e (\sigma + j\omega\epsilon) \zeta^{-1} e^{-\zeta(h-y)}$$

$$(\sigma + j\omega\epsilon) \tilde{E}_x = \tilde{E}_x^e (\sigma + j\omega\epsilon) e^{-\zeta(h-y)}$$

$$(\sigma + j\omega\epsilon) \tilde{E}_y = \tilde{E}_x^e (\sigma + j\omega\epsilon) jk \zeta^{-1} e^{-\zeta(h-y)} \quad (5)$$

$$\zeta^2 = k^2 - \omega^2 \mu_0 \epsilon + j\omega \mu_0 \sigma, \quad \text{Re}(\zeta) \geq 0$$

$$\tilde{E}_x^e = V_0 \delta(k - \omega/c + j/x_0) / c$$

$$B. \quad \text{for } \sigma_2 \rightarrow \infty, \quad E_x^e = V_0 \delta(ct - x) \exp(-x/x_0), \quad \sigma_1 = \sigma, \quad \epsilon_1 = \epsilon, \quad 0 \leq y \leq h$$

$$\tilde{H}_z = \tilde{E}_x^e (\sigma + j\omega\epsilon) \zeta^{-1} (\sinh(\zeta h))^{-1} \cosh(\zeta y)$$

$$(\sigma + j\omega\epsilon)\tilde{E}_x = \tilde{E}_x^e(\sigma + j\omega\epsilon)(\sinh(\zeta h))^{-1}\sinh(\zeta y)$$

$$(\sigma + j\omega\epsilon)\tilde{E}_y = \tilde{E}_x^e(\sigma + j\omega\epsilon)jk\zeta^{-1}(\sinh(\zeta h))^{-1}\cosh(\zeta y) \quad (6)$$

$$\zeta^2 = k^2 - \omega^2\mu_0\epsilon + j\omega\mu_0\sigma, \quad \tilde{E}_x^e = V_0\delta(k - \omega/c + j/x_0)/c$$

Using the second equation of Equation 1, one can calculate the (t,x)-domain fields from their corresponding (ω,k)-domain solutions given above. Due to the presence of the term $\delta(k - \omega/c + j/x_0)$, one can easily perform the k-integrals to reduce the two-dimensional Fourier integrals to one-dimensional integrals, the evaluation of which generally requires some contour deformations in the complex ω -planes. Here, the evaluation will be performed for the special cases (a) and (b) described above.

$$A. \quad \sigma_1 = \sigma_2 = \sigma, \quad \epsilon_1 = \epsilon_2 = \epsilon, \quad E_x^e = V_0\delta(ct - x)\exp(-x/x_0), \quad y \leq h$$

For this case, two different situations may arise depending on whether or not ϵ equals the free-space permittivity ϵ_0 .

$$(1) \quad \epsilon = \epsilon_0$$

For this case, one finds from Equations 1 and 5 that all the ω -integrals are of the following form:

$$\int_{\tilde{C}_1} f_1(\omega) e^{-\sqrt{j\omega\mu_0\sigma(1-2/R) - 1/x_0^2}(h-y)} e^{j\omega\tau} d\omega$$

where $\tau = t - x/c$, $R = \mu_0\sigma cx_0$ and \tilde{C}_1 is the integration contour. Obviously, the integrand of the above integral has a branch point at $-j(c/x_0)(R-2)^{-1}$. A branch cut can be drawn from this point to infinity along the imaginary axis, so that in the proper Riemann sheet $\text{Re}\left(\sqrt{j\omega\mu_0\sigma(1-2/R) - 1/x_0^2}\right) \geq 0$. The integration path \tilde{C}_1 can then be deformed to either the upper or lower complex ω -plane. The value of the original integral then becomes a

summation of residues at the poles and an integral along the branch cut. After carrying out this procedure, one obtains the following expressions for the field distributions:

$$\begin{aligned}
 H_z &= \frac{V_o}{hZ_o} \left(\frac{t_d}{\pi\tau B} \right)^{\frac{1}{2}} \left(1 - \frac{t_r}{2\tau} + \frac{Bt_r t_d}{4\tau^2} + \frac{1}{BR^2} \right) e^{-\frac{Bt_d}{4\tau}} e^{-\frac{\tau}{Bt_{dx_o}}} e^{-\frac{x}{x_o}} U(\tau) \\
 (\sigma + \epsilon_o \frac{\partial}{\partial t}) E_x &= \frac{V_o}{2h^2 Z_o} \left(\frac{Bt_d^3}{\pi\tau^3} \right)^{\frac{1}{2}} e^{-\frac{Bt_d}{4\tau}} e^{-\frac{\tau}{Bt_{dx_o}}} e^{-\frac{x}{x_o}} U(\tau) \\
 &\quad \times \left(1 - \frac{3t_r}{2\tau} + \frac{Bt_r t_d}{4\tau^2} + \frac{1}{BR^2} \right) \\
 (\sigma + \epsilon_o \frac{\partial}{\partial t}) E_y &= \frac{H_z}{x_o} - \frac{V_o}{2h^2 Z_o} \left(\frac{t_r t_d^2}{\pi B \tau^3} \right)^{\frac{1}{2}} e^{-\frac{Bt_d}{4\tau}} e^{-\frac{\tau}{Bt_{dx_o}}} e^{-\frac{x}{x_o}} U(\tau) \\
 &\quad \times \left\{ \left(1 + \frac{2}{BR^2} \right) - \frac{2}{Bt_{dx_o}} \left(1 + \frac{1}{BR^2} \right) - \left(\frac{3t_r}{2\tau} + \frac{Bt_d}{2\tau} + \frac{t_d}{\tau R^2} \right) \right. \\
 &\quad \left. + \frac{3Bt_r t_d}{2\tau^2} - \frac{B^2 t_r t_d^2}{8\tau^3} \right\}
 \end{aligned} \tag{7}$$

where $Z_o = \sqrt{\mu_o/\epsilon_o}$ is the free-space impedance, $t_r = \epsilon_o/\sigma$ is the relaxation time, $t_d = \mu_o \sigma h^2$ and $t_{dx_o} = \mu_o \sigma x_o^2$ are, respectively, the diffusion times for the distances h and x_o , $B = 1 - 2/R = 1 - 2(\mu_o \sigma c x_o)^{-1}$, and $U(\tau)$ is the unit-step function. Although Equation 7 gives the field and current density only at $y=0$, one can directly obtain the field and current distributions at an arbitrary $y < h$ by simply replacing h and t_d with $(h-y)$ and $t_d(1-y/h)^2$.

To derive Equation 7 it has been assumed that $R > 2$, i.e., $B > 0$. When $2 \geq R \geq 0$ (i.e., $B \leq 0$), one can show that all three quantities become infinite at a finite h . This is due to the fact that the source field is

unrealistic in that it increases exponentially in the negative x-direction, and the conductivity of the medium is not large enough to damp the infinitely large fields created by the infinitely large source field at $x/x_0 \rightarrow -\infty$. However, for the source region to be simulated, one expects that x_0 is in the order of 200-300 meters. The R-value will then be larger than 2 if the conductivity of the simulator is larger than 3×10^{-5} mho/m which is a relatively low conductivity. Thus, from a practical point of view the case $0 \leq R \leq 2$ can be excluded.

An examination of Equation 7 shows that the field and current densities become infinitely large as $\tau \rightarrow \infty$ at a finite x, say $x=0$. This arises because the source field goes as $\exp(-x/x_0)$ and this infinitely large source field at $x \rightarrow -\infty$ will diffuse into the finite-x region as $\tau \rightarrow \infty$. However, for a simulator, h is of 1 to 2 meters, i.e., $x_0/h \geq 100$. If one is mainly interested in the range of τ up to $10^2 t_d B$ or even $10^3 t_d B$, τ is still too small to allow this unrealistic phenomenon to occur.

The field and total current density are presented in Figures 2, 3, and 4 for $x_0/h = 200, 10$; $t_r/t_d = 10, 5, 1, 0.5, 0.25, 0.01$; and for τ up to a few t_d . As can be seen, the results are quite different for $x_0/h = 200$ and 10. The case for $x_0/h = 200$ is more realistic for source region simulation and, thus, its corresponding curves are more interesting. For $x_0/h \geq 100$, $x_0 \geq 200m$, $\sigma \geq 3 \times 10^{-4}$ mho/m, and $\tau < 10^2 t_d$, one can approximate Equation 7 by setting $B = 1$, $R^2 \rightarrow \infty$, $\tau/t_{dx_0} \rightarrow 0$ and retaining only one or two terms for the field and current distributions.

From the approximate equation and the curves in Figures 2,3 and 4, one obtains the following approximate and accurate expressions for the field and current densities in Tables 1 and 2. In the tables, the rise and fall times are respectively the τ -values where the peak value and $1/e$ of the peak value are obtained. When $0.01 < t_r/t_d < 0.5$, one expects the behaviors of the field and current densities to be somewhat between the tabulated extreme situations.

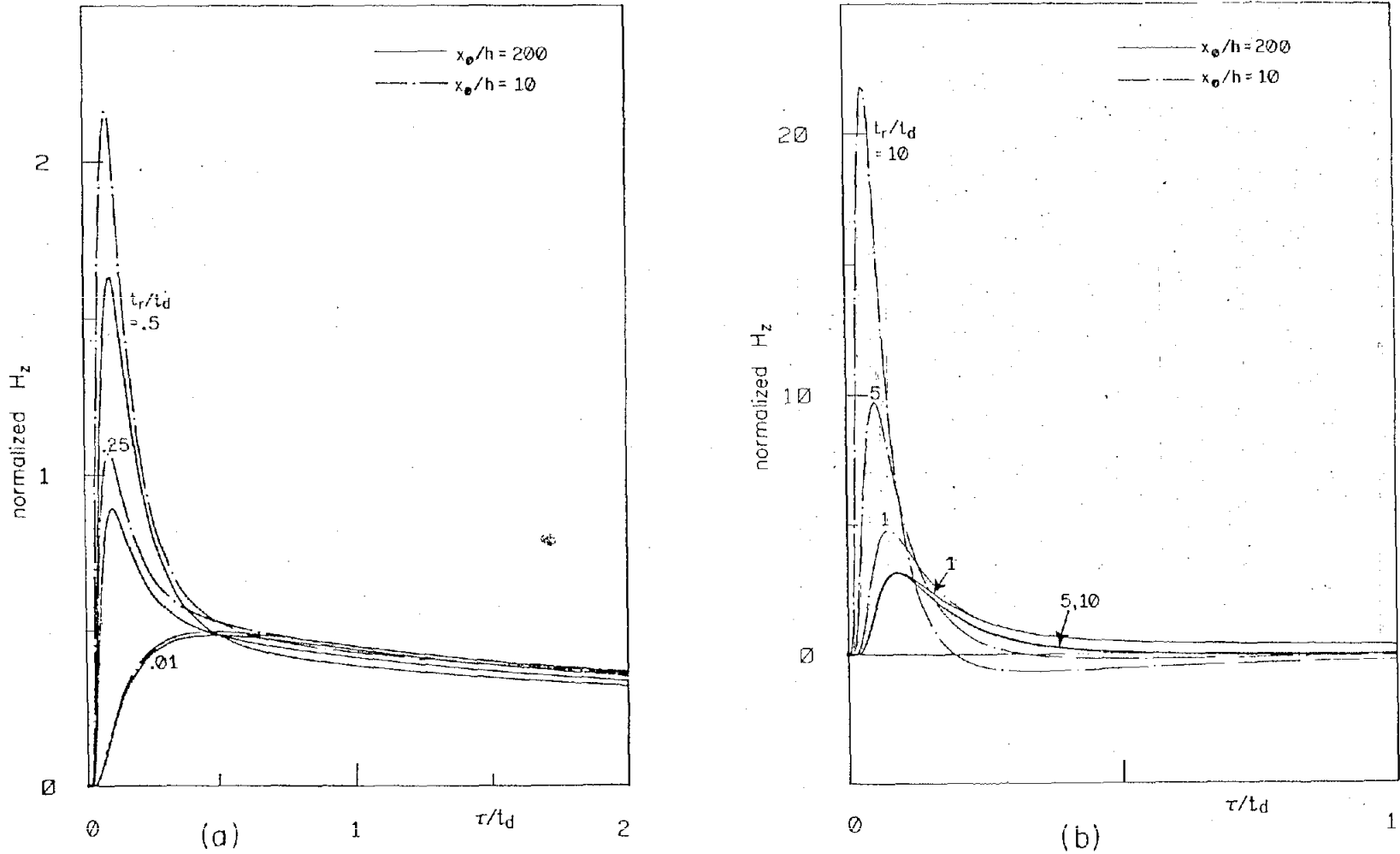


Figure 2. (a) H_z/H_0 , (b) $(t_d/t_r)H_z/H_0$ at $y=0$ as functions of τ/t_d for $x_0/h=200$ and 10, and various t_r/t_d , for the simulator with $\sigma_1 = \sigma_2 = \sigma$, $\epsilon_1 = \epsilon_2 = \epsilon_0$, $E_x^e = V_0 \delta(ct-x) \exp(-x/x_0)$. Here, $H_0 = V_0 \exp(-x/x_0) \times (hZ_0)^{-1}$, $Z_0 = (\mu_0/\epsilon_0)^{1/2}$, $t_r = \epsilon_0/\sigma$, $t_d = \mu_0 \sigma h^2$, $\tau = t - x/c$.

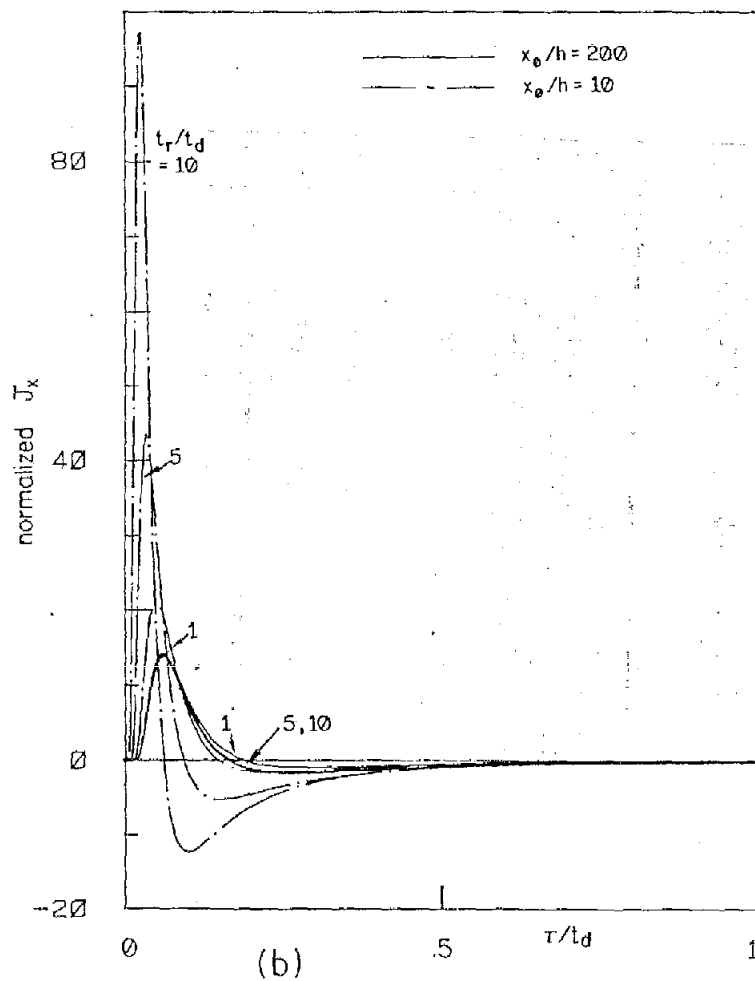
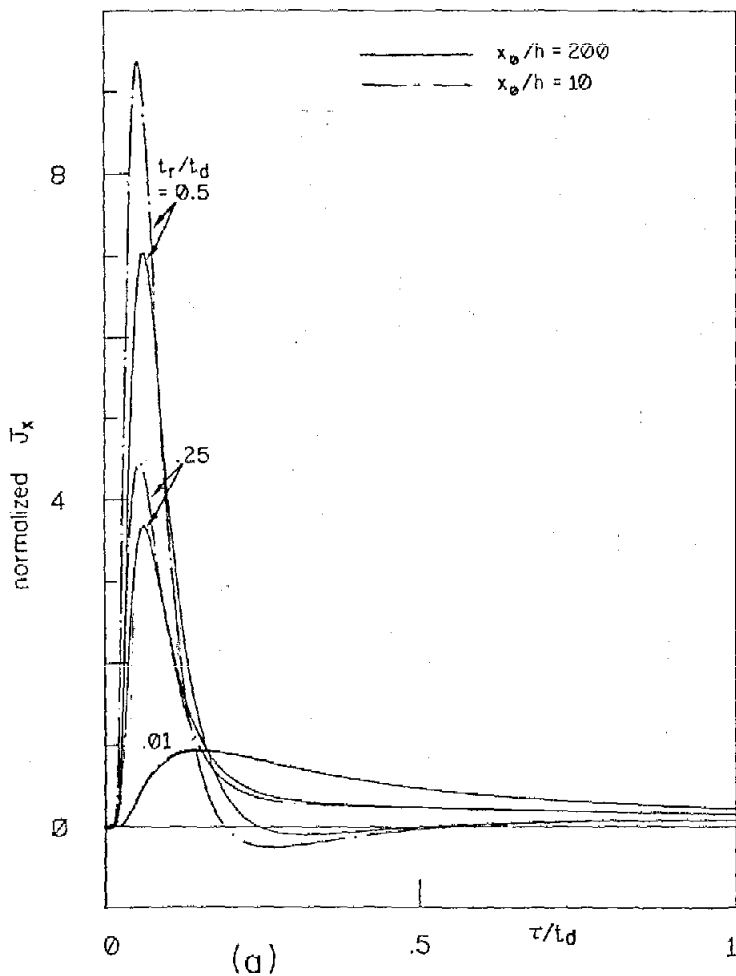


Figure 3. (a) J_x/J_0 , (b) $(t_d/t_r)J_x/J_0$ at $y=0$ as functions of τ/t_d for $x_0/h = 200$ and 10 , and various t_r/t_d , for the simulator with $\sigma_1 = \sigma_2 = \sigma$, $\epsilon_1 = \epsilon_2 = \epsilon_0$, $E_x^e = V_0 \delta(ct - x) \exp(-x/x_0)$. Here, $J_x = (\sigma + \epsilon_0 \frac{\partial}{\partial t})E_x$, $J_0 = V_0 \exp(-x/x_0) (h^2 Z_0)^{-1}$, $Z_0 = (\mu_0/\epsilon_0)^{1/2}$, $t_r = \epsilon_0/\sigma$, $t_d = \mu_0 \sigma h^2$, $\tau = t - x/c$.

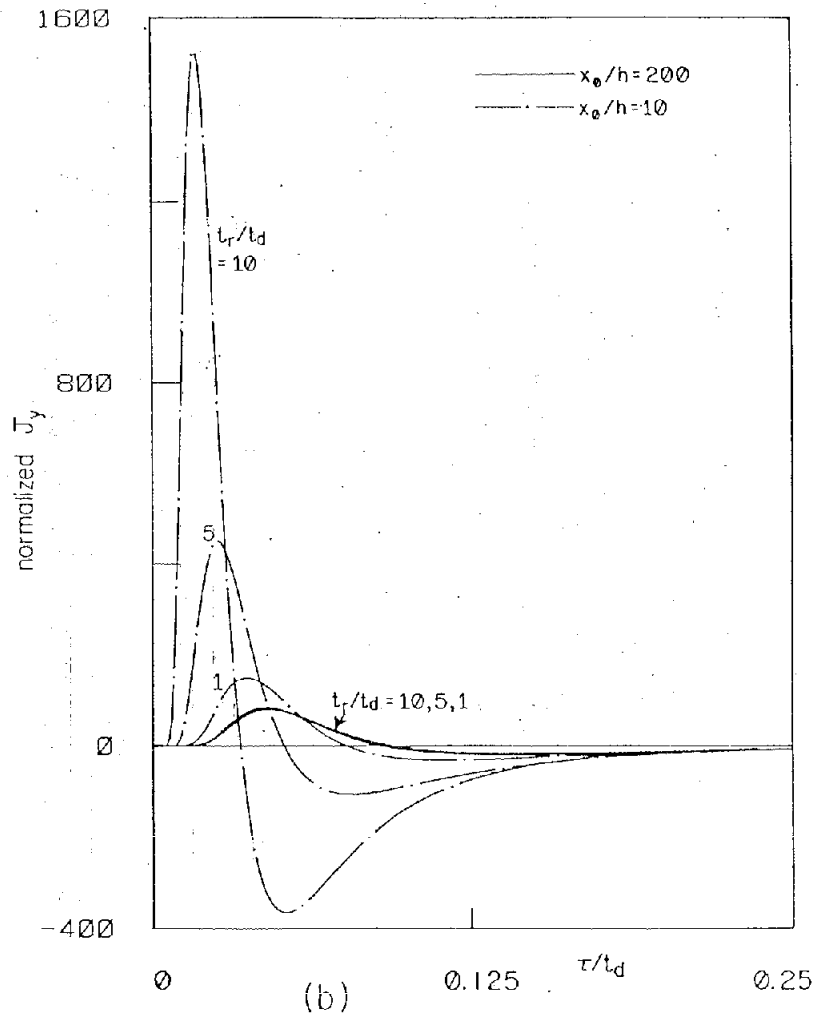
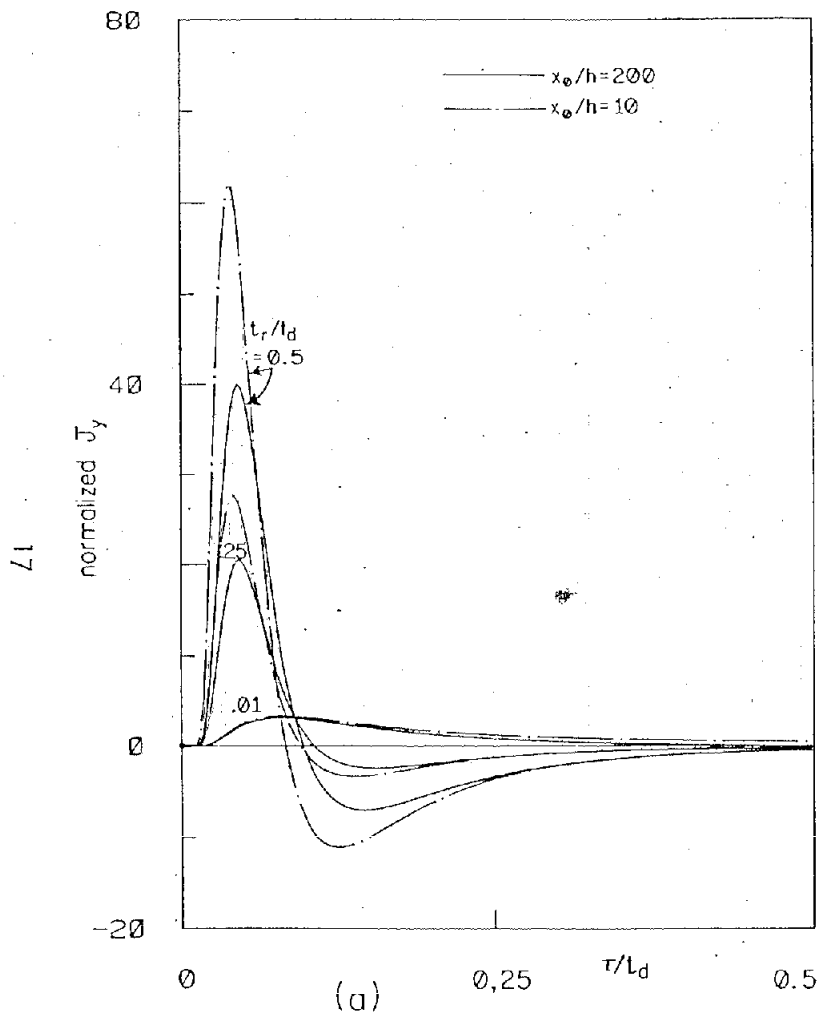


Figure 4. (a) $(t_d/t_r)^{1/2} J_y/J_0$, (b) $(t_d/t_r)^{3/2} J_y/J_0$ at $y=0$ as functions of τ/t_d for $x_0/h=200$ and 10, and various t_r/t_d , for the simulator with $\sigma_1 = \sigma_2 = \sigma$, $\epsilon_1 = \epsilon_2 = \epsilon_0$, $E_x^e = V_0 \delta(ct-x) \exp(-x/x_0)$. Here, $J_y = (\sigma + \epsilon_0 \frac{\partial}{\partial t}) E_y$, $J_0 = V_0 \exp(-x/x_0) (h^2 Z_0^2)^{-1}$, $Z_0 = (\mu_0/\epsilon_0)^{1/2}$, $t_r = \epsilon_0/\sigma$, $t_d = \mu_0 \sigma h^2$, $\tau = t - x/c$.

TABLE 1. FIELD AND CURRENT DENSITY FOR $t_r/t_d \leq 0.01$ ($\sigma h \geq 10^{-2}$ mho)[†]

Quantity	Rise Time	Fall Time	Peak Value	Normalizing Factor
H_z/H_o	$0.5 t_d$	$9.5 t_d$	0.5	$H_o = \frac{V_o e^{-x/x_o}}{hZ_o}$
$(\sigma + \epsilon_o \frac{\partial}{\partial t}) E_x/J_o$	$0.17 t_d$	$0.7 t_d$	0.9	$J_o = \frac{V_o e^{-x/x_o}}{h^2 Z_o}$
$(\sigma + \epsilon_o \frac{\partial}{\partial t}) E_y/J_o$	$0.1 t_d$	$0.4 t_d$	$3(t_r/t_d)^{1/2}$	$J_o = \frac{V_o e^{-x/x_o}}{h^2 Z_o}$

[†] $t_r = \epsilon_o/\sigma$, $t_d = \mu_o \sigma h^2$, $\sigma_1 = \sigma_2 = \sigma$, $\epsilon_1 = \epsilon_2 = \epsilon_o$, $E_x^e = V_o \delta(ct-x) \exp(-x/x_o)$,
 $x_o \geq 200$, $\sigma \geq 3 \times 10^{-4}$ mho/m, $y=0$, $\tau < t_{dx_o} = \mu_o \sigma x_o^2$, $x_o/h \geq 100$.

TABLE 2. FIELD AND CURRENT DENSITY FOR $t_r/t_d \geq 0.5$
 $(4 \times 10^{-3}$ mho $\geq \sigma h)$ [†]

Quantity	Rise Time	Fall Time	Peak Value	Normalizing Factor
H_z/H_o	$0.09 t_d$	several tenths of t_d	$3.3(t_r/t_d)$	$H_o = \frac{V_o e^{-x/x_o}}{hZ_o}$
$(\sigma + \epsilon_o \frac{\partial}{\partial t}) E_x/J_o$	$0.06 t_d$	$0.1 t_d$	$14(t_r/t_d)$	$J_o = \frac{V_o e^{-x/x_o}}{h^2 Z_o}$
$(\sigma + \epsilon_o \frac{\partial}{\partial t}) E_y/J_o$	$0.05 t_d$	$0.08 t_d$	$80(t_r/t_d)^{3/2}$	$J_o = \frac{V_o e^{-x/x_o}}{h^2 Z_o}$

[†] Same as that of Table 1.

$$(2) \quad \epsilon/\epsilon_0 = \epsilon_r > 1$$

The ω -integrals to be evaluated are of the form

$$\int_{\tilde{C}_1} f_2(\omega) e^{-\zeta(h-y)} e^{j\omega\tau} d\omega$$

where $\zeta^2 = \left(\omega^2 \mu_0 \epsilon_0 (1 - \epsilon_r) + j\omega \mu_0 \sigma (1 - 2/R) - 1/x_0^2 \right)$, $\text{Re}(\zeta) \geq 0$, and \tilde{C}_1 is the integration path. The branch points are at $j(2t'_r)^{-1} \left(1 \pm \sqrt{1 + 4t'_r/(B^2 t_{dx_0})} \right)$, where $t'_r = \epsilon_0(\epsilon_r - 1)/\sigma$. A branch cut is drawn between these two branch points, so that $\text{Re}(\zeta) \geq 0$ along \tilde{C}_1 . By a proper deformation of the contour \tilde{C}_1 the following expressions for the field and current density distributions at $y=0$ are obtained:

$$H_z = \frac{V_0}{hZ_0} \left(\frac{t_d}{t'_r} \right)^{1/2} e^{-\frac{x}{x_0}} e^{-\frac{B\tau}{2t'_r}} \left\{ \left(1 - \frac{\epsilon_r B}{2(\epsilon_r - 1)} \right) I_0(A) + \frac{\epsilon_r B}{2(\epsilon_r - 1)} \sqrt{1 + \frac{4t'_r}{B^2 t_{dx_0}}} \frac{\tau}{\sqrt{\tau^2 - t'_t{}^2}} I_1(A) \right\} U(\tau - t'_t)$$

$$\begin{aligned} (\sigma + \epsilon \frac{\partial}{\partial t}) E_x &= \frac{V_0}{h^2 Z_0} \left(\frac{t_d}{t'_r} \right)^{1/2} e^{-\frac{x}{x_0}} e^{-\frac{B\tau}{2t'_r}} \frac{Bt_d}{4(\epsilon_r - 1)} \sqrt{1 + \frac{4t'_r}{B^2 t_{dx_0}}} \times \\ &\times \left\{ \frac{(2-B)\epsilon_r - 2}{\sqrt{\tau^2 - t'_t{}^2}} I_1(A) + \frac{\epsilon_r B\tau}{\tau^2 - t'_t{}^2} \sqrt{1 + \frac{4t'_r}{B^2 t_{dx_0}}} I_2(A) \right\} U(\tau - t'_t) \end{aligned} \quad (8)$$

$$\begin{aligned} (\sigma + \epsilon \frac{\partial}{\partial t}) E_y &= \frac{H_z}{x_0} - \frac{V_0}{h^2 Z_0} \frac{t_d}{t'_r} \frac{\epsilon_r B}{4(\epsilon_r - 1)^{3/2}} e^{-\frac{x}{x_0}} e^{-\frac{B\tau}{2t'_r}} \times \\ &\times \left[2 - B - \frac{2}{\epsilon_r} - \frac{B}{2} \left(1 + \frac{4t'_r}{B^2 t_{dx_0}} \right) \right] I_0(A) \end{aligned}$$

$$\begin{aligned}
& + \left(2B - 2 + \frac{2}{\epsilon_r} \right) \sqrt{1 + \frac{4t'_r}{B^2 t_{dx_0}} \frac{\tau}{\sqrt{\tau^2 - t'_t{}^2}}} I_1(A) \\
& - \frac{B}{2} \left(1 + \frac{4t'_r}{B^2 t_{dx_0}} \right) \frac{\tau^2 + t'_t{}^2}{\tau^2 - t'_t{}^2} I_2(A) \left. \right\} U(\tau - t'_t)
\end{aligned}$$

where $A = B \sqrt{\tau^2 - t'_t{}^2} \sqrt{1 + 4t'_r/(B^2 t_{dx_0})}^{-1} / (2t'_r)$, $t'_t{}^2 = h^2(\epsilon_r - 1)/c^2 = t'_d t'_r$, and $I_n(A)$ is the modified Bessel function of the first kind of order n .

In Equation 8, the responses of the form $\delta(\tau - t'_t)$ and $\delta'(\tau - t'_t)$ at $\tau = t'_t$ have been omitted. They should be included if one uses the above results for the calculation of the field and current density by convolution due to an arbitrary source field $f(ct - x)$, such as a unit step $U(ct - x)$, which will be considered in the next section.

To derive Equation 8 it has been assumed that $R > 2$ (i.e., $B > 0$). The case where $2 \geq R \geq 0$ is of no practical interest, as has been discussed before, since $x_0 \approx 200 - 300$ meters.

Another point to be mentioned is that Equation 8 shows that, in addition to diffusion, the Cerenkov process also plays an important role. This should be borne in mind when a medium with $\epsilon \neq \epsilon_0$ is used in a simulator with the source field propagating at a speed faster than $c/\sqrt{\epsilon_r}$.

Based on Equation 8, several curves are presented in figures 5, 6, and 7 for $x_0/h = 200, 10$; $(t'_d/t'_r)^{1/2} = t'_d/t'_t = 10, 5, 1, 0.5, 0.1, 0.05$. In the figures, $\epsilon_r = 20$ is used. From Equation 8, one can see that the field and current densities do not change much for $40 \geq \epsilon_r \geq 10$ (say, within a factor of 2), once t'_d/t'_t is fixed. Thus, these curves can also be used for a simulator with $10 \leq \epsilon_r \leq 40$. As can be seen, Equation 8 is extremely complicated. However, for the practical situation with $x_0 \approx 200 - 300$ m, $\sigma \geq 3 \times 10^{-4}$ mho/m and $\epsilon_r \approx 10 - 40$, one can generally approximate Equation 8 by setting $B = 1$ and $1 + 4t'_r/(B^2 t_{dx_0}) = 1$, and the early- and late-time (defined respectively by $\sqrt{\tau^2 - t'_t{}^2} \ll 2t'_r$ and $\sqrt{\tau^2 - t'_t{}^2} \gg 2t'_r$) approximations are obtained as follows:

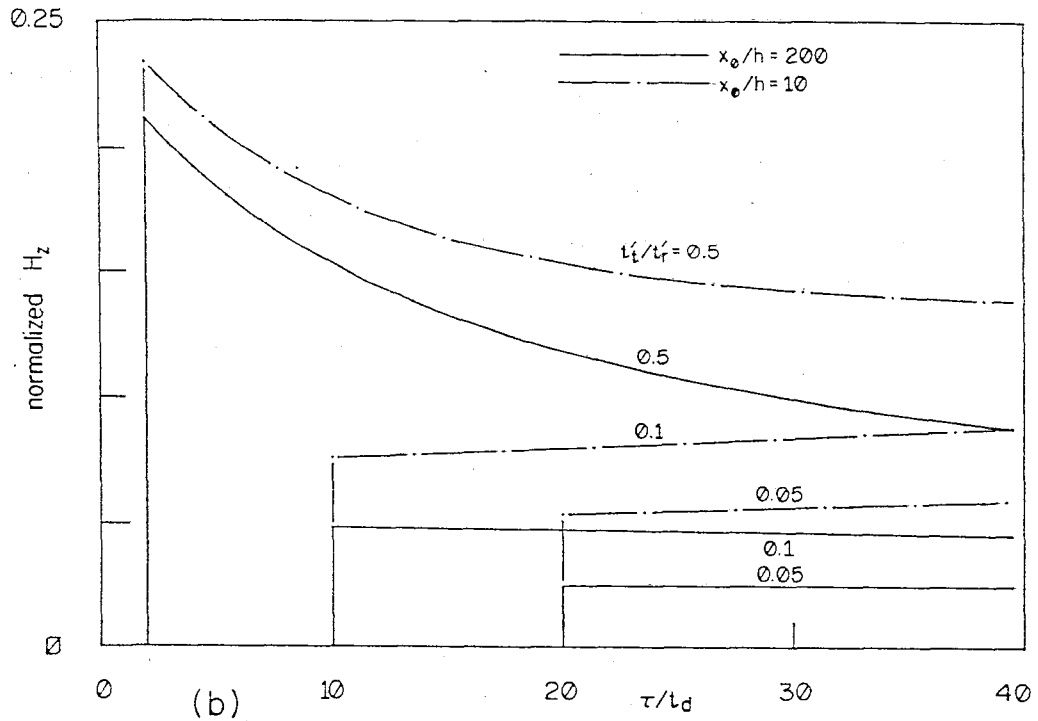
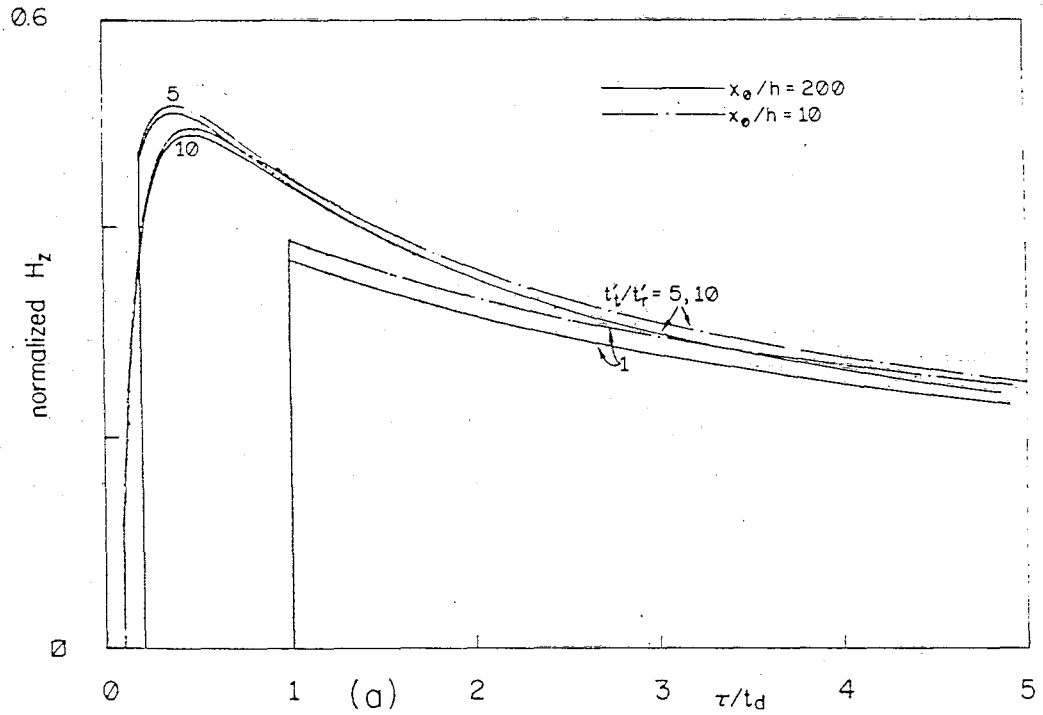


Figure 5. (a) H_z/H_0 , (b) $(t'_t/t'_r)H_z/H_0$ at $y=0$ as functions of τ/t_d for $x_0/h=200$ and 10 , $\epsilon_r=20$, and various t'_t/t'_r , for the simulator with $\sigma_1=\sigma_2=\sigma$, $\epsilon_1=\epsilon_2=\epsilon=\epsilon_r\epsilon_0$, $E_x^e=V_0\delta(ct-x)\exp(-x/x_0)$. Here $H_0=V_0\exp(-x/x_0)(hZ_0)^{-1}$, $Z_0=(\mu_0/\epsilon_0)^{1/2}$, $t_d=\mu_0\sigma h^2$, $t'_t=h\sqrt{\epsilon_r-1}/c$, $t'_r=\epsilon_0(\epsilon_r-1)/\sigma$, $t'_t/t'_r=t_d/t'_t=(t_d/t'_t)^{1/2}$, $\tau=t-x/c$.

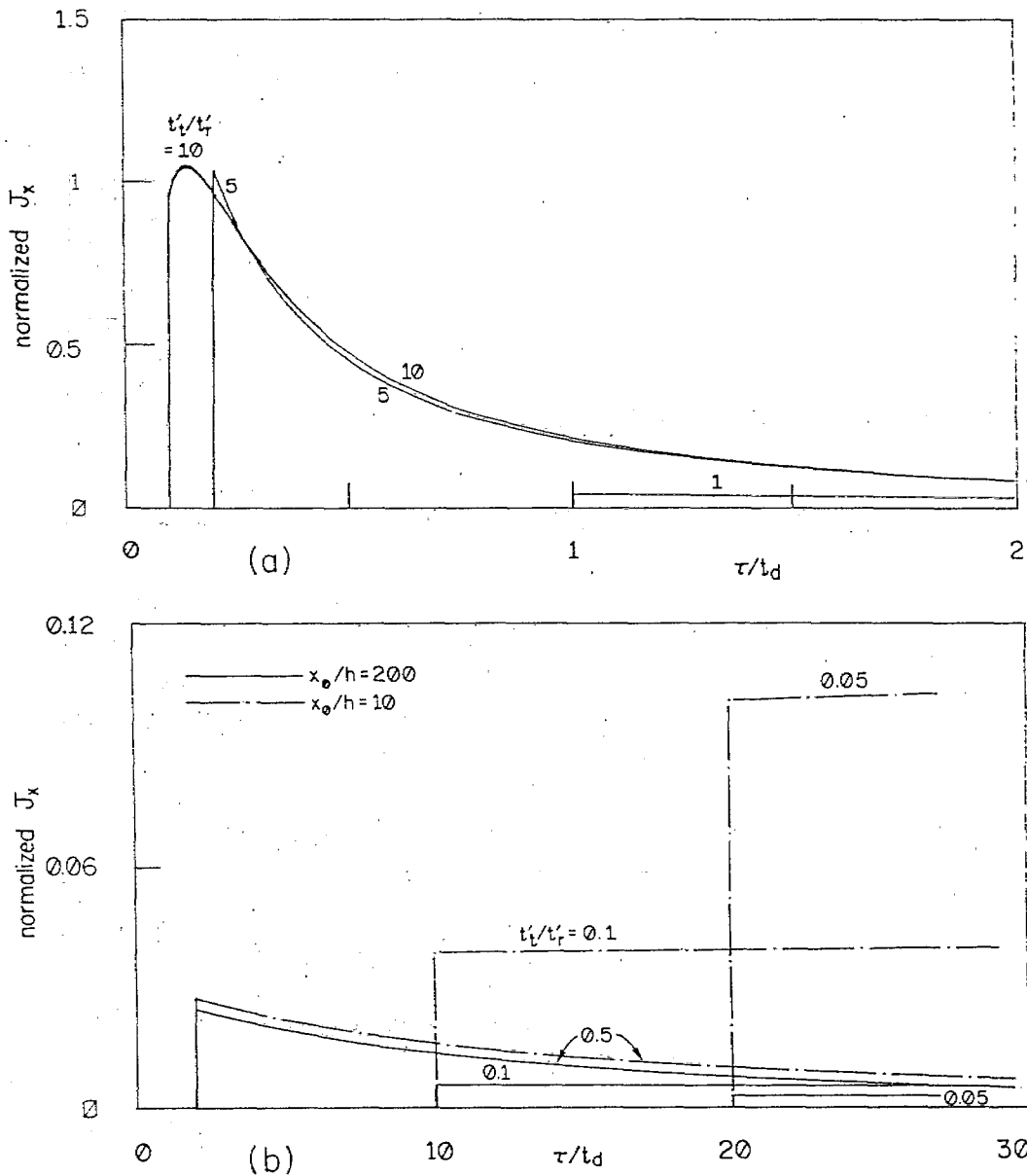


Figure 6. (a) J_x/J_0 , (b) $(t'_t/t'_r)^2 J_x/J_0$ at $y=0$ as functions of τ/t_d for $x_0/h=200$ and 10 , $\epsilon_r=20$ and various t'_t/t'_r , for the simulator with $\sigma_1=\sigma_2=\sigma$, $\epsilon_1=\epsilon_2=\epsilon=\epsilon_r\epsilon_0$, $E_x^e=V_0\delta(ct-x)\exp(-x/x_0)$. Here $J_x=(\sigma+\epsilon\frac{\partial}{\partial t})E_x$, $J_0=V_0\exp(-x/x_0)(h^2Z_0)^{-1}$, $Z_0=(\mu_0/\epsilon_0)^{1/2}$, $t_d=\mu_0\sigma h^2$, $t'_t=h/\sqrt{\epsilon_r-1}/c$, $t'_r=\epsilon_0(\epsilon_r-1)/\sigma$, $t'_t/t'_r=t_d/t'_t=(t_d/t'_r)^{1/2}$, $\tau=t-x/c$. (Note, the difference in J_x/J_0 between $x_0/h=200$ and 10 is small for $t'_t/t'_r \geq 1$).

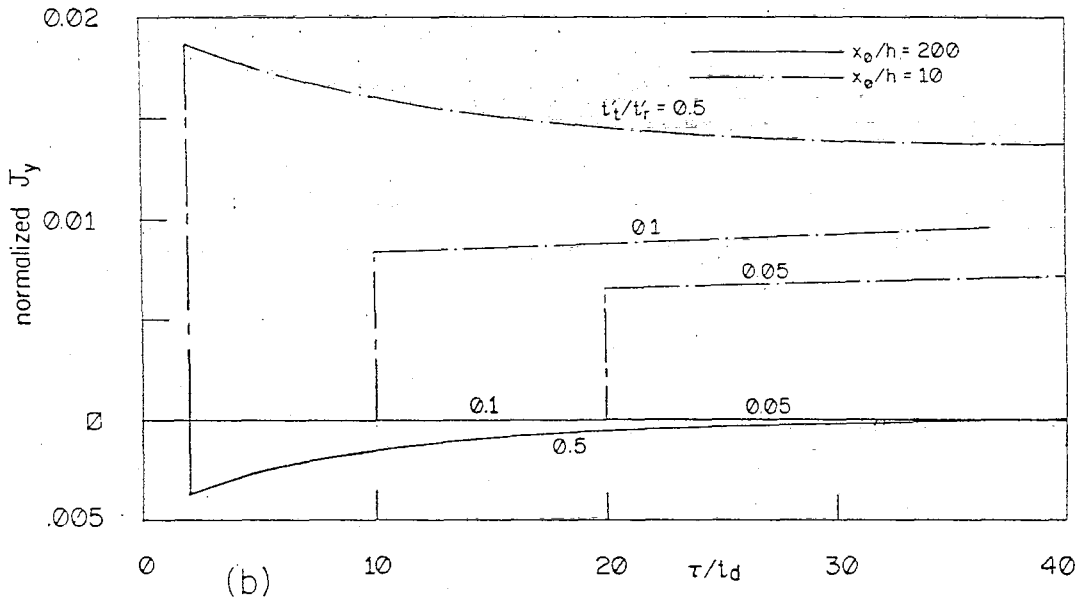
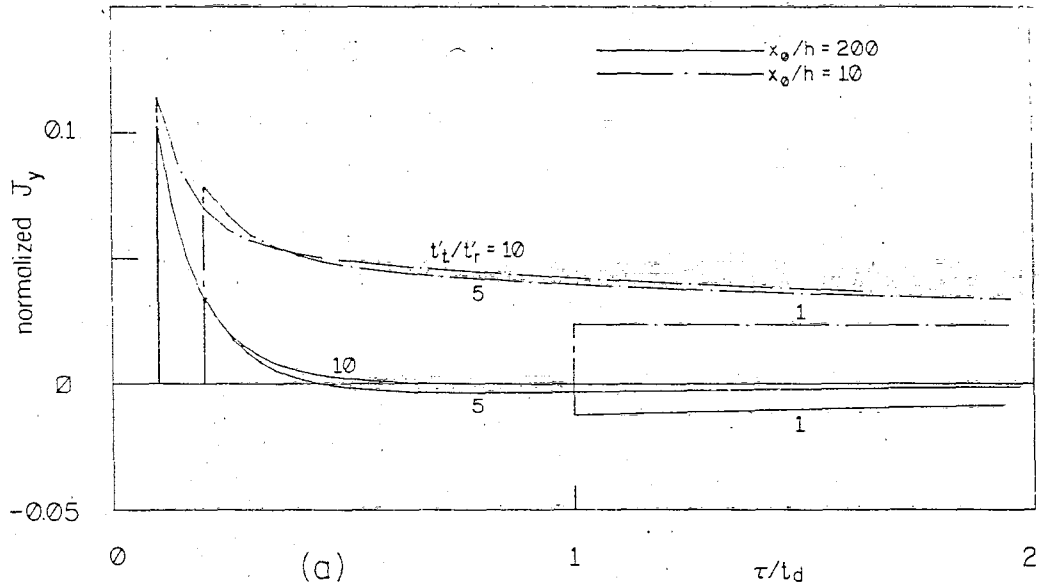


Figure 7. J_y/J_0 at $y=0$ as a function of τ/t_d for $x_0/h = 200$ and 10 , $\epsilon_r = 20$, and various t'_t/t'_r , for the simulator with $\sigma_1 = \sigma_2 = \sigma$, $\epsilon_1 = \epsilon_2 = \epsilon = \epsilon_r \epsilon_0$, $E_x^e = V_0 \delta(ct - x) \exp(-x/x_0)$. Here, $J_y = (\sigma + \epsilon \frac{\partial}{\partial t}) E_y$, $J_0 = V_0 \exp(-x/x_0) (h^2 Z_0)^{-1}$, $Z_0 = (\mu_0/\epsilon_0)^{1/2}$, $t_d = \mu_0 \sigma h^2$, $t'_t = h\sqrt{\epsilon_r - 1}/c$, $t'_r = \epsilon_0(\epsilon_r - 1)/\sigma$, $t'_t/t'_r = t_d/t'_t = (t_d/t'_t)^{1/2}$, $\tau = t - x/c$.

(a) at early times ($\sqrt{\tau^2 - t_t'^2} \ll 2t_r'$, $\tau > t_t'$):

$$H_z \approx \frac{V_o}{hZ_o} \left(\frac{t_d}{t_r'} \right)^{1/2} e^{-\frac{x}{x_o}} e^{-\frac{\tau}{2t_r'}} \frac{\epsilon_r - 2}{2(\epsilon_r - 1)} \left(1 + \frac{\epsilon_r}{4(\epsilon_r - 2)} \frac{\tau}{t_r'} \right)$$

$$\left(\sigma + \epsilon \frac{\partial}{\partial t} \right) E_x \approx \frac{V_o}{h^2 Z_o} \left(\frac{t_d}{t_r'} \right)^{3/2} e^{-\frac{x}{x_o}} e^{-\frac{\tau}{2t_r'}} \frac{\epsilon_r - 2}{16(\epsilon_r - 1)} \left(1 + \frac{\epsilon_r}{8(\epsilon_r - 2)} \frac{\tau}{t_r'} \right) \quad (9)$$

$$\left(\sigma + \epsilon \frac{\partial}{\partial t} \right) E_y \approx \frac{H_z}{x_o} - \frac{V_o}{h^2 Z_o} \frac{t_d}{t_r'} e^{-\frac{x}{x_o}} e^{-\frac{\tau}{2t_r'}} \frac{\epsilon_r - 4}{8(\epsilon_r - 1)^{3/2}} \times$$

$$\times \left(1 + \frac{1}{\epsilon_r - 4} \frac{\tau}{t_r'} - \frac{\epsilon_r}{32(\epsilon_r - 4)} \frac{\tau^2 + t_t'^2}{t_r'^2} \right)$$

(b) at late times ($\sqrt{\tau^2 - t_t'^2} \gg 2t_r'$, $\tau > t_t'$):

$$H_z \approx \frac{V_o}{hZ_o} \left(\frac{t_d}{\pi \sqrt{\tau^2 - t_t'^2}} \right)^{1/2} e^{-\frac{x}{x_o}} e^{-(\tau - \sqrt{\tau^2 - t_t'^2}) / (2t_r')} \frac{(\epsilon_r - 2)}{2(\epsilon_r - 1)} \times$$

$$\times \left(1 + \frac{\epsilon_r}{\epsilon_r - 2} \frac{\tau}{\sqrt{\tau^2 - t_t'^2}} \right)$$

$$\left(\sigma + \epsilon \frac{\partial}{\partial t} \right) E_x \approx \frac{V_o}{h^2 Z_o} \left(\frac{t_d}{\sqrt{\tau^2 - t_t'^2}} \right)^{3/2} e^{-\frac{x}{x_o}} e^{-(\tau - \sqrt{\tau^2 - t_t'^2}) / (2t_r')} \frac{(\epsilon_r - 2)}{4\sqrt{\pi}(\epsilon_r - 1)} \times$$

$$\times \left(1 + \frac{\epsilon_r}{\epsilon_r - 2} \frac{\tau}{\sqrt{\tau^2 - t_t'^2}} \right) \quad (10)$$

$$\begin{aligned}
\left(\sigma + \epsilon \frac{\partial}{\partial t}\right) E_y &\approx \frac{H_z}{x_o} - \frac{V_o}{h^2 Z_o} \frac{t_d}{\left(\pi t_r' \sqrt{\tau^2 - t_t'^2}\right)^{1/2}} e^{-\frac{x}{x_o}} e^{-(\tau - \sqrt{\tau^2 - t_t'^2}) / (2t_r')} \frac{1}{8(\epsilon_r - 1)^{3/2}} \times \\
&\times \left(\left[(\epsilon_r - 4) + 4 \frac{\tau}{\sqrt{\tau^2 - t_t'^2}} - \epsilon_r \frac{\tau^2 + t_t'^2}{\tau^2 - t_t'^2} \right] \right. \\
&\left. + \frac{t_r'}{4\sqrt{\tau^2 - t_t'^2}} \left[(\epsilon_r - 4) - \frac{12\tau}{\sqrt{\tau^2 - t_t'^2}} + 15\epsilon_r \frac{\tau^2 + t_t'^2}{\tau^2 - t_t'^2} \right] \right) \quad (10)
\end{aligned}$$

If, furthermore, $\tau \gg t_d$, one has

$$\begin{aligned}
H_z &\approx \frac{V_o}{h Z_o} \left(\frac{t_d}{\pi \tau} \right)^{1/2} e^{-\frac{x}{x_o}} e^{-\frac{t_d}{4\tau}} \\
\left(\sigma + \epsilon \frac{\partial}{\partial t}\right) E_x &\approx \frac{V_o}{h^2 Z_o} \frac{1}{2\sqrt{\pi}} \left(\frac{t_d}{\tau} \right)^{3/2} e^{-\frac{x}{x_o}} e^{-\frac{t_d}{4\tau}} \quad (11) \\
\left(\sigma + \epsilon \frac{\partial}{\partial t}\right) E_y &\approx \frac{H_z}{x_o} - \frac{V_o}{h^2 Z_o} \frac{1}{2\sqrt{\pi}} \frac{t_d}{\tau} \left(\frac{t_r}{\tau} \right)^{1/2} e^{-\frac{x}{x_o}} e^{-\frac{t_d}{4\tau}}
\end{aligned}$$

Equation 11 is similar to Equation 7 when $\tau \gg t_r, t_d, B \rightarrow 1, R^2 \rightarrow \infty$. Thus, at very late times, one expects that the diffusion is the dominant process.

From Figures 5,6,7 and Equations 8, 9, 10 and 11, one can summarize the approximate behaviors of the field and current quantities in Table 3. For $(\sigma + \epsilon(\partial/\partial t))E_x/J_o$ with $5 \geq t_d/t_t' \geq 1$ and $(\sigma + \epsilon(\partial/\partial t))E_y/J_o$ with $5 \geq t_d/t_t' \geq 2$, the behaviors are expected to be approximately between the tabulated extreme situations.

TABLE 3. FIELD AND CURRENT DENSITY FOR $\epsilon_r \approx 10-40$, $x_o \geq 200$ m, $\sigma \geq 3 \times 10^{-4}$ mho/m, $x_o/h \geq 100^\dagger$

Quantity	Rise Time (τ_r)	Fall Time	Peak Value	Condition
$\frac{H_z}{H_o}$	$t'_t + 0.3 t_d \geq \tau_r \geq t'_t$	$8 t_d$	0.5	$(t_d/t'_t)^{1/2} = t_d/t'_t = t'_t/t'_r \geq 1$
	t'_t	$8t'_r$	$0.5 t_d/t'_t$	$1 \geq t_d/t'_t$
$\frac{(\sigma + \epsilon \frac{\partial}{\partial t}) E_x}{J_o}$	$t'_t + 0.2 t_d \geq \tau_r \geq t'_t$	$0.5 t_d$	1	$t_d/t'_t \geq 5$
	t'_t	$5t'_r$	$(t_d/t'_t)^3/16$	$1 \geq t_d/t'_t$
$\frac{(\sigma + \epsilon \frac{\partial}{\partial t}) E_y^*}{J_o}$	t'_t	$0.3 t_d$	$0.002 t_d^2/t'_r^2 \exp(-0.5 t_d/t'_t)$	$t_d/t'_t \geq 5$
	t'_t	several t'_r	$-0.025 t_d/t'_r \exp(-0.5 t_d/t'_t)$	$2 \geq t_d/t'_t \geq 0.1$

* For $0.1 \geq t_d/t'_t$, $(\sigma + \epsilon \frac{\partial}{\partial t}) E_y/J_o$ is in the order of $(H_z/H_o) \times (h/x_o)$, which is very small.
 For $t_d/t'_t \geq 5$, the peak value has a maximum ≈ 0.15 , at $t_d/t'_t \approx 8$.

$\dagger t_d = \mu_o \sigma h^2$, $t'_t = h\sqrt{\epsilon_r - 1} / c$, $t'_r = \epsilon_o(\epsilon_r - 1)/\sigma$, $\sigma_1 = \sigma_2 = \sigma$, $\epsilon_1 = \epsilon_2 = \epsilon = \epsilon_r \epsilon_o$, $E_x^e = V_o \delta(ct - x) \exp(-x/x_o)$,
 $H_o = hJ_o = V_o(hZ_o)^{-1} \exp(-x/x_o)$, $\tau < t_{dx_o} = \mu_o \sigma x_o^2$, $y=0$, and the δ -function responses at $\tau = t'_t$ are excluded.

$$B. \quad \sigma_2 \rightarrow \infty, \quad \sigma_1 = \sigma, \quad \epsilon_1 = \epsilon, \quad E_x^e = V_0 \delta(ct - x) \exp(-x/x_0), \quad 0 \leq y \leq h$$

Two cases will be considered depending on whether or not ϵ equals ϵ_0 .

$$(1) \quad \epsilon = \epsilon_0$$

From Equations 1 and 6 it is seen that all the ω -integrals are of the form

$$\text{and} \quad \int_{\tilde{C}_1} f_1(\omega) \zeta^{-1} (\sinh(\zeta h))^{-1} \cosh(\zeta y) e^{j\omega\tau} d\omega \quad (12)$$

$$\int_{\tilde{C}_1} f_2(\omega) (\sinh(\zeta h))^{-1} \sinh(\zeta y) e^{j\omega\tau} d\omega$$

where $\zeta = \sqrt{j\omega\mu_0\sigma B - 1/x_0^2}$, and \tilde{C}_1 is the integration path. The integrands have poles at the zeros of $\sinh(\zeta h)$, i.e., at $\omega = j(m^2\pi^2 - h^2/x_0^2)/(t_d B)$, $m = 0, 1, 2, \dots$, but no branch points. The integration path \tilde{C}_1 can then be deformed and the following results are obtained:

$$H_z = \frac{2V_0}{hZ_0 B} e^{-\frac{x}{x_0}} \sum_{m=0}^{\infty} \frac{(-1)^m \cos(m\pi y/h)}{1 + \delta_{m0}} \left(1 - \frac{m^2\pi^2 - h^2/x_0^2}{B} \frac{t_r}{t_d} \right) \times$$

$$\times e^{-\frac{m^2\pi^2 - h^2/x_0^2}{B} \frac{\tau}{t_d}} U(\tau)$$

$$\left(\sigma + \epsilon_0 \frac{\partial}{\partial t} \right) E_x = \frac{-2V_0}{h^2 Z_0 B} e^{-\frac{x}{x_0}} \sum_{m=1}^{\infty} (-1)^m m\pi \sin(m\pi y/h) \times$$

$$\times \left(1 - \frac{m^2\pi^2 - h^2/x_0^2}{B} \frac{t_r}{t_d} \right) e^{-\frac{m^2\pi^2 - h^2/x_0^2}{B} \frac{\tau}{t_d}} U(\tau)$$

$$\begin{aligned}
\left(\sigma + \epsilon_0 \frac{\partial}{\partial t}\right) E_y &= \frac{-2V_0}{h^2 Z_0 B} e^{-\frac{x}{x_0}} \sum_{m=0}^{\infty} \frac{(-1)^m \cos(m\pi y/h)}{1 + \delta_{m0}} \left(1 - \frac{m^2 \pi^2 - h^2/x_0^2}{B} \frac{t_r}{t_d}\right) \times \\
&\times \left[\frac{m^2 \pi^2 - h^2/x_0^2}{B} \left(\frac{t_r}{t_d}\right)^{\frac{1}{2}} - \frac{h}{x_0} \right] e^{-\frac{m^2 \pi^2 - h^2/x_0^2}{B} \frac{\tau}{t_d}} U(\tau) \quad (13)
\end{aligned}$$

where δ_{m0} is the Kronecker delta function, which is zero when $m \neq 0$, unity when $m = 0$. From Equation 13 one observes that when $\tau > t_d$ one requires only a couple of terms with small m 's to obtain good approximations for the field and current density. But, when $0 \leq \tau \ll t_d$, one can see that the series representation of Equation 13 converges very slowly and one has to look for alternative representations.

One alternative representation good for $0 \leq \tau \ll t_d$ can be obtained by deforming the original integration path \tilde{C}_1 to the lower half plane, and the following expressions are obtained.

$$\begin{aligned}
H_z &= \frac{V_0}{hZ_0} \left(\frac{t_d}{\pi B \tau}\right)^{\frac{1}{2}} \sum_{n=-\infty}^{\infty} \left(1 - \frac{t_r}{2\tau} + \frac{1}{BR^2} + \frac{Bt_r t_d^{(n)}}{4\tau^2}\right) e^{-\frac{Bt_d^{(n)}}{4\tau} \frac{\tau}{Bt_d x_0}} e^{-\frac{x}{x_0}} U(\tau) \\
\left(\sigma + \epsilon_0 \frac{\partial}{\partial t}\right) E_x &= \frac{V_0}{2h^2 Z_0} \left(\frac{Bt_d^3}{\pi \tau^3}\right)^{\frac{1}{2}} \sum_{n=-\infty}^{\infty} (2n+1 - y/h) e^{-\frac{Bt_d^{(n)}}{4\tau} \frac{\tau}{Bt_d x_0}} e^{-\frac{x}{x_0}} U(\tau) \times \\
&\times \left(1 - \frac{3t_r}{2\tau} + \frac{1}{BR^2} + \frac{Bt_r t_d^{(n)}}{4\tau^2}\right) \\
\left(\sigma + \epsilon_0 \frac{\partial}{\partial t}\right) E_y &= \frac{H_z}{x_0} - \frac{V_0}{2h^2 Z_0} \left(\frac{t_r t_d^2}{\pi B \tau^3}\right)^{\frac{1}{2}} e^{\frac{\tau}{Bt_d x_0}} e^{-\frac{x}{x_0}} U(\tau) \times
\end{aligned}$$

$$\begin{aligned}
& \times \sum_{n=-\infty}^{\infty} \left\{ \left(1 + \frac{2}{BR^2} \right) - \frac{2\tau}{Bt_{dx_0}} \left(1 + \frac{1}{BR^2} \right) - \left(\frac{3t_r}{2\tau} + \frac{Bt_{dy}^{(n)}}{2\tau} + \frac{t_{dy}^{(n)}}{\tau R^2} \right) + \right. \\
& \left. + \frac{3Bt_r t_{dy}^{(n)}}{2\tau^2} - \frac{B^2 t_r t_{dy}^{(n)2}}{8\tau^3} \right\} e^{-\frac{Bt_{dy}^{(n)}}{4\tau}} \quad (14)
\end{aligned}$$

where $t_{dy}^{(n)} = t_d(2n+1-y/h)^2$. As is obvious from Equation 14, when $\tau < t_d$, one needs only a couple of terms with small n 's to get good approximations for the field and current density distributions.

To derive Equations 13 and 14, it has been assumed that $R > 2$ (i.e., $B > 0$). The situation with $R \leq 2$ will be excluded from the discussion since it is of no practical interest.

From Equations 13 and 14, one finds that the fields and current densities are determined by the diffusion process and the bounce between $y = 0$ and $y = h$ planes. Based on Equations 13 and 14, several curves for $x_0/h = 200; 10;$ $t_r/t_d = 1, 0.3, 0.1, 0.08, 0.03, 0.01;$ $y/h = 0, 0.5$ are presented in Figures 8-12, for τ up to t_d . Of course, one is mainly interested in the case with $x_0/h = 200$ so that $R \gg 2$, and $B \approx 1$. From the figures, one can see that all quantities reach their maximums in a few tenths of t_d . In this range of τ , Equation 14 is a good representation for the field and current density. Actually, one needs only the term with $n = 0$ for the region $\frac{1}{2} \leq y/h < 1$, and possibly, the terms with $n = 0, -1$ for the region $\frac{1}{2} > y \geq 0$ to get good estimates of the three field quantities. That is, one needs only to consider the direct "illumination" for the region relatively far away from the ground plane $y = 0$, and possibly has to include the first reflection from $y = 0$ for the region close to the ground plane. And, definitely, for these $n = 0, -1$ terms, one can approximate them further, similar to what has been done on Equation 7 for the case (A-1).

Based on these considerations and the curves in Figures 8-12, the field and current densities are obtained and summarized in Tables 4 and 5.

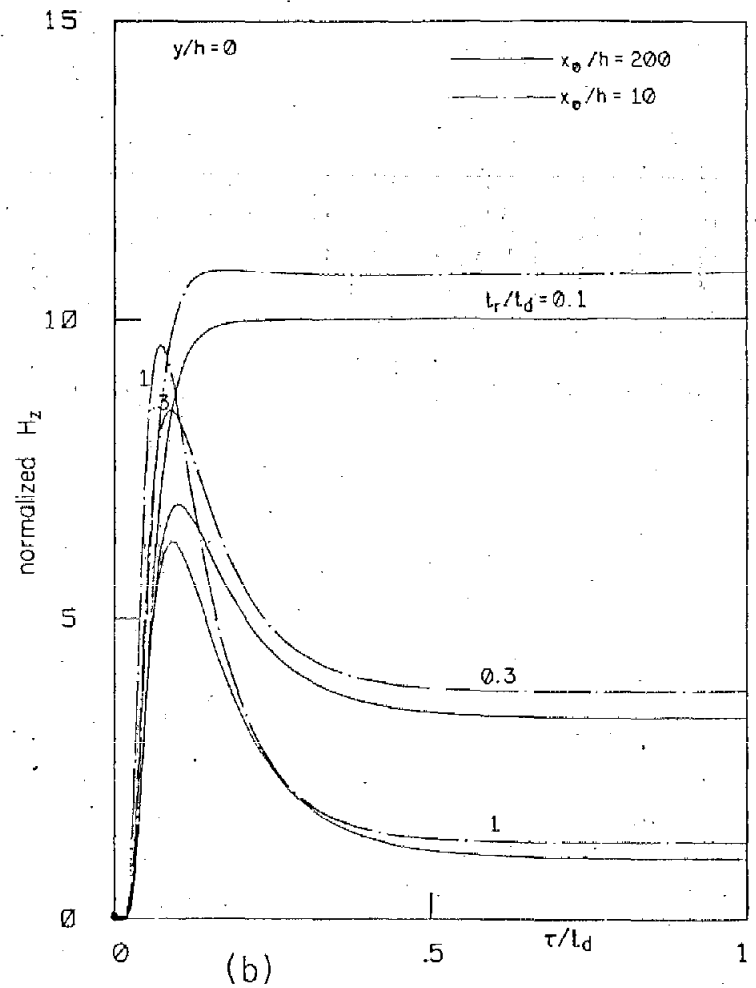
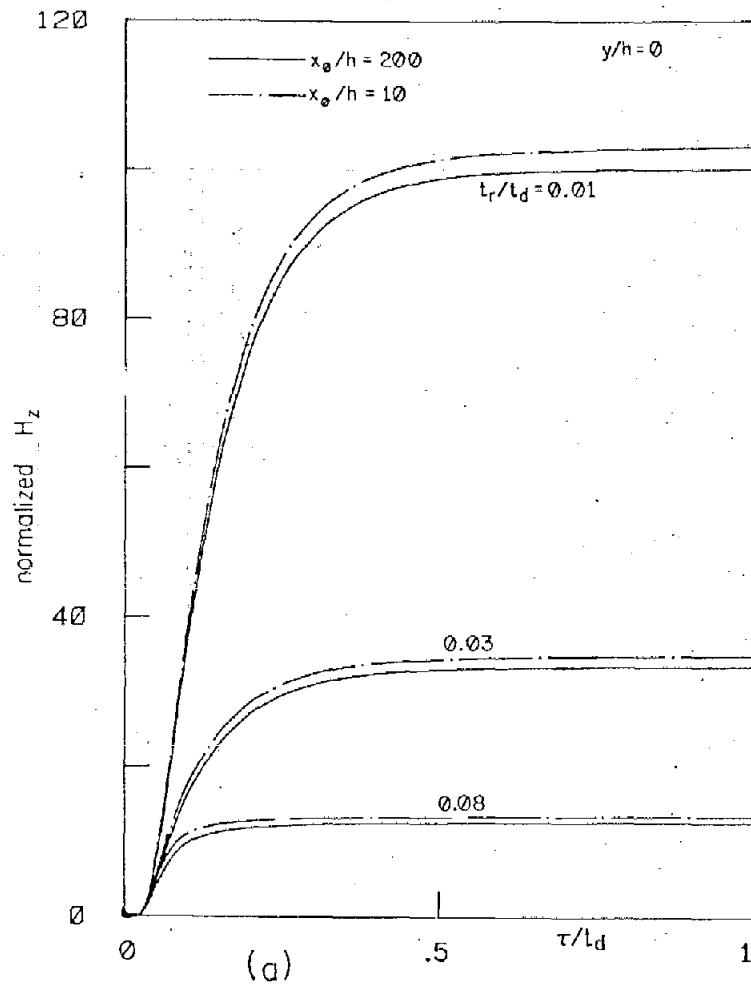


Figure 8. $(t_d/t_r)H_z/H_0$ at $y=0$ as a function of τ/t_d for $x_0/h = 200, 10$ and various t_r/t_d , for the simulator with $\sigma_2 \rightarrow \infty$, $\sigma_1 = \sigma$, $\epsilon_1 = \epsilon_0$, $E_x^e = V_0 \exp(-x/x_0) \delta(ct-x)$. Here, $H_0 = V_0 (hZ_0)^{-1} \exp(-x/x_0)$, $Z_0 = (\mu_0/\epsilon_0)^{1/2}$, $t_r = \epsilon_0/\sigma$, $t_d = \mu_0 \sigma h^2$, $\tau = t - x/c$.

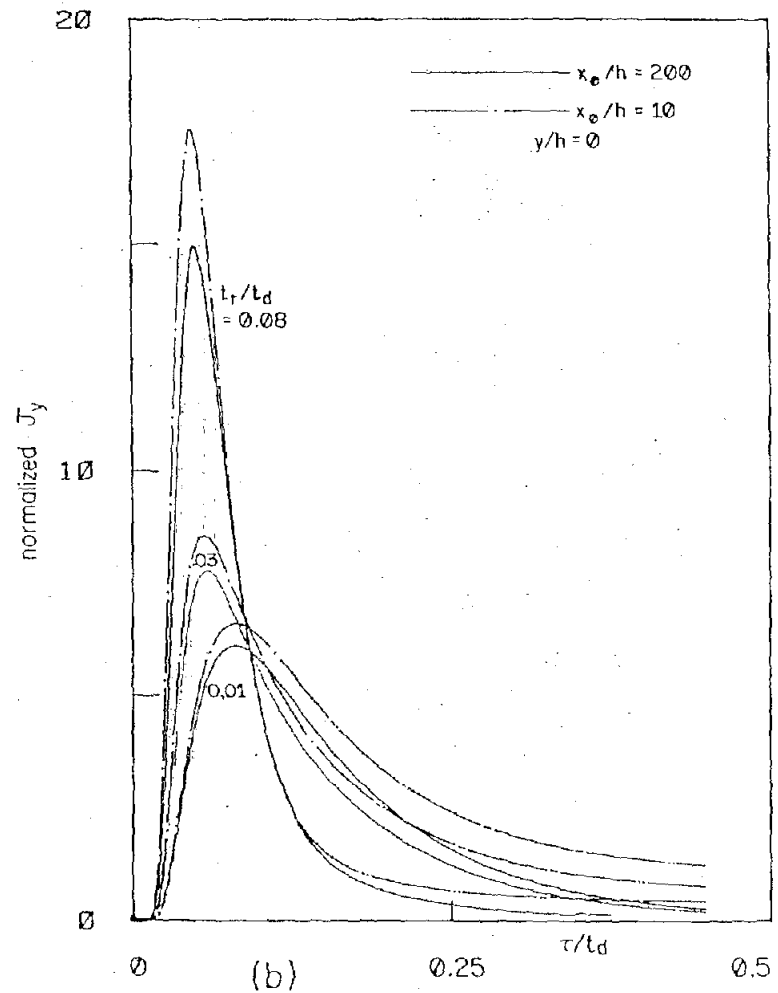
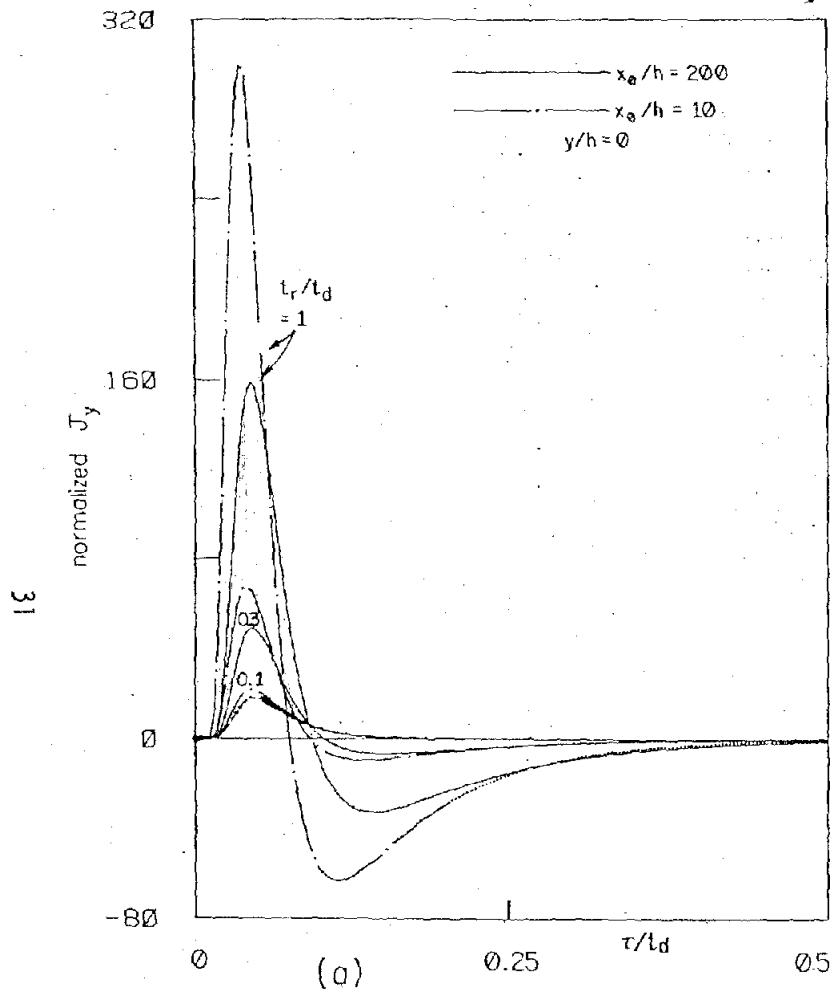


Figure 9. $(t_d/t_r)^{1/2} J_y/J_0$ at $y=0$ as a function of τ/t_d for $x_0/h = 200, 10$ and various t_r/t_d , for the simulator with $\sigma_2 \rightarrow \infty$, $\sigma_1 = \sigma$, $\epsilon_1 = \epsilon_0$, $E_x^e = V_0 \exp(-x/x_0) \delta(ct-x)$. Here, $J_y = (\sigma + \epsilon_0 \frac{\partial}{\partial t}) E_y$, $J_0 = V_0 (h^2 Z_0)^{-1} \exp(-x/x_0)$, $Z_0 = (\mu_0/\epsilon_0)^{1/2}$, $t_r = \epsilon_0/\sigma$, $t_d = \mu_0 \sigma h^2$, $\tau = t - x/c$.

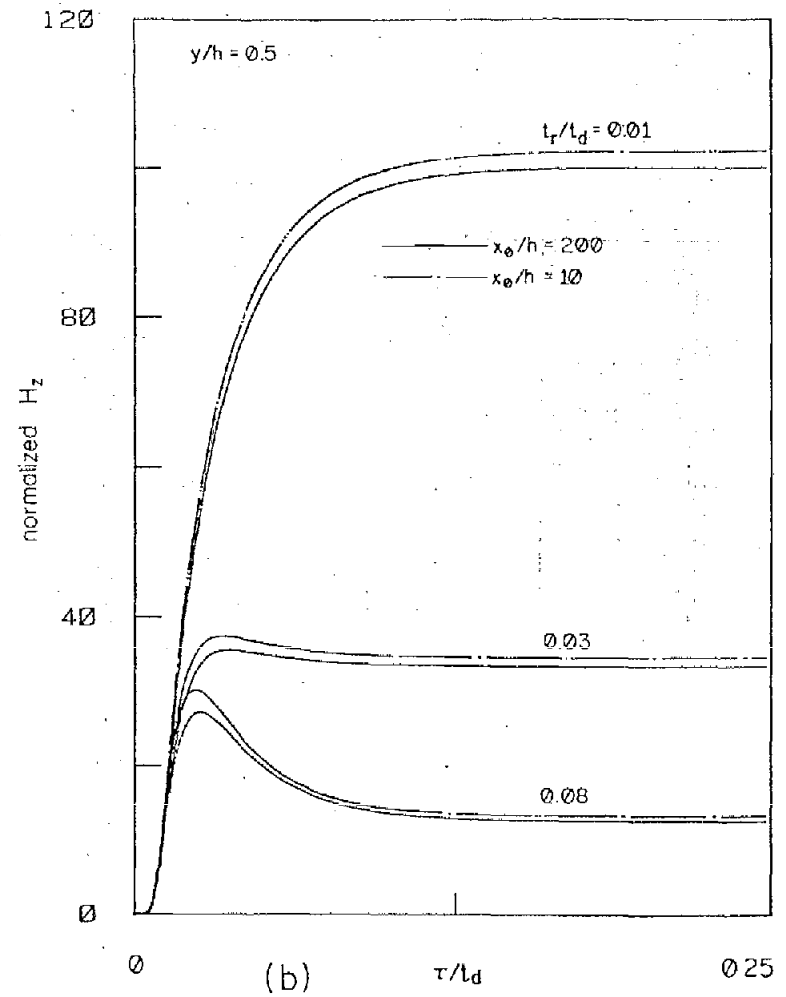
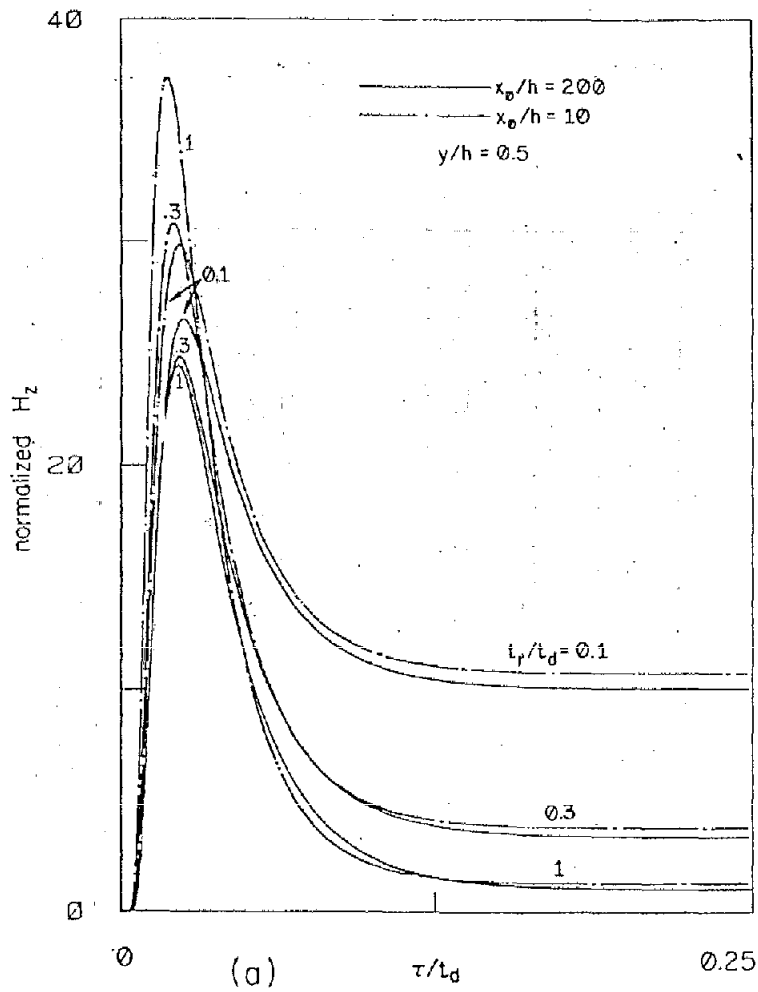


Figure 10. $(t_d/t_r)H_z/H_0$ at $y/h = 0.5$ as a function of τ/t_d for $x_0/h = 200, 10$, and various t_r/t_d , for the simulator with $\sigma_2 \rightarrow \infty$, $\sigma_1 = \sigma$, $\epsilon_1 = \epsilon_0$, $E_x^e = V_0 \exp(-x/x_0) \delta(ct - x)$. Here, $H_0 = V_0 (hZ_0)^{-1} \times \exp(-x/x_0)$, $Z_0 = (\mu_0/\epsilon_0)^{1/2}$, $t_r = \epsilon_0/\sigma$, $t_d = \mu_0 \sigma h^2$, $\tau = t - x/c$.

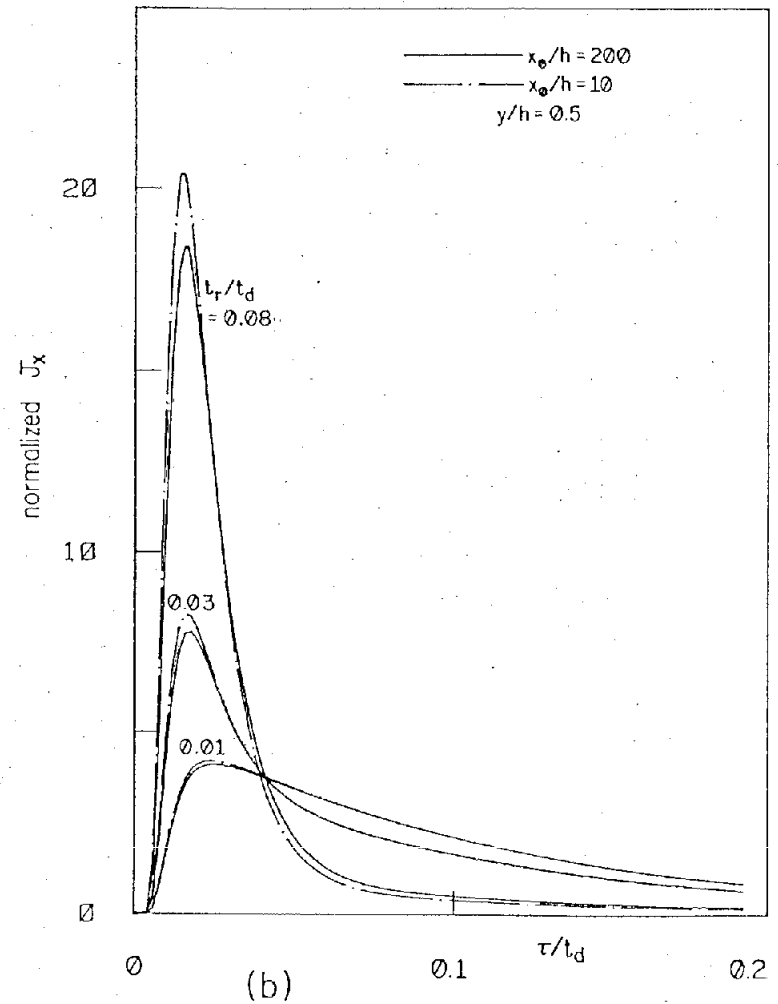
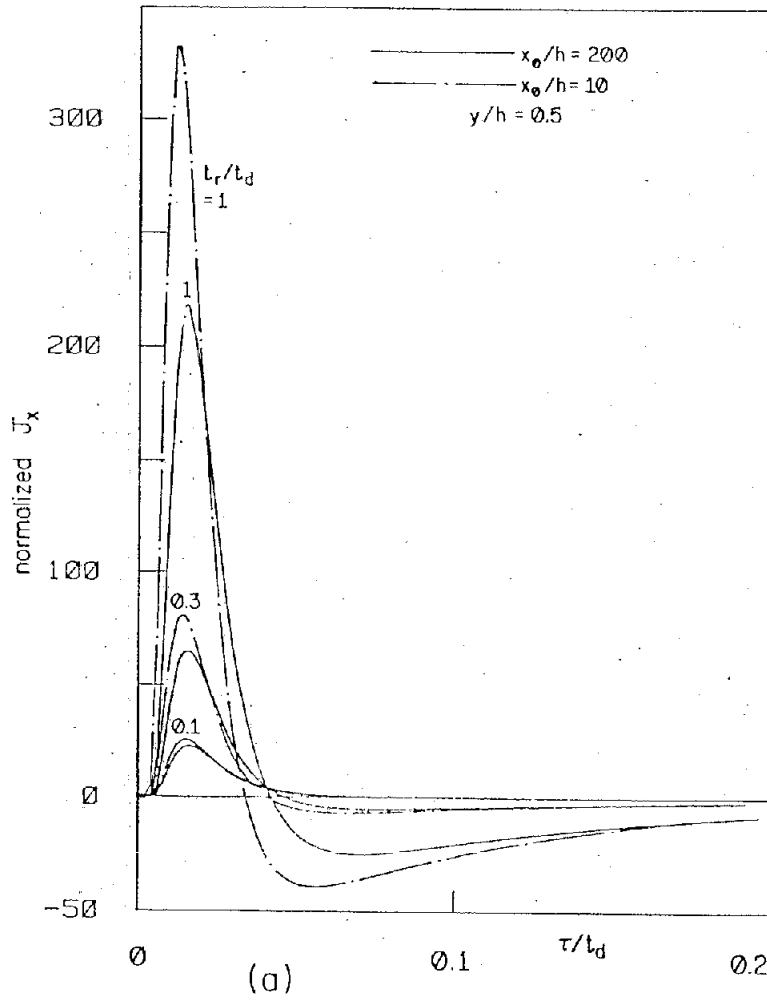


Figure 11. J_x/J_0 at $y/h = 0.5$ as a function of τ/t_d for $x_0/h = 200, 10$ and various t_r/t_d , for the simulator with $\sigma_2 \rightarrow \infty$, $\sigma_1 = \sigma$, $\epsilon_1 = \epsilon_0$, $E_x^e = V_0 \exp(-x/x_0) \delta(ct - x)$. Here $J_x = (\sigma + \epsilon_0 \frac{\partial}{\partial t}) E_x$, $J_0 = V_0 (h^2 Z_0)^{-1} \exp(-x/x_0)$, $Z_0 = (\mu_0/\epsilon_0)^{1/2}$, $t_r = \epsilon_0/\sigma$, $t_d = \mu_0 \sigma h^2$, $\tau = t - x/c$.

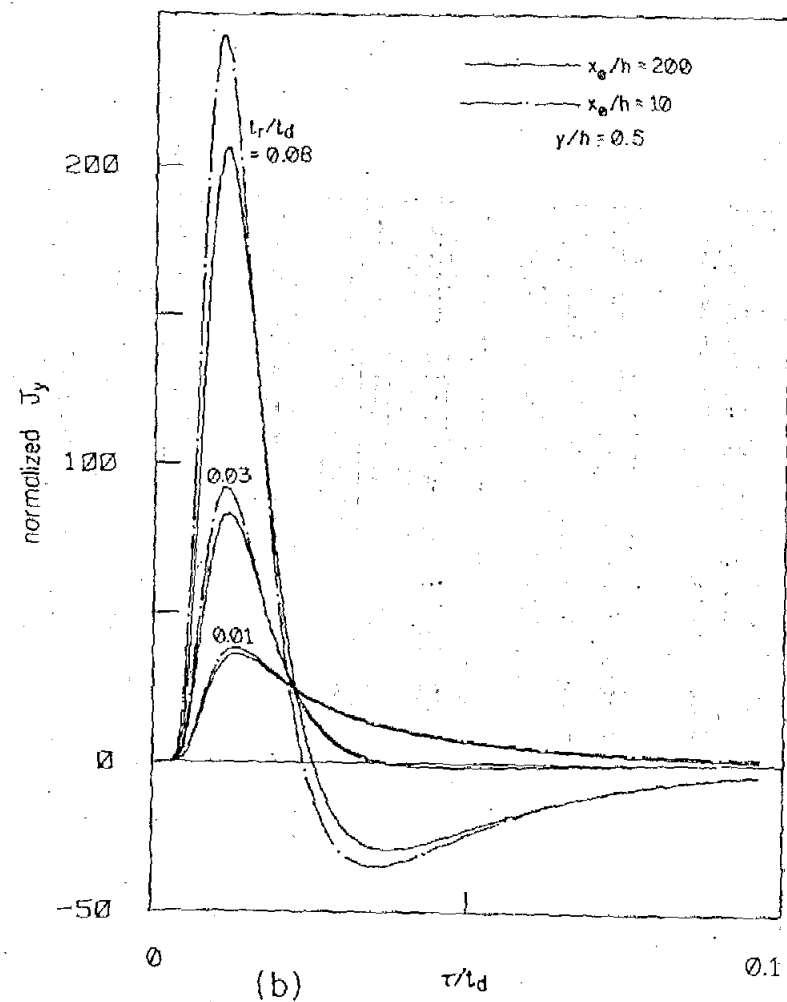
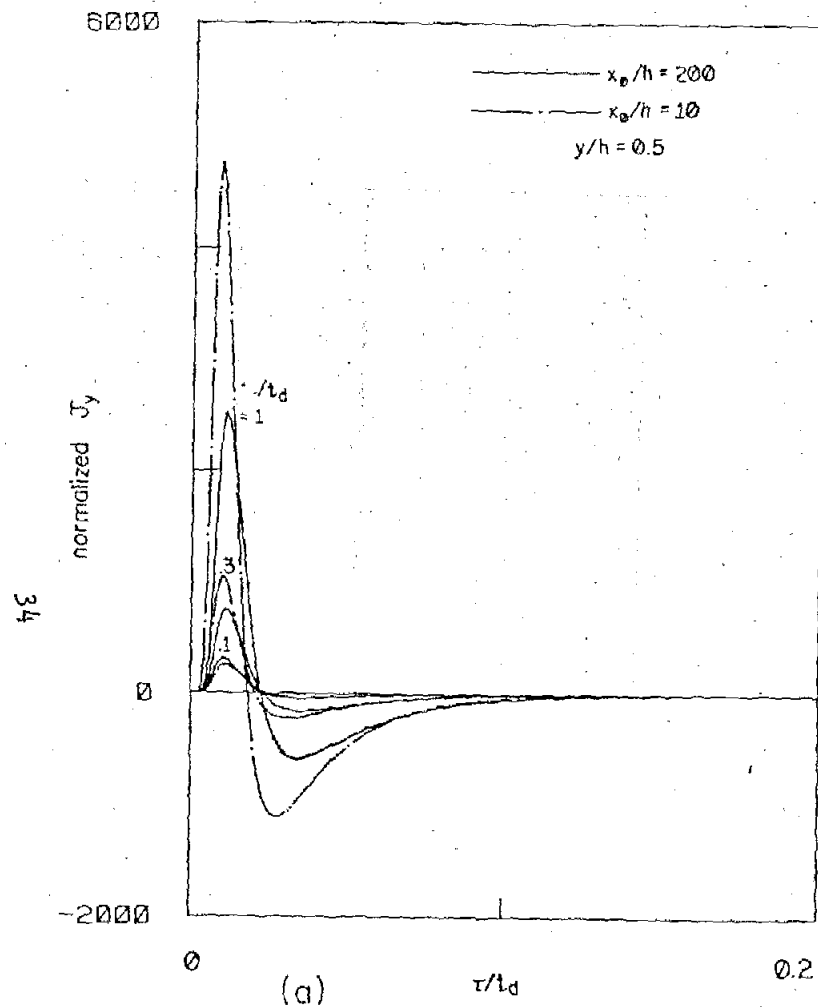


Figure 12. $(t_d/t_r)^{1/2} J_y/J_0$ at $y/h = 0.5$ as a function of τ/t_d for $x_0/h = 200, 10$ and various t_r/t_d , for the simulator with $\sigma_2 \rightarrow \infty, \sigma_1 = \sigma, \epsilon_1 = \epsilon_0, E_x^e = V_0 \exp(-x/x_0) \delta(ct-x)$. Here $J_y = (\sigma + \epsilon_0 \frac{\partial}{\partial t}) E_y, J_0 = V_0 (h^2 Z_0)^{-1} \exp(-x/x_0), Z_0 = (\mu_0/\epsilon_0)^{1/2}, t_r = \epsilon_0/\sigma, t_d = \mu_0 \sigma h^2, \tau = t - x/c$.

TABLE 4. FIELD AND CURRENT DENSITY AT $y/h \approx 0$ FOR $\sigma_2 \rightarrow \infty$, $\tau < t_{dx_0} = \mu_0 \sigma x_0^2$, $\sigma_1 \geq 3 \times 10^{-4}$ mho/m, $x_0 \geq 200$ m AND $x_0/h \geq 100$ [†]

Quantity	Rise Time (in t_d)	Fall Time (in t_d)	Peak Value	Condition
$\frac{H_z}{H_0}$	0.5	does not fall	1	$t_r/t_d \leq 0.01$
	0.09	0.5*	$6.6 t_r/t_d$	$0.5 \leq t_r/t_d$
$\frac{(\sigma + \epsilon_0 \frac{\partial}{\partial t}) E_y}{J_0}$	0.1	0.25	$6(t_r/t_d)^{1/2}$	$t_r/t_d \leq 0.01$
	0.05	0.08	$160(t_r/t_d)^{3/2}$	$0.5 \leq t_r/t_d$

$${}^\dagger t_r = \epsilon_0/\sigma, \quad t_d = \mu_0 \sigma h^2, \quad (\sigma + \epsilon_0 \frac{\partial}{\partial t}) E_x \approx 0, \quad E_x^e = V_0 \delta(ct - x) \exp(-x/x_0).$$

* Here, the fall time is the τ -value where H_z/H_0 reduces to approximately unity.

TABLE 5. FIELD AND CURRENT DENSITY AT $1 > y/h \geq 0.5$ FOR $\sigma_2 \rightarrow \infty$, $x_0/h \geq 100$, AND $\sigma_1 \geq 3 \times 10^{-4}$ mho/m, $x_0 \geq 200$ m[†]

Quantity	Rise Time (in t_{dy})	Fall Time (in t_{dy})	Peak Value	Condition
$\frac{H_z}{H_0}$	0.5	does not fall	1	$t_r/t_{dy} \leq 0.01$
	0.09	0.5*	$3.3 \frac{t_r}{t_d} \left(1 - \frac{y}{h}\right)^{-3}$	$0.5 \leq \frac{t_r}{t_{dy}}$
$\frac{(\sigma + \epsilon_0 \frac{\partial}{\partial t}) E_x}{J_0}$	0.17	0.7	$0.9(1 - y/h)^{-2}$	$t_r/t_{dy} \leq 0.01$
	0.06	0.1	$14 \frac{t_r}{t_d} \left(1 - \frac{y}{h}\right)^{-4}$	$0.5 \leq \frac{t_r}{t_{dy}}$
$\frac{(\sigma + \epsilon_0 \frac{\partial}{\partial t}) E_y}{J_0}$	0.1	0.4	$3 \left(\frac{t_r}{t_d}\right)^{1/2} \left(1 - \frac{y}{h}\right)^{-3}$	$t_r/t_{dy} \leq 0.01$
	0.05	0.08	$80 \left(\frac{t_r}{t_d}\right)^{3/2} \left(1 - \frac{y}{h}\right)^{-5}$	$0.5 \leq \frac{t_r}{t_{dy}}$

$${}^\dagger t_{dy} = t_d(1 - y/h)^2 = \mu_0 \sigma (h - y)^2, \quad E_x^e = V_0 \delta(ct - x) \exp(-x/x_0), \quad \tau < t_{dx_0}$$

* Here, the fall time is the τ -value where H_z/H_0 reduces to approximately unity.

$$(2) \quad \epsilon/\epsilon_0 = \epsilon_r > 1.$$

For this case, one finds that the ω -integrals are of the forms of Equation 12, but with $\zeta^2 = \omega^2 \mu_0 \epsilon_0 (1 - \epsilon_r) + j\omega \mu_0 \sigma B - 1/x_0^2$. The integrands have poles at the zeros of $\sinh(\zeta h)$ which are now at $\omega = j\omega_m^\pm = jB(2t'_r)^{-1} \times \left(1 \pm \sqrt{1 - 4t'_r(m^2 \pi^2 - h^2/x_0^2)/(B^2 t_d)} \right)$, $m=0,1,2,\dots$, but no branch points. By deforming the integration path, one gets the following representations for the field and current densities.

$$\begin{aligned}
 H_z &= \frac{2V_0}{hZ_0 B} e^{-\frac{x}{x_0}} \sum_{m=0}^{\infty} \frac{(-1)^m \cos(m\pi y/h) U(\tau - t'_{ty})}{(1 + \delta_{m0}) \sqrt{1 - 4t'_r(m^2 \pi^2 - h^2/x_0^2)/(B^2 t_d)}} \times \\
 &\quad \times \left[e^{-\omega_m^- \tau} \left(1 - \frac{\epsilon_r}{\epsilon_r - 1} \omega_m^- t'_r \right) - e^{-\omega_m^+ \tau} \left(1 - \frac{\epsilon_r}{\epsilon_r - 1} \omega_m^+ t'_r \right) \right] \\
 (\sigma + \epsilon \frac{\partial}{\partial t}) E_x &= \frac{-2V_0}{h^2 Z_0 B} e^{-\frac{x}{x_0}} \sum_{m=1}^{\infty} \frac{(-1)^m m\pi \sin(m\pi y/h) U(\tau - t'_{ty})}{\sqrt{1 - 4t'_r(m^2 \pi^2 - h^2/x_0^2)/(B^2 t_d)}} \times \\
 &\quad \times \left[e^{-\omega_m^- \tau} \left(1 - \frac{\epsilon_r}{\epsilon_r - 1} \omega_m^- t'_r \right) - e^{-\omega_m^+ \tau} \left(1 - \frac{\epsilon_r}{\epsilon_r - 1} \omega_m^+ t'_r \right) \right] \\
 (\sigma + \epsilon \frac{\partial}{\partial t}) E_y &= \frac{-2V_0}{h^2 Z_0 B} e^{-\frac{x}{x_0}} \sum_{m=0}^{\infty} \frac{(-1)^m \cos(m\pi y/h) U(\tau - t'_{ty})}{(1 + \delta_{m0}) \sqrt{1 - 4t'_r(m^2 \pi^2 - h^2/x_0^2)/(B^2 t_d)}} \times \\
 &\quad \times \left[e^{-\omega_m^- \tau} \left(\omega_m^- t_t - \frac{h}{x_0} \right) \left(1 - \frac{\epsilon_r}{\epsilon_r - 1} \omega_m^- t'_r \right) - e^{-\omega_m^+ \tau} \left(\omega_m^+ t_t - \frac{h}{x_0} \right) \left(1 - \frac{\epsilon_r}{\epsilon_r - 1} \omega_m^+ t'_r \right) \right]
 \end{aligned} \tag{15}$$

where $t_t = h/c$, and $t'_{ty} = (h-y)\sqrt{\epsilon_r - 1}/c$.

As in Equation 8, the infinite responses (i.e., δ -functions) at $\tau = t'_{ty}$ in Equation 15 are not included. Equation 15 reduces to Equation 13 when $\epsilon_r \rightarrow 1$, as expected. From Equation 15, one observes that only a couple of terms with smaller $\text{Re}(\omega_m^\pm)$'s are required for good approximations to the field quantities when $\tau \gg 2t'_r, t'_d$. But, when $\tau \leq 2t'_r$, the series representation of Equation 15 does not converge at all and one has to seek for alternative representations.

An alternative representation can be obtained by expressing the hyperbolic functions in Equation 12 in terms of exponential functions, using the Taylor expansions and then applying the techniques used to get Equation 8. The results are given as follows (for $\tau > t'_{ty}$, of course):

$$\begin{aligned}
 H_z &= \frac{V_o}{hZ_o} \left(\frac{t_d}{t'_r} \right)^{1/2} e^{-\frac{x}{x_o}} e^{-\frac{B\tau}{2t'_r}} \sum_{n=-\infty}^{\infty} U(\tau_{yn}^2) \times \\
 &\times \left\{ \left[1 - \frac{\epsilon_r B}{2(\epsilon_r - 1)} \right] I_o(AA) + \frac{\epsilon_r B}{2(\epsilon_r - 1)} \sqrt{1 + \frac{4t'_r}{B^2 t_{dx_o}} \frac{\tau}{\tau_{yn}}} I_1(AA) \right\} \\
 (\sigma + \epsilon \frac{\partial}{\partial t}) E_x &= \frac{V_o}{h^2 Z_o} \left(\frac{t_d}{t'_r} \right)^{1/2} \frac{B}{4(\epsilon_r - 1)} \sqrt{1 + \frac{4t'_r}{B^2 t_{dx_o}}} e^{-\frac{x}{x_o}} e^{-\frac{B\tau}{2t'_r}} \sum_{n=-\infty}^{\infty} U(\tau_{yn}^2) \times \\
 &\times \frac{t_d(2n+1-y/h)}{\tau_{yn}} \left\{ \left[(2-B)\epsilon_r - 2 \right] I_1(AA) + \frac{\epsilon_r B\tau}{\tau_{yn}} \sqrt{1 + \frac{4t'_r}{B^2 t_{dx_o}}} I_2(AA) \right\} \\
 (\sigma + \epsilon \frac{\partial}{\partial t}) E_y &= \frac{H_z}{x_o} - \frac{V_o}{h^2 Z_o} \frac{t_d}{t'_r} \frac{\epsilon_r B}{4(\epsilon_r - 1)^{3/2}} e^{-\frac{x}{x_o}} e^{-\frac{B\tau}{2t'_r}} \sum_{n=-\infty}^{\infty} U(\tau_{yn}^2) \times \\
 &\times \left\{ \left[\frac{(2-B)\epsilon_r - 2}{\epsilon_r} - \frac{B}{2} \left(1 + \frac{4t'_r}{B^2 t_{dx_o}} \right) \right] I_o(AA) \right\}
 \end{aligned}$$

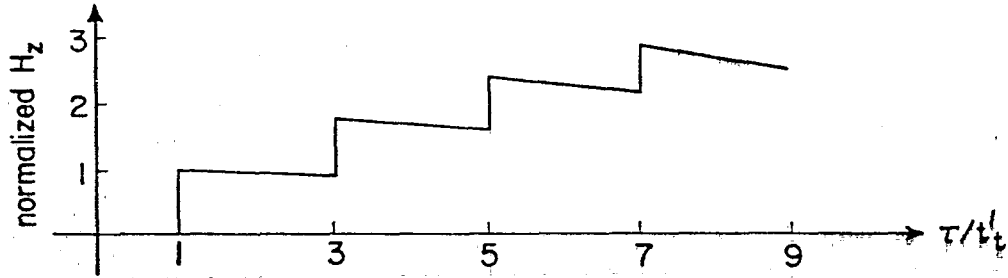
$$\begin{aligned}
& + \frac{(2B-2)\epsilon_r + 2}{\epsilon_r} \sqrt{1 + \frac{4t'_r}{B^2 t_{dx_0}}} \frac{\tau}{\tau_{yn}} I_1(AA) \\
& - \frac{B}{2} \left(1 + \frac{4t'_r}{B^2 t_{dx_0}} \right) \frac{2\tau^2 - \tau_{yn}^2}{\tau_{yn}^2} I_2(AA) \left. \right\} \quad (16)
\end{aligned}$$

where $AA = B\tau_{yn} \sqrt{1 + 4t'_r/(B^2 t_{dx_0})} / (2t'_r)$, $\tau_{yn} = (\tau^2 - t_{ty}'(n)^2)^{1/2}$ and $t_{ty}'(n) = \sqrt{(2n+1)h-y}^2 (\epsilon_r - 1) / c$. From the above equation, one can see that the smaller τ is, the fewer terms are required for the calculations. In Equation 16, the infinite responses at $\tau = t_{ty}'(n)$ (i.e., $\delta(\tau - t_{ty}'(n))$, etc.) are not shown.

To derive Equations 15 and 16, it has been assumed that $R > 2$ (i.e., $B > 0$). The results for the situation with $2 \geq R \geq 0$ are different. However, for most of the practical situations, $R \gg 2$ and the approximations $B \approx 1$, $1 + 4t'_r/(B^2 t_{dx_0}) \approx 1$ can always be made to simplify Equations 15 and 16.

In the series representation of Equation 16, one can see that every term (i.e., with a specific n) is exactly the same as Equation 8, if $t_{ty}'(n)$ is replaced by t'_t . That is, in addition to the diffusion and Cerenkov processes, the field and current density distributions are determined by the bounces between $y=0$ and $y=h$ planes. And, the field and current density distributions of the present case can be easily constructed from the solutions represented by Equation 8. One set of example curves given for $t'_t/t'_r = 0.2$, $\epsilon_r = 10$ and $y=0$ is presented in Figure 13. The t'_t/t'_r value given for this example is relatively small. Thus, as can be seen from Figure 13, one needs several bounces to reach the late-time behaviors of $H_z/H_o \rightarrow 1$, $(\sigma + \epsilon \frac{\partial}{\partial t}) E_x / J_o \rightarrow 0$, $(\sigma + \epsilon \frac{\partial}{\partial t}) E_y / J_o \rightarrow 0$ which can be implied from Equation 15 when $\tau \gg t'_r, t'_d$. However, when t'_t/t'_r is large, one does not need many bounces to reach those late-time values.

(a)



(b)

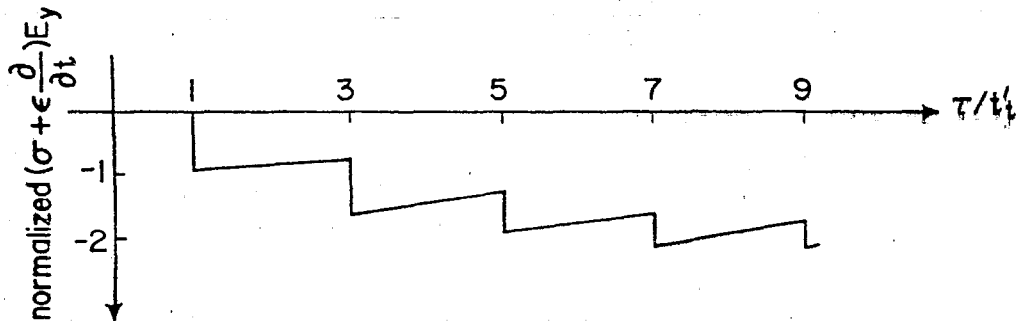


Figure 13. (a) $9(t'_r/t'_t)H_z/(8H_0)$, (b) $18(t'_r/t'_d) \left(\sigma + \epsilon \frac{\partial}{\partial t} \right) E_y/J_0$ at $y=0$ as functions of τ/t'_t for $x_0/h \geq 200$, $\epsilon_r = 10$ and $t'_t/t'_r = 0.2$, for the simulator with $\sigma_2 \rightarrow \infty$, $\sigma_1 = \sigma$, $\epsilon_1 = \epsilon = \epsilon_r \epsilon_0$, $E_x^e = V_0 \delta(ct-x) \exp(-x/x_0)$. Here $H_0 = hJ_0 = V_0 (hZ_0)^{-1} \exp(-x/x_0)$, $Z_0 = (\mu_0/\epsilon_0)^{1/2}$, $t_d = \mu_0 \sigma h^2$, $t'_t = h\sqrt{\epsilon_r - 1}/c$, $t'_r = \epsilon_0(\epsilon_r - 1)/\sigma$, $t'_t/t'_r = t_d/t'_t = (t_d/t'_r)^{1/2}$, $\tau = t - x/c$.

IV. UNIT-STEP SOURCE FIELD

In the last section, the field and current density distributions for two special simulator geometries with a δ -function source field $E_x^e = V_0 \delta(ct - x) \times \exp(-x/x_0)$ have been obtained. In this section, the corresponding distributions for the same special simulator geometries, but with a unit-step source field $E_x^e = E_0 U(t - x/c) \exp(-x/x_0)$, will be sought.

For the simulator with a unit-step source field, one finds that the (ω, k) -domain solutions are still given by Equations 5 and 6, except that \tilde{E}_x^e has a new value $E_0 \delta(k - \omega/c + j/x_0)/(j\omega)$. The (t, x) -domain solutions can then be calculated from the inverse Fourier-transform integrals, the second equation of Equation 1. Due to the presence of the term $\delta(k - \omega/c + j/x_0)$, the k -integral can be easily performed. To calculate the remaining ω -integrals, one can either deform the integration paths as was done in Section III or compute convolution integrals of the form

$$\int_{-\infty}^{\infty} F_1(\tau') U(\tau - \tau') d\tau'$$

where F_1 is the solution with a δ -function source field.

From Section III, it is observed that for the situations of practical interest the approximations $R = \mu_0 \sigma c x_0 \rightarrow \infty$, $B = 1 - 2/R \rightarrow 1$ and $\tau/t_{dx_0} \rightarrow 0$ can always be used. That is, the field and current density distributions in a simulator with a source field containing the factor $\exp(-x/x_0)$ can be approximated with $\exp(-x/x_0)$ times the distributions derived for a source field which does not contain this factor (i.e., $x_0 \rightarrow \infty$). This argument will now be applied throughout this section to simplify the calculations. The approximated solutions are presented as follows.

$$A. \quad \sigma_1 = \sigma_2 = \sigma, \quad \epsilon_1 = \epsilon_2 = \epsilon, \quad E_x^e = E_0 U(t - x/c) \exp(-x/x_0), \quad y \leq h$$

The two cases will be considered depending on whether or not ϵ equals to ϵ_0 .

$$(1) \quad \epsilon = \epsilon_0$$

For this case, the following expressions for the field and current density distributions at $y=0$ are obtained.

$$\begin{aligned}
 H_z &\approx \frac{E_0}{Z_0} \left\{ \left[\left(\frac{t_r}{\pi\tau} \right)^{\frac{1}{2}} + \left(\frac{4\tau}{\pi t_r} \right)^{\frac{1}{2}} \right] e^{-\frac{t_d}{4\tau}} \right. \\
 &\quad \left. - \left(\frac{t_d}{t_r} \right)^{\frac{1}{2}} \left[1 - \operatorname{erf} \left(\sqrt{\frac{t_d}{4\tau}} \right) \right] \right\} e^{-\frac{x}{x_0}} U(\tau) \\
 (\sigma + \epsilon_0 \frac{\partial}{\partial t}) E_x &\approx \frac{E_0}{hZ_0} \left\{ \frac{t_d}{2\tau} \left(\frac{t_r}{\pi\tau} \right)^{\frac{1}{2}} e^{-\frac{t_d}{4\tau}} \right. \\
 &\quad \left. + \left(\frac{t_d}{t_r} \right)^{\frac{1}{2}} \left[1 - \operatorname{erf} \left(\sqrt{\frac{t_d}{4\tau}} \right) \right] \right\} e^{-\frac{x}{x_0}} U(\tau) \\
 (\sigma + \epsilon_0 \frac{\partial}{\partial t}) E_y &\approx \frac{H_z}{x_0} + \frac{E_0}{hZ_0} \left(\frac{t_d}{\pi\tau} \right)^{\frac{1}{2}} e^{-\frac{t_d}{4\tau}} e^{-\frac{x}{x_0}} U(\tau) \times \\
 &\quad \times \left(1 - \frac{t_r}{2\tau} + \frac{t_r t_d}{4\tau^2} \right)
 \end{aligned} \tag{17}$$

where $\operatorname{erf}(z)$ is the error function defined as

$$\operatorname{erf}(z) = \frac{2}{\sqrt{\pi}} \int_0^z e^{-p^2} dp$$

The field and current density distributions at an arbitrary $y < h$ can be calculated by simply replacing h and t_d in Equation 17 with $(h-y)$ and t_{dy} .

Based on Equation 17, several curves are presented in Figures 14 - 16 for various t_r/t_d . At very early and late times (defined respectively by $\tau \ll t_d$ and $\tau \gg t_d$), Equation 17 can be simplified by using the asymptotic approximations for the error function and retaining only one or two terms in the equation. From the simplified equation and the curves in Figures 14 - 16, one can summarize the behaviors of the field and current densities in Table 6.

$$(2) \quad \epsilon/\epsilon_0 = \epsilon_r > 1$$

In section III, it was mentioned that some δ -function responses have to be added to Equation 8 to obtain complete solutions for this simulator geometry with a δ -function source field. These δ -function responses are now given as below.

$$H_z : \quad \frac{V_0}{c} \frac{\epsilon_r}{Z_0 \sqrt{\epsilon_r - 1}} e^{-\frac{t'_t}{2t'_r}} \delta(\tau - t'_t)$$

$$\left(\sigma + \epsilon \frac{\partial}{\partial t}\right) E_x : \quad \frac{V_0}{c} e^{-\frac{t'_t}{2t'_r}} \left[\sigma \delta(\tau - t'_t) + \epsilon_r \epsilon_0 \delta'(\tau - t'_t) \right] \quad (18)$$

$$\left(\sigma + \epsilon \frac{\partial}{\partial t}\right) E_y : \quad \frac{V_0}{c} \frac{1}{\sqrt{\epsilon_r - 1}} e^{-\frac{t'_t}{2t'_r}} \left[\sigma \delta(\tau - t'_t) + \epsilon_r \epsilon_0 \delta'(\tau - t'_t) \right]$$

By using the combination of Equations 8 and 18 for F_1 in the convolution integrals, the following expressions for the field and current density distributions at $y=0$ are obtained:

$$H_z \approx \frac{E_0}{Z_0} \frac{\epsilon_r}{\sqrt{\epsilon_r - 1}} e^{-\frac{x}{x_0}} U(\tau - t'_t) \times \left\{ e^{-\frac{\tau}{2t'_r}} I_0 \left[\frac{1}{2t'_r} \sqrt{\tau^2 - t'^2_2} \right] + \right.$$

$$\left. + \frac{(\epsilon_r - 1)}{\epsilon_r t'_r} \int_{t'_t}^{\tau} e^{-\frac{\tau'}{2t'_r}} I_0 \left[\frac{1}{2t'_r} \sqrt{\tau'^2 - t'^2_2} \right] d\tau' \right\}$$

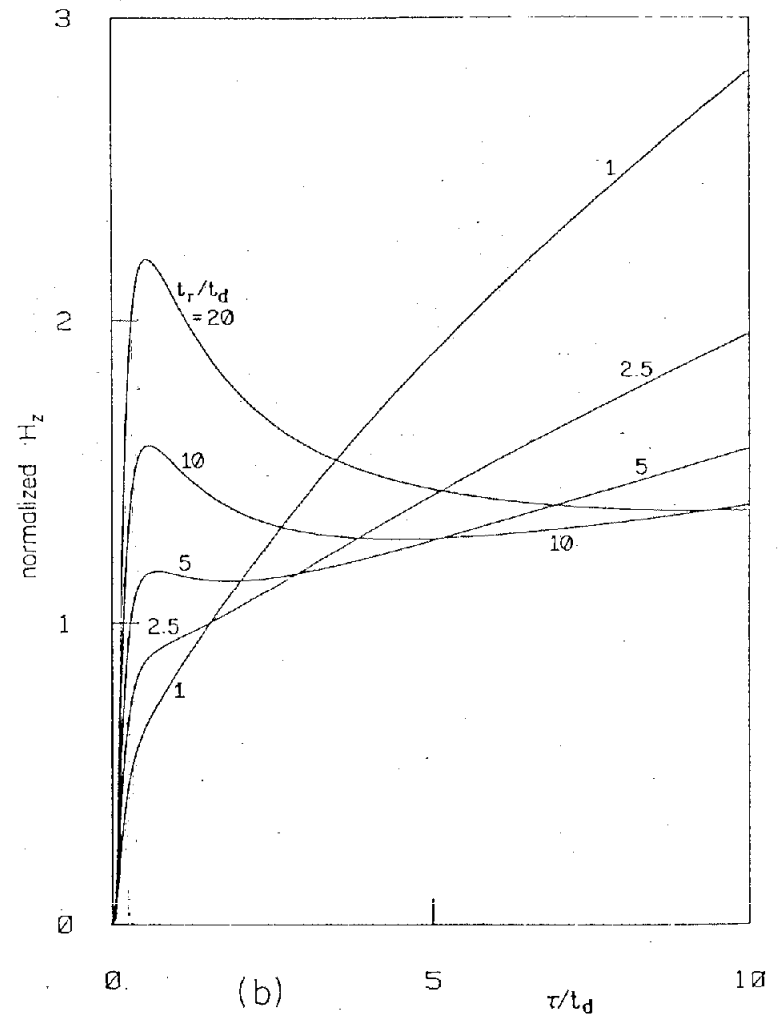
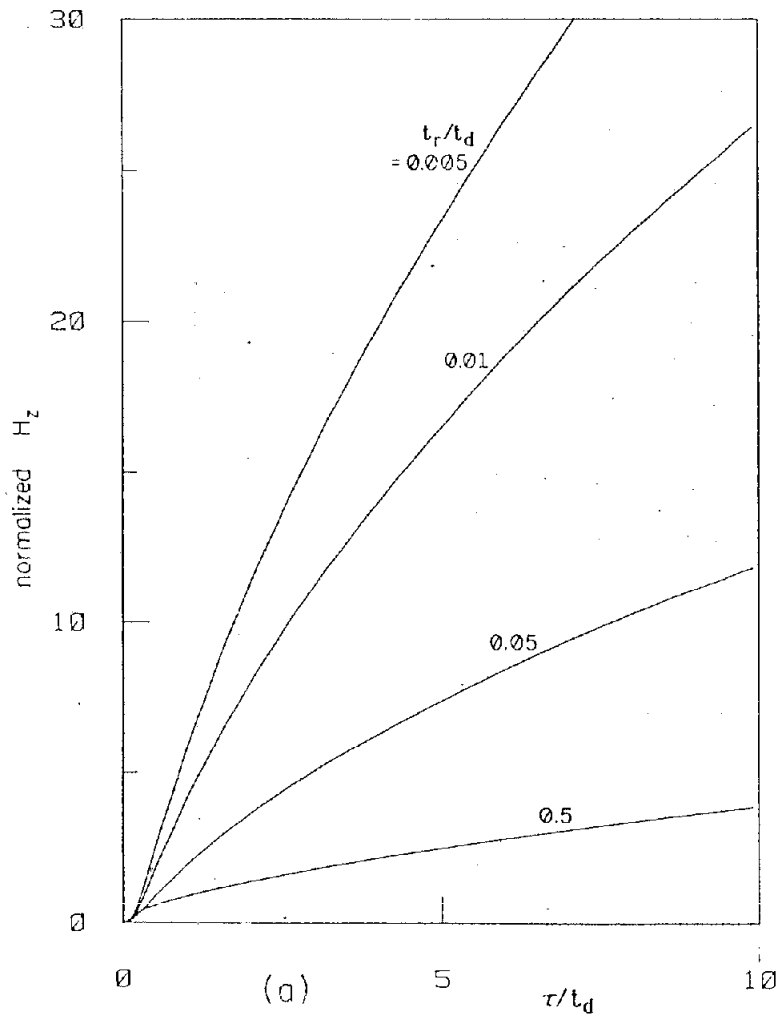


Figure 14. H_z/H'_0 at $y=0$ as a function of τ/t_d for $x_0/h \geq 200$ and various t_r/t_d , for the simulator with $\sigma_1 = \sigma_2 = \sigma$, $\epsilon_1 = \epsilon_2 = \epsilon_0$, $E_x^e = E_0 \exp(-x/x_0)U(t-x/c)$. Here, $H'_0 = E_0 \exp(-x/x_0)Z_0^{-1}$, $Z_0 = (\mu_0/\epsilon_0)^{1/2}$, $t_r = \epsilon_0/\sigma$, $t_d = \mu_0 ch^2$, $\tau = t-x/c$.

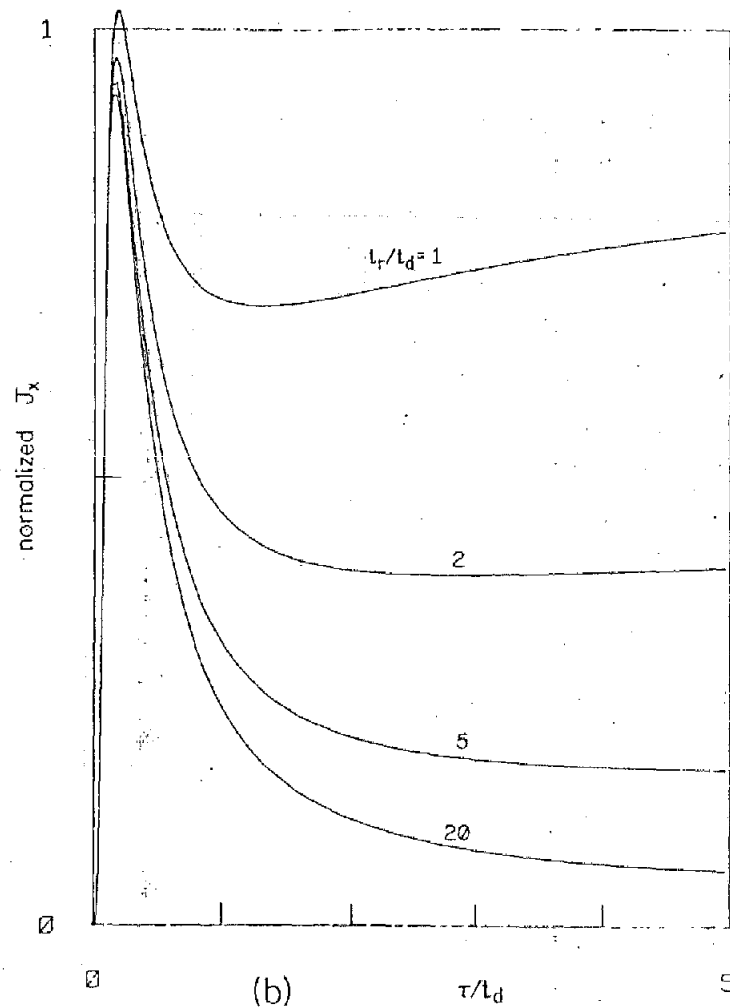
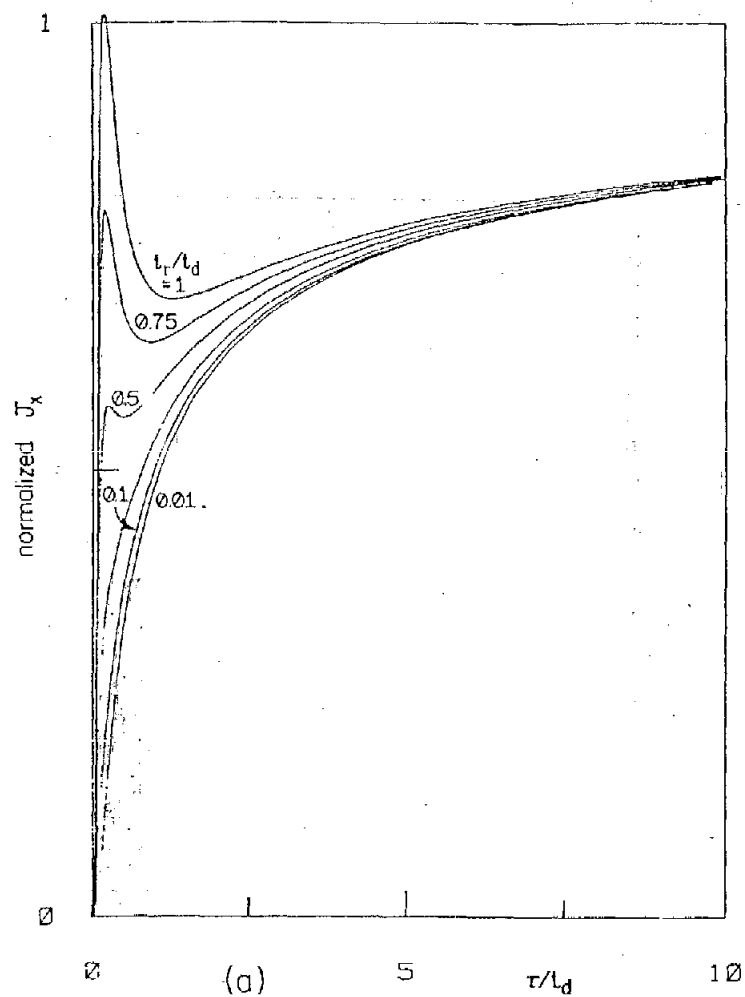


Figure 15. (a) $(t_r/t_d)^{1/2} J_x/J'_0$, (b) $(t_d/t_r)^{1/2} J_x/J'_0$ at $y=0$ as functions of τ/t_d for $x_0/h \geq 200$ and various t_r/t_d , for the simulator with $\sigma_1 = \sigma_2 = \sigma$, $\epsilon_1 = \epsilon_2 = \epsilon_0$, $E_x^e = E_0 \exp(-x/x_0) U(t-x/c)$. Here, $J_x = (\sigma + \epsilon_0 \frac{\partial}{\partial t}) E_x$, $J'_0 = E_0 (hZ_0)^{-1} \exp(-x/x_0)$, $Z_0 = (\mu_0/\epsilon_0)^{1/2}$, $t_r = \epsilon_0/\sigma$, $t_d = \mu_0 \sigma h^2$, $\tau = t - x/c$.

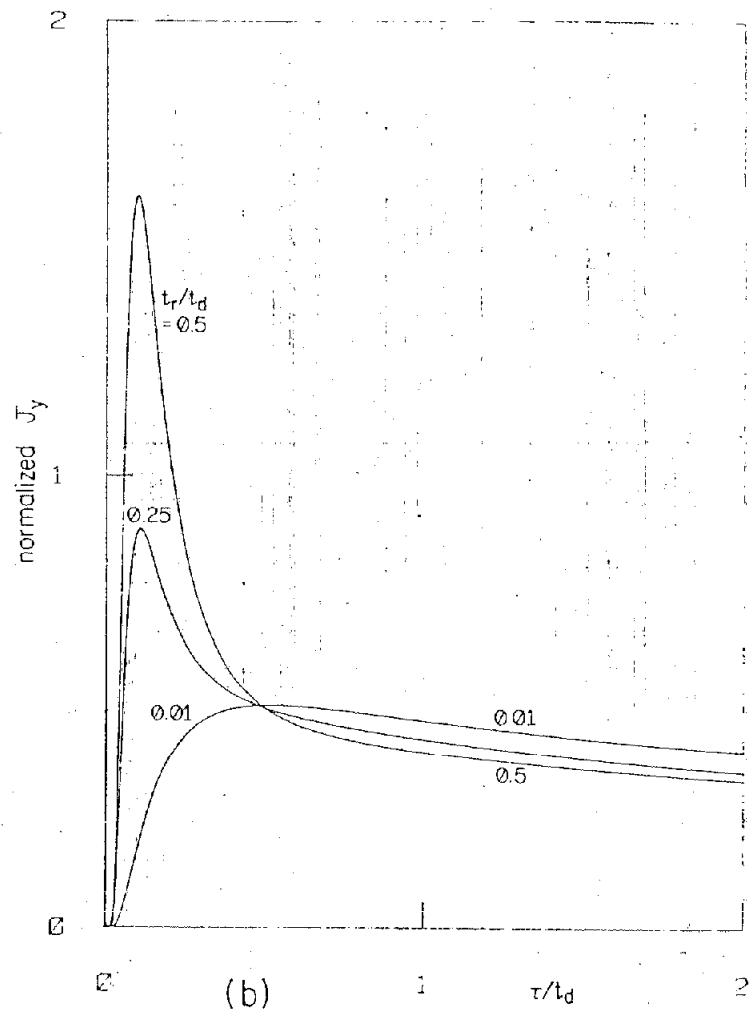
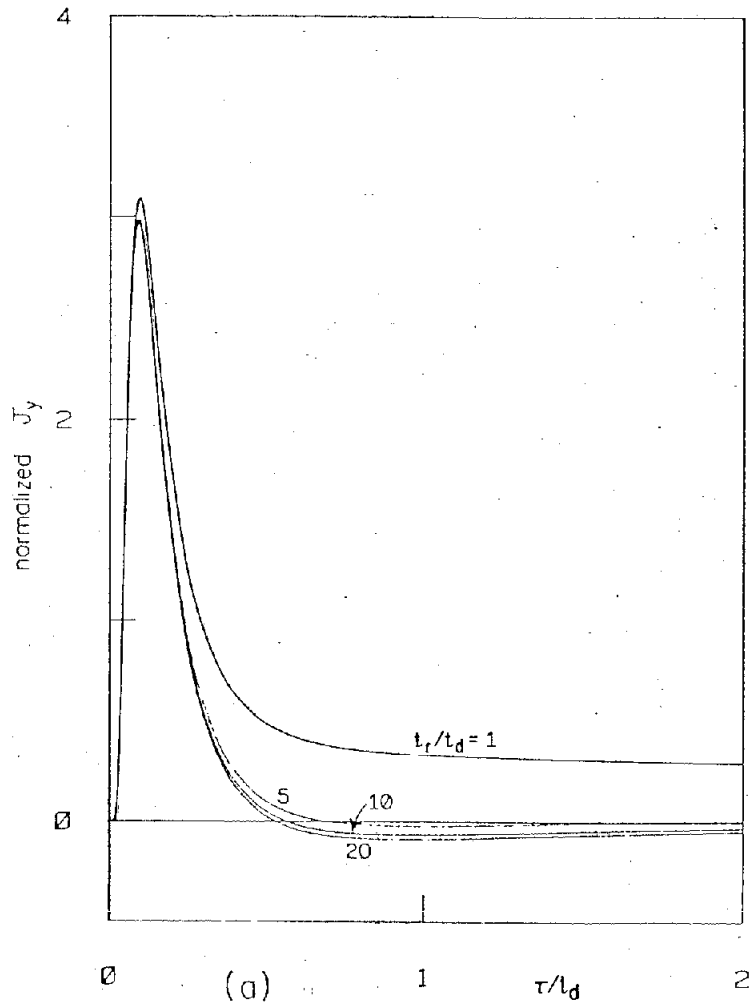


Figure 16. (a) $(t_d/t_r)J_y/J'_0$, (b) J_y/J'_0 at $y=0$ as functions of τ/t_d for $x_0/h \geq 200$ and various t_r/t_d , for the simulator with $\sigma_1 = \sigma_2 = \sigma$, $\epsilon_1 = \epsilon_2 = \epsilon_0$, $E_x^e = E_0 \exp(-x/x_0)U(t-x/c)$. Here, $J_y = (\sigma + \epsilon_0 \frac{\partial}{\partial t})E_y$, $J'_0 = E_0 (hZ_0)^{-1} \exp(-x/x_0)$, $Z_0 = (\mu_0/\epsilon_0)^{1/2}$, $t_r = \epsilon_0/\sigma$, $t_d = \mu_0 \sigma h^2$, $\tau = t - x/c$.

TABLE 6. FIELD AND CURRENT DENSITY FOR UNIT-STEP SOURCE FIELD AT $y=0$ FOR
 $\sigma_1 = \sigma_2 = \sigma$, $\epsilon_1 = \epsilon_2 = \epsilon_0$, $x_0 \geq 200$ m, $\sigma \geq 3 \times 10^{-4}$ mho/m AND $x_0/h \geq 200$ [†]

Quantity	First Maximum*		First Minimum*		Late Time Value $t_{dx_0} > \tau \gg t_r, t_d$	Condition
	τ	Value	τ	Value		
$\frac{H_z}{H'_0}$	$t_d \geq \tau \geq \frac{t_d}{2}$	$0.5 \left(\frac{t_r}{t_d} \right)^{\frac{1}{2}}$	$0.5 t_r$	Less than 1.5	$\left(\frac{4\tau}{\pi t_r} \right)^{\frac{1}{2}}$	$t_r/t_d \geq 4$
	Monotonically increasing					
$\frac{(\sigma + \epsilon_0 \frac{\partial}{\partial t}) E_x}{J'_0}$	$\frac{t_d}{3} \geq \tau \geq \frac{t_d}{6}$	$\left(\frac{t_r}{t_d} \right)^{\frac{1}{2}}$	$1.5 t_r$	$(t_d/t_r)^{\frac{1}{2}} > \text{value}$ $> 0.5(t_d/t_r)^{\frac{1}{2}}$	$\left(\frac{t_d}{t_r} \right)^{\frac{1}{2}}$	$t_r/t_d \geq \frac{4}{9}$
	Monotonically increasing					
$\frac{(\sigma + \epsilon_0 \frac{\partial}{\partial t}) E_y}{J'_0}$ **	$0.09 t_d$	$3 t_r/t_d$	Fall to 1/e of the maximum at $\tau \sim 0.5 t_d$		0	$t_r/t_d \geq 0.5$
	$0.5 t_d$	0.5	Fall to 1/(2e) at $\tau \sim 9.5 t_d$			$t_r/t_d \leq 0.01$

[†] $t_d = \mu_0 \sigma h^2$, $t_r = \epsilon_0 / \sigma$, $H'_0 = E_0 \exp(-x/x_0) Z_0^{-1}$, $J'_0 = h^{-1} H'_0$, $t_{dx_0} = \mu_0 \sigma x_0^2$

* See Figures 14 - 16, referred to the local maximum and minimum.

** For $0.5 > t_r/t_d > 0.01$, the behaviors are between the tabulated extreme situations.

$$\begin{aligned}
\left(\sigma + \varepsilon \frac{\partial}{\partial t}\right) E_x &\approx E_0 e^{-\frac{x}{x_0}} e^{-\frac{t'_t}{2t'_r}} \left[\varepsilon_r \varepsilon_0 \delta(\tau - t'_t) + \sigma U(\tau - t'_t) \right] \\
&+ \frac{E_0}{2hZ_0} \frac{\varepsilon_r}{\sqrt{\varepsilon_r - 1}} e^{-\frac{x}{x_0}} U(\tau - t'_t) \times \left\{ \frac{t_d}{\sqrt{\tau^2 - t'_t{}^2}} e^{-\frac{\tau}{2t'_r}} I_1 \left[\frac{1}{2t'_r} \sqrt{\tau^2 - t'_t{}^2} \right] + \right. \\
&\left. + \frac{\varepsilon_r - 1}{\varepsilon_r t'_r} \int_{t'_t}^{\tau} \frac{t_d}{\sqrt{\tau'^2 - t'_t{}^2}} e^{-\frac{\tau'}{2t'_r}} I_1 \left[\frac{1}{2t'_r} \sqrt{\tau'^2 - t'_t{}^2} \right] d\tau' \right\}
\end{aligned} \tag{19}$$

$$\begin{aligned}
\left(\sigma + \varepsilon \frac{\partial}{\partial t}\right) E_y &\approx \frac{H_z}{x_0} + \frac{E_0}{2hZ_0} \left(\frac{t_d}{t'_r}\right)^{\frac{1}{2}} \frac{(\varepsilon_r - 2)}{(\varepsilon_r - 1)} e^{-\frac{x}{x_0}} e^{-\frac{\tau}{2t'_r}} U(\tau - t'_t) \times \\
&\times \left\{ I_0 \left[\frac{1}{2t'_r} \sqrt{\tau^2 - t'_t{}^2} \right] + \frac{\varepsilon_r}{\varepsilon_r - 2} \frac{\tau}{\sqrt{\tau^2 - t'_t{}^2}} I_1 \left[\frac{1}{2t'_r} \sqrt{\tau^2 - t'_t{}^2} \right] \right\} \\
&+ \frac{E_0}{\sqrt{\varepsilon_r - 1}} \varepsilon_r \varepsilon_0 e^{-\frac{t'_t}{2t'_r}} \delta(\tau - t'_t)
\end{aligned}$$

The results at an arbitrary $y < h$ can be calculated by replacing h , t_d and t'_t in Equation 19 with $(h - y)$, t_{dy} and $t'_t(1 - y/h)$, respectively.

Equation 19 involves integrals of Bessel's functions which in principle can be evaluated by numerical integrations. However, instead of going through this complicated, time-consuming process, only the asymptotic approximations of Equation 19 at early and late times will be analyzed, from which together with the results for the δ -function source field case (see Table 3 and Figures 5 - 7), the approximate behaviors of the field and current density distributions are summarized in Table 7.

TABLE 7. FIELD AND CURRENT DENSITY FOR UNIT-STEP SOURCE FIELD FOR $\sigma_1 = \sigma_2 = \sigma$, $\epsilon_1 = \epsilon_2 = \epsilon = \epsilon_r \epsilon_0$,
 $40 \geq \epsilon_r \geq 10$, $\sigma \geq 3 \times 10^{-4}$ mho/m, $x_0 \geq 200$ m AND $x_0/h \geq 200$ [†]

Quantity	Initial Value at $\tau = t'_t$	Late Time Value for $t_{dx_0} > \tau \gg t'_r, t'_t, t'_d$	Approximate Behavior Between t'_t and the Late Time.
$\frac{H_z}{H'_0}$	$\sqrt{\epsilon_r} e^{-\frac{t'_t}{2t'_r}}$	$\left(\frac{4\tau}{\pi t'_r}\right)^{1/2}$	Monotonically increasing
$\frac{(\sigma + \epsilon \frac{\partial}{\partial t}) E_x}{J'_0}$	$\left(\frac{t'_d}{t'_r}\right)^{1/2} \left[1 + \frac{1}{8} \left(\frac{t'_d}{t'_r}\right)^{1/2} \right] e^{-t'_t/(2t'_r)}$	$\left(\frac{t'_d}{t'_r}\right)^{1/2}$	Monotonically increasing, reach $\sim (t'_d/t'_r)^{1/2}$ at approximately tens of t'_r or tens of t'_t , whichever is larger
$\frac{(\sigma + \epsilon \frac{\partial}{\partial t}) E_y}{J'_0}$	$\frac{1}{2} \left(\frac{t'_d}{t'_r}\right)^{1/2} \left(1 + \frac{t'_t}{4t'_r} \right) e^{-t'_t/(2t'_r)}$	0	Same as that of H_z/H'_0 of Table 3 (i.e., results due to a δ -function source field)

[†] $t'_r = \epsilon_0/\sigma$, $t'_t = \epsilon_0(\epsilon_r - 1)/\sigma$, $t'_d = \mu_0 \sigma h^2$, $t'^2_t = h^2(\epsilon_r)/c^2 = t'_d t'_r$, $H'_0 = hJ'_0 = E_0 Z_0^{-1} \exp(-x/x_0)$.

And the δ -function responses at t'_t are excluded. $t_{dx_0} = \mu_0 \sigma x_0^2$.

B. $\sigma_2 \rightarrow \infty$, $\sigma_1 = \sigma$, $\epsilon_1 = \epsilon$, $E_x^e = E_0 U(t - x/c) \exp(-x/x_0)$, $0 \leq y < h$

Two cases depending on whether or not ϵ equals ϵ_0 will be considered.

(1) $\epsilon = \epsilon_0$

Two different series representations are obtained for the field and current density distributions. The one to be used for late times ($t_{dx_0} > \tau > t_d$) is given by (for $y \neq h$)

$$\begin{aligned}
 H_z &\approx \frac{E_0}{Z_0} \left(\frac{t_r}{t_d} \right)^{\frac{1}{2}} e^{-\frac{x}{x_0}} U(\tau) \left\{ \frac{\tau}{t_r} - \frac{t_d}{6t_r} \left(1 - \frac{3y^2}{h^2} \right) + 1 + \right. \\
 &\quad \left. + 2 \sum_{m=1}^{\infty} (-1)^m \cos \left(\frac{m\pi y}{h} \right) e^{-\frac{m^2 \pi^2 \tau}{t_d}} \left(1 - \frac{t_d}{m^2 \pi^2 t_r} \right) \right\} \\
 \left(\sigma + \epsilon_0 \frac{\partial}{\partial t} \right) E_x &\approx \frac{E_0}{hZ_0} \left(\frac{t_r}{t_d} \right)^{\frac{1}{2}} e^{-\frac{x}{x_0}} U(\tau) \left\{ \frac{t_d y}{t_r h} - \right. \\
 &\quad \left. - 2 \sum_{m=1}^{\infty} (-1)^m m\pi \sin \left(\frac{m\pi y}{h} \right) e^{-\frac{m^2 \pi^2 \tau}{t_d}} \left(1 - \frac{t_d}{m^2 \pi^2 t_r} \right) \right\} \quad (20) \\
 \left(\sigma + \epsilon_0 \frac{\partial}{\partial t} \right) E_y &\approx \frac{H_z}{x_0} + \frac{2E_0}{hZ_0} e^{-\frac{x}{x_0}} U(\tau) \sum_{m=0}^{\infty} \frac{(-1)^m \cos(m\pi y/h)}{1 + \delta_{m0}} \times \\
 &\quad \times \left(1 - \frac{m^2 \pi^2 t_r}{t_d} \right) e^{-\frac{m^2 \pi^2 \tau}{t_d}}
 \end{aligned}$$

The representation appropriate for early times ($\tau \ll t_d$) is given by

$$H_z \approx \frac{E_o}{Z_o} e^{-\frac{x}{x_o}} U(\tau) \sum_{n=-\infty}^{\infty} \left\{ \left[\left(\frac{t_r}{\pi\tau} \right)^{\frac{1}{2}} + \left(\frac{4\tau}{\pi t_r} \right)^{\frac{1}{2}} \right] e^{-\frac{t_{dy}^{(n)}}{4\tau}} - \left(\frac{t_{dy}^{(n)}}{t_r} \right)^{\frac{1}{2}} \left[1 - \operatorname{erf} \left(\sqrt{\frac{t_{dy}^{(n)}}{4\tau}} \right) \right] \right\}$$

$$\left(\sigma + \epsilon_o \frac{\partial}{\partial t} \right) E_x \approx \frac{E_o}{hZ_o} \left(\frac{t_d}{t_r} \right)^{\frac{1}{2}} e^{-\frac{x}{x_o}} U(\tau) \times \sum_{n=-\infty}^{\infty} (2n + 1 - y/h) \times \quad (21)$$

$$\times \left\{ \frac{t_r}{2\tau} \left(\frac{t_d}{\pi\tau} \right)^{\frac{1}{2}} e^{-\frac{t_{dy}^{(n)}}{4\tau}} + \left[1 - \operatorname{erf} \left(\sqrt{\frac{t_{dy}^{(n)}}{4\tau}} \right) \right] |2n + 1 - y/h|^{-1} \right\}$$

$$\left(\sigma + \epsilon_o \frac{\partial}{\partial t} \right) E_y \approx \frac{H_z}{x_o} + \frac{E_o}{hZ_o} \left(\frac{t_d}{\pi\tau} \right)^{\frac{1}{2}} e^{-\frac{x}{x_o}} U(\tau) \times \sum_{n=-\infty}^{\infty} \left(1 - \frac{t_r}{2\tau} + \frac{t_r t_{dy}^{(n)}}{4\tau^2} \right) e^{-\frac{t_{dy}^{(n)}}{4\tau}}$$

Based on Equations 20 and 21 several curves are presented in Figures 17-21, for $y=0, 0.5h$, and various t_r/t_d . At very early ($\tau \ll t_d$) and late ($\tau \gg t_d$) times, Equations 20 and 21 can be approximated with only one or two terms corresponding to small m 's and n 's. With this approximation and the curves in Figures 17-21, the analytical behaviors of the field and current densities can be obtained and are summarized in Table 8.

$$(2) \epsilon/\epsilon_o = \epsilon_r > 1$$

Two different series representations are obtained for the field and current density distributions. The one to be used for late times ($t_{dx_o} > \tau \gg t_r, t_d$) is given by (for $y \neq h$)

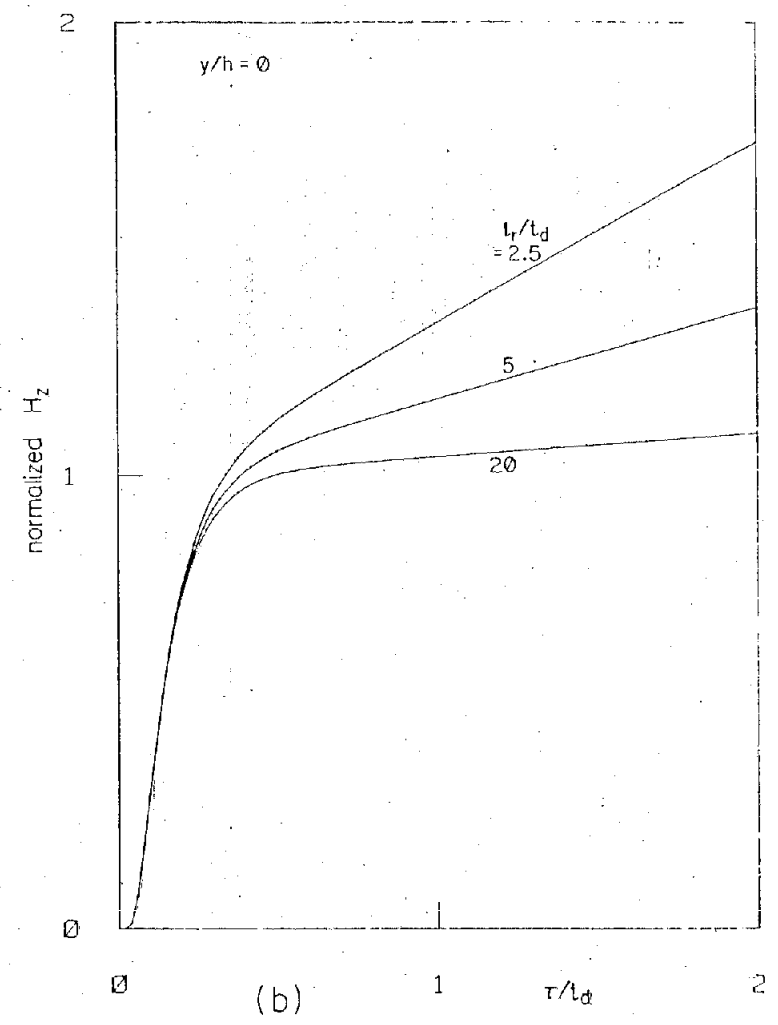
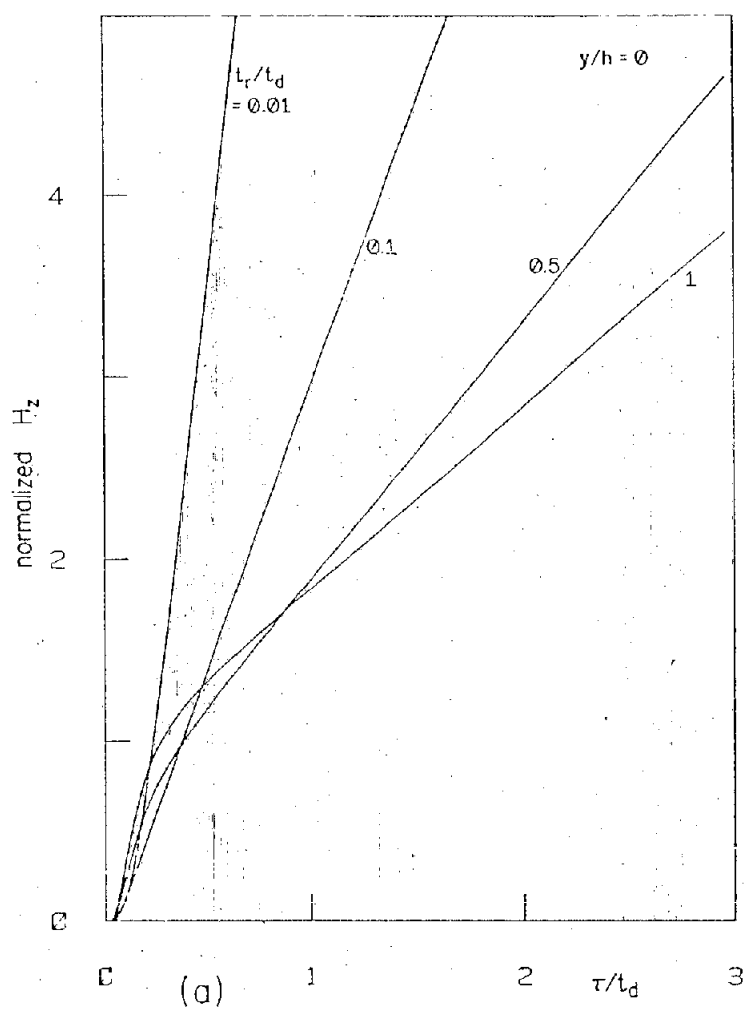


Figure 17. (a) H_z/H'_0 , (b) $(t_d/t_r)^{1/2} H_z/H'_0$ at $y=0$ as functions of τ/t_d for $x_0/h \geq 200$ and various t_r/t_d , for the simulator with $\sigma_2 \rightarrow \infty$, $\sigma_1 = \sigma$, $\epsilon_1 = \epsilon_0$, $E_x^e = E_0 \exp(-x/x_0) U(t-x/c)$. Here, $H'_0 = E_0 Z_0^{-1} \exp(-x/x_0)$, $Z_0 = (\mu_0/\epsilon_0)^{1/2}$, $t_r = \epsilon_0/\sigma$, $t_d = \mu_0 \sigma h^2$, $\tau = t-x/c$.

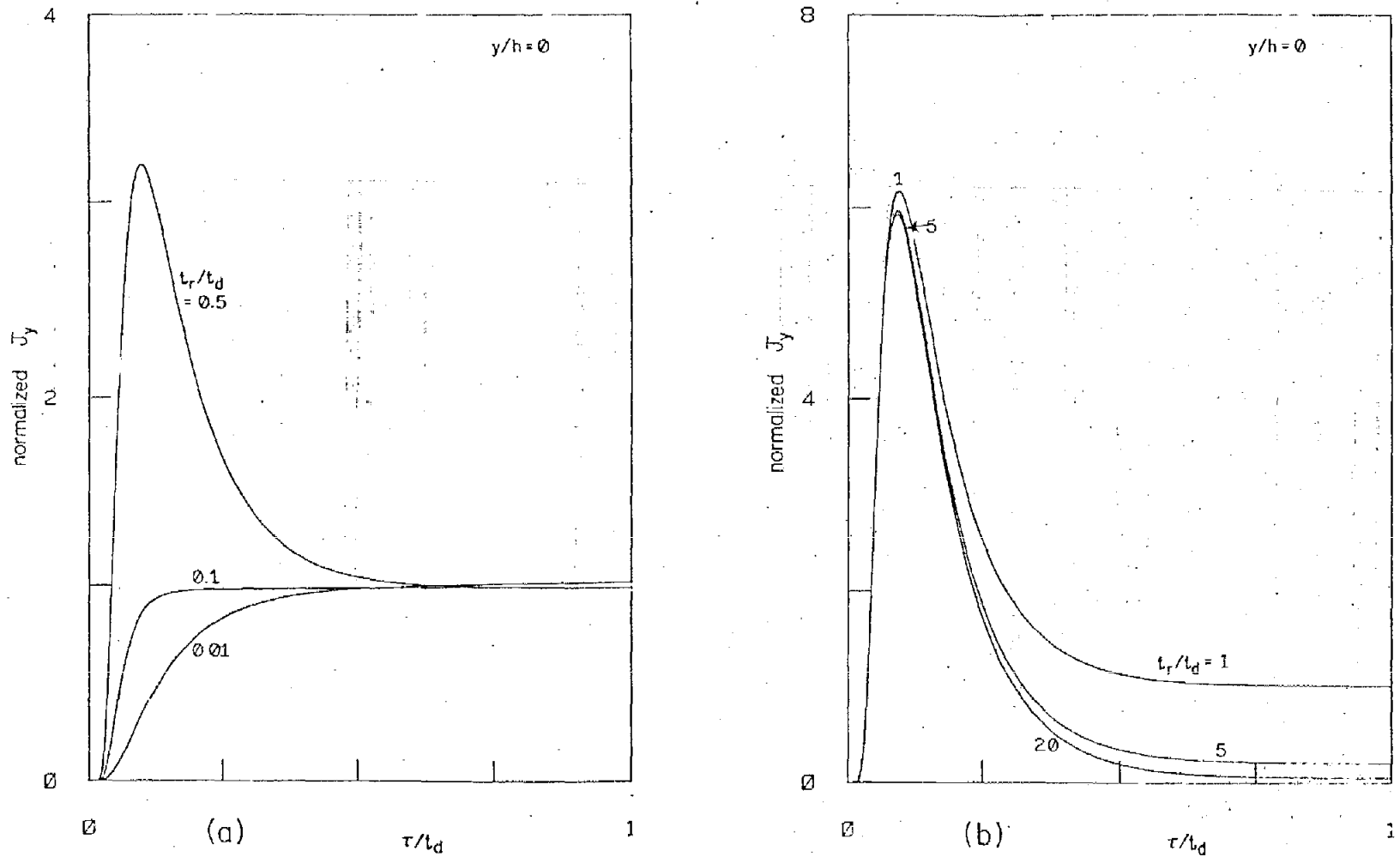


Figure 18. (a) J_y/J'_0 , (b) $(t_d/t_r)J_y/J'_0$ at $y=0$ as functions of τ/t_d for $x_0/h \geq 200$ and various t_r/t_d , for the simulator with $\sigma_2 \rightarrow \infty$, $\sigma_1 = \sigma$, $\epsilon_1 = \epsilon_0$, $E_x^e = E_0 \exp(-x/x_0)U(t-x/c)$. Here, $J_y = (\sigma + \epsilon_0 \frac{\partial}{\partial t})E_y$, $J'_0 = E_0(hZ_0)^{-1} \exp(-x/x_0)$, $Z_0 = (\mu_0/\epsilon_0)^{1/2}$, $t_r = \epsilon_0/\sigma$, $t_d = \mu_0 \sigma h^2$, $\tau = t - x/c$.

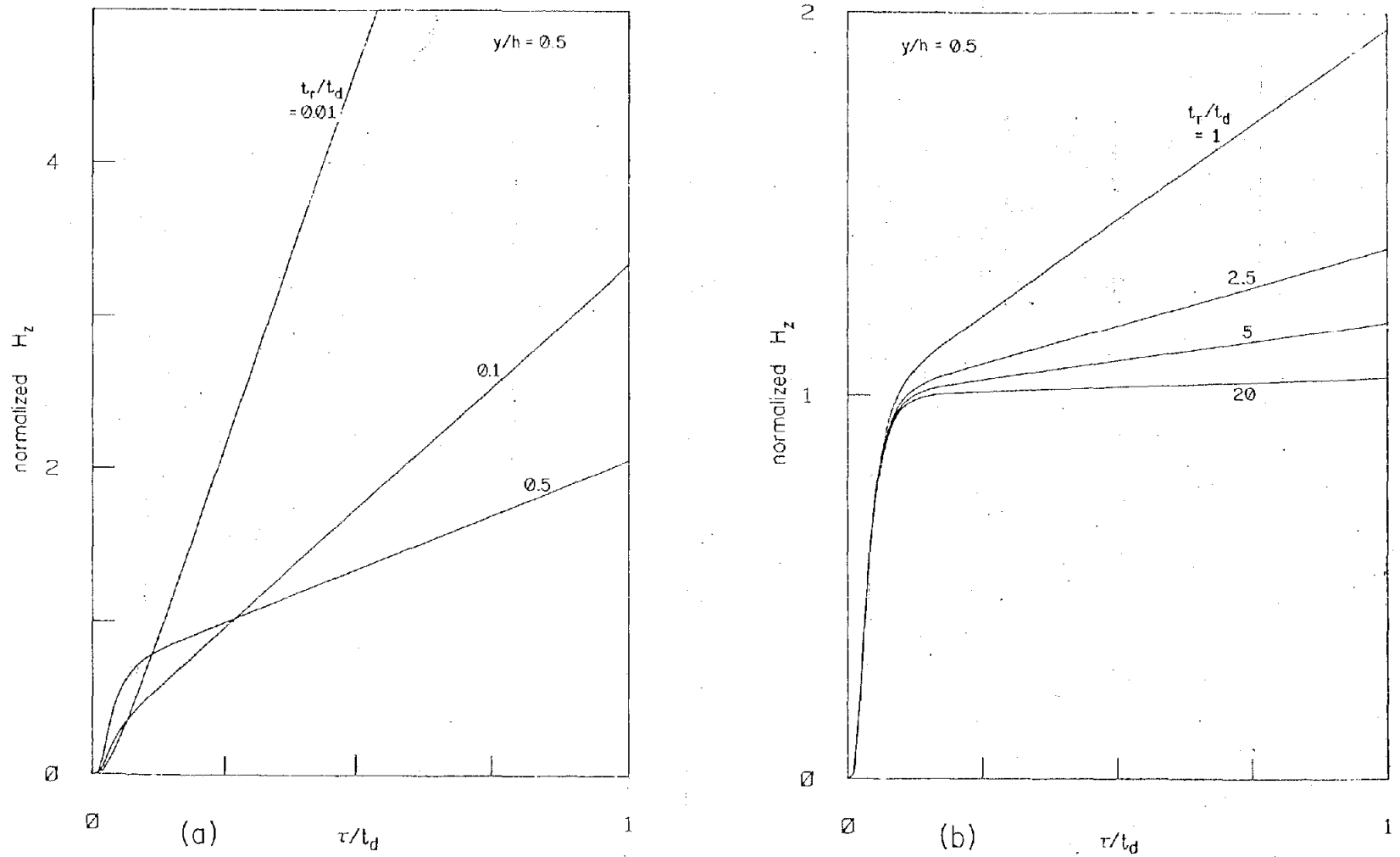


Figure 19. (a) H_z/H'_0 , (b) $(t_d/t_r)^{1/2} H_z/H'_0$ at $y/h = 0.5$ as functions of τ/t_d for $x_0/h \geq 200$ and various t_r/t_d , for the simulator with $\sigma_2 \rightarrow \infty$, $\sigma_1 = \sigma$, $\epsilon_1 = \epsilon_0$, $E_x^e = E_0 \exp(-x/x_0) U(t - x/c)$. Here, $H'_0 = E_0 Z_0^{-1} \times \exp(-x/x_0)$, $Z_0 = (\mu_0/\epsilon_0)^{1/2}$, $t_r = \epsilon_0/\sigma$, $t_d = \mu_0 \sigma h^2$, $\tau = t - x/c$.

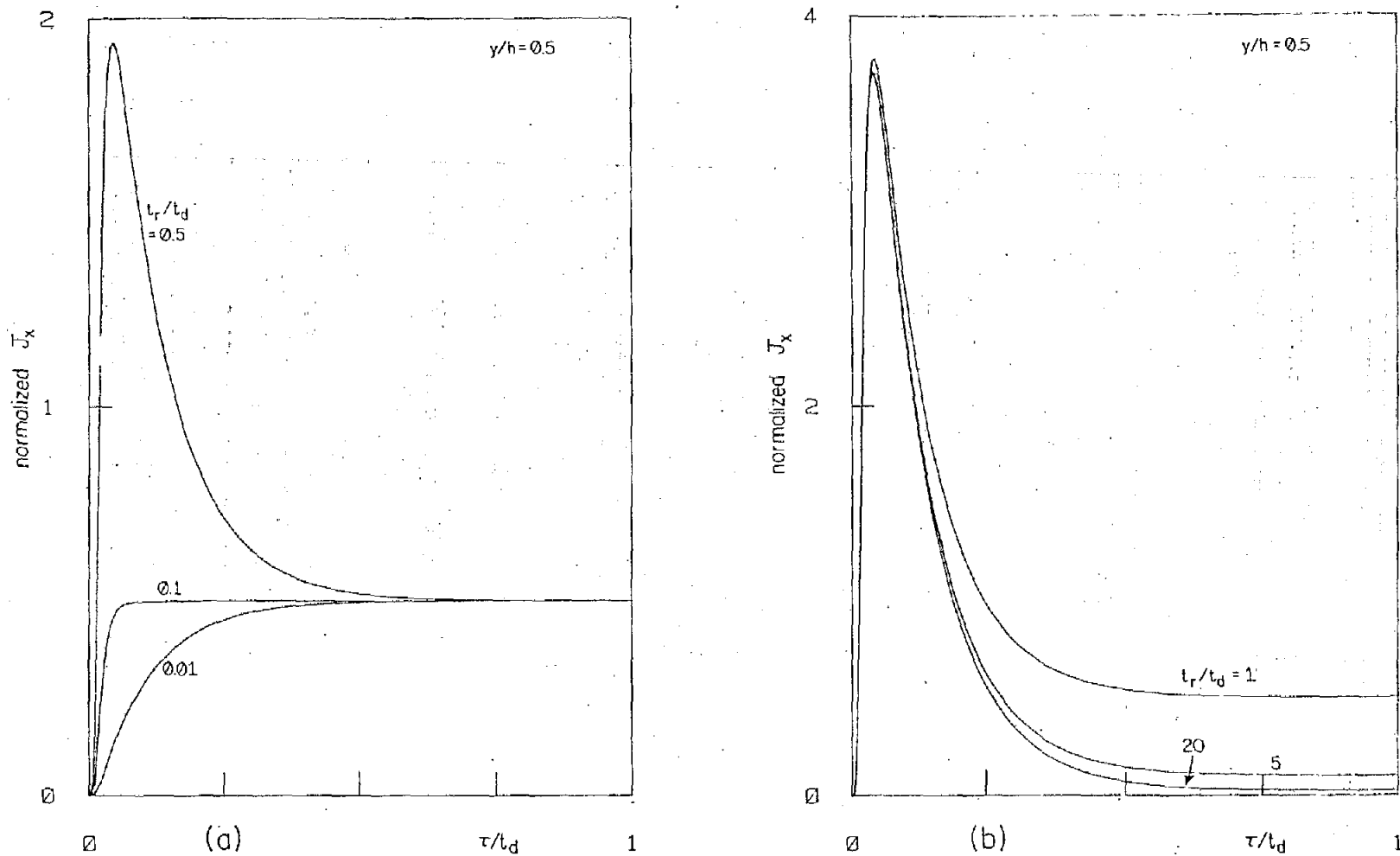


Figure 20. (a) $(t_r/t_d)^{1/2} J_x / J'_0$, (b) $(t_d/t_r)^{1/2} J_x / J'_0$ at $y/h = 0.5$ as functions of τ/t_d for $x_0/h \geq 200$ and various t_r/t_d , for the simulator with $\sigma_2 \rightarrow \infty$, $\sigma_1 = \sigma$, $\epsilon_1 = \epsilon_0$, $E_x^e = E_0 \exp(-x/x_0) U(t - x/c)$. Here, $J_x = (\sigma + \epsilon_0 \frac{\partial}{\partial t}) E_x$, $J'_0 = E_0 (hZ_0)^{-1} \exp(-x/x_0)$, $Z_0 = (\mu_0/\epsilon_0)^{1/2}$, $t_r = \epsilon_0/\sigma$, $t_d = \mu_0 \sigma h^2$, $\tau = t - x/c$.

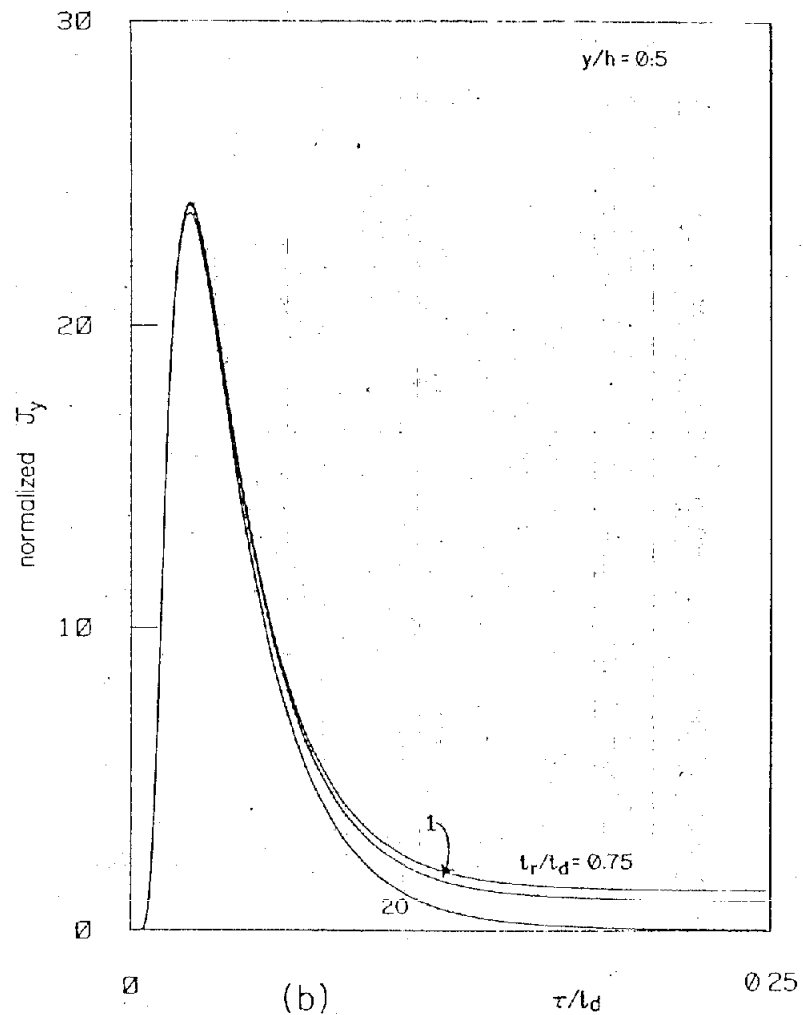
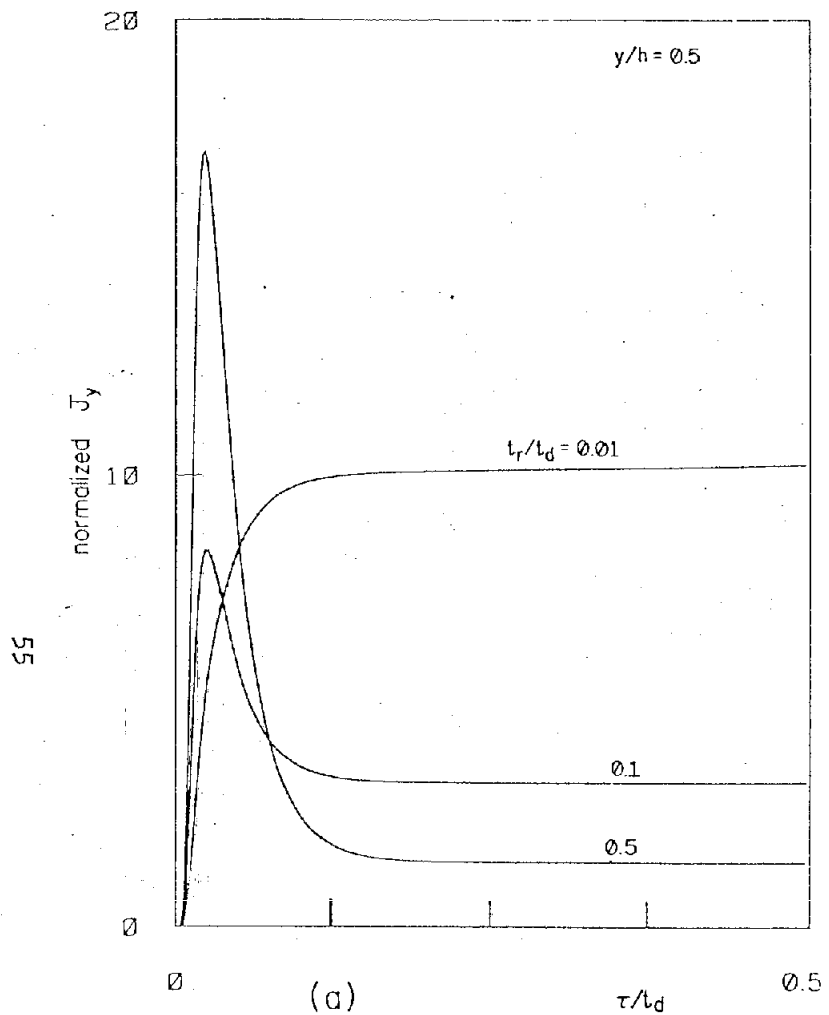


Figure 21. (a) $(t_d/t_r)^{1/2} J_y/J'_0$, (b) $(t_d/t_r) J_y/J'_0$ at $y/h = 0.5$, as functions of τ/t_d for $x_0/h \geq 200$ and various t_r/t_d , for the simulator with $\sigma_2 \rightarrow \infty$, $\sigma_1 = \sigma$, $\epsilon_1 = \epsilon_0$, $E_x^e = E_0 \exp(-x/x_0) U(t-x/c)$. Here, $J_y = (\sigma + \epsilon_0 \frac{\partial}{\partial t}) E_y$, $J'_0 = E_0 (hZ_0)^{-1} \exp(-x/x_0)$, $Z_0 = (\mu_0/\epsilon_0)^{1/2}$, $t_r = \epsilon_0/\sigma$, $t_d = \mu_0 \sigma h^2$, $\tau = t - x/c$.

TABLE 8. FIELD AND CURRENT DENSITY FOR UNIT-STEP SOURCE FIELD FOR $\sigma_2 \rightarrow \infty$, $\sigma_1 = \sigma$, $\epsilon_1 = \epsilon_0$,
 $\sigma \geq 3 \times 10^{-4}$ mho/m, $x_0 \geq 200$ m, AND $x_0/h \geq 100^\dagger$

Quantity	Location y/h	Local Maximum		Late Time Value ($t_{dx_0} > \tau \gg t_r, t_d$)	Condition
		Value	Time to Reach Maximum (τ)		
$\frac{H_z}{H'_0}$	$1 > \frac{y}{h} \geq 0$	Monotonically increasing. At early time, the larger y/h is, the faster it increases.		$\frac{\tau}{(t_r t_d)^{1/2}}$	any t_r/t_d
$\frac{(\sigma + \epsilon_0 \frac{\partial}{\partial t}) E_x}{J'_0}$	y/h = 0	= 0		$\left(\frac{t_d}{t_r}\right)^{1/2} \frac{y}{h}$	None
	$1 > \frac{y}{h} \geq \frac{1}{2}$	Monotonically increasing			$t_r/t_{dy} \leq 4/9$
$\left(\frac{t_r}{t_d}\right)^{1/2} \left(1 - \frac{y}{h}\right)^{-2}$		$\frac{t_{dy}}{3} \geq \tau \geq \frac{t_{dy}}{6}$			$\frac{t_r}{t_{dy}} \geq \frac{4}{9}$
$\frac{(\sigma + \epsilon_0 \frac{\partial}{\partial t}) E_y}{J'_0}$	$\frac{y}{h} = 0$	Monotonically increasing, reach ~ 1 at or before 0.5 t_d		1	$t_r/t_d \leq 0.1$
		$6(t_r/t_d)$	$0.09 t_d$		$t_r/t_d \geq 0.5$
	$1 > \frac{y}{h} \geq \frac{1}{2}$	Monotonically increasing, reach ~ 1 at or before 0.5 t_{dy}			$t_r/t_{dy} \leq 0.1$
		$3 \frac{t_r}{t_d} \left(1 - \frac{y}{h}\right)^{-3}$	$0.09 t_{dy}$		$\frac{t_r}{t_{dy}} \geq 0.5$

56

$^\dagger t_{dy} = t_d(1-y/h)^2 = \mu_0 \sigma h^2 (1-y/h)^2$, $H'_0 = h J'_0 = E_0 Z_0^{-1} \exp(-x/x_0)$, $t_{dx_0} = \mu_0 \sigma x_0^2$.

* Same as H_z/H_0 of Tables 4 and 5.

$$\begin{aligned}
H_z \approx & \frac{E_0}{Z_0} \left(\frac{t_r}{t_d} \right)^{\frac{1}{2}} e^{-\frac{x}{x_0}} U(\tau - t'_{ty}) \left\{ \frac{\tau}{t_r} - \frac{t_d}{6t_r} \left(1 - \frac{3y^2}{h^2} \right) + 1 - e^{-\frac{\tau}{t'_r}} \right. \\
& + 2 \sum_{m=1}^{\infty} \frac{(-1)^m \cos(m\pi y/h)}{\sqrt{1 - 4t'_m{}^2 \pi^2 / t_d}} \left(\frac{\epsilon_r \omega_m^- t_r - 1}{\omega_m^- t_r} e^{-\omega_m^- \tau} - \frac{\epsilon_r \omega_m^+ t_r - 1}{\omega_m^+ t_r} e^{-\omega_m^+ \tau} \right) \left. \right\} \\
(\sigma + \epsilon \frac{\partial}{\partial t}) E_x \approx & \frac{E_0}{hZ_0} \left(\frac{t_r}{t_d} \right)^{\frac{1}{2}} e^{-\frac{x}{x_0}} U(\tau - t'_{ty}) \left\{ \frac{t_d}{t_r} \frac{y}{h} - \right. \\
& \left. - 2 \sum_{m=1}^{\infty} \frac{(-1)^m m\pi \sin(m\pi y/h)}{\sqrt{1 - 4t'_m{}^2 \pi^2 / t_d}} \left(\frac{\epsilon_r \omega_m^- t_r - 1}{\omega_m^- t_r} e^{-\omega_m^- \tau} - \frac{\epsilon_r \omega_m^+ t_r - 1}{\omega_m^+ t_r} e^{-\omega_m^+ \tau} \right) \right\}
\end{aligned} \tag{22}$$

$$\begin{aligned}
(\sigma + \epsilon \frac{\partial}{\partial t}) E_y \approx & \frac{E_0}{hZ_0} e^{-\frac{x}{x_0}} U(\tau - t'_{ty}) \left\{ 1 + \frac{1}{\epsilon_r - 1} e^{-\frac{\tau}{t'_r}} \right. \\
& + 2 \sum_{m=1}^{\infty} \frac{(-1)^m \cos(m\pi y/h)}{\sqrt{1 - 4t'_m{}^2 \pi^2 / t_d}} \left((1 - \epsilon_r \omega_m^- t_r) e^{-\omega_m^- \tau} - (1 - \epsilon_r \omega_m^+ t_r) e^{-\omega_m^+ \tau} \right) \left. \right\} + \frac{H_z}{x_0}
\end{aligned}$$

$$\text{where } \omega_m^{\pm} = \left(1 \pm \sqrt{1 - 4t'_m{}^2 \pi^2 / t_d} \right) / (2t'_r).$$

The representation appropriate for early times (i.e., for τ up to several t'_t) is given by

$$\begin{aligned}
H_z \approx & \frac{E_0}{Z_0} \frac{\epsilon_r}{\sqrt{\epsilon_r - 1}} e^{-\frac{x}{x_0}} \sum_{n=-\infty}^{\infty} U(\tau - t'_{ty}^{(n)}) \times \left\{ e^{-\frac{\tau}{2t'_r}} I_0 \left(\frac{\tau y_n}{2t'_r} \right) + \right. \\
& \left. + \frac{1}{\epsilon_r t_r} \int_{t'_{ty}^{(n)}}^{\tau} e^{-\frac{\tau'}{2t'_r}} I_0 \left(\frac{\tau' y_n}{2t'_r} \right) d\tau' \right\}
\end{aligned} \tag{23}$$

$$\begin{aligned} \left(\sigma + \varepsilon \frac{\partial}{\partial t} \right) E_x \approx E_o e^{-\frac{x}{x_o}} \sum_{n=-\infty}^{\infty} \frac{(2n+1-y/h)}{|2n+1-y/h|} e^{-\frac{t'_y(n)}{2t'_r}} \left[\varepsilon_r \varepsilon_o \delta(\tau - t'_y(n)) + \sigma U(\tau - t'_y(n)) \right] \\ + \frac{E_o}{2hZ_o} \frac{\varepsilon_r}{\sqrt{\varepsilon_r - 1}} e^{-\frac{x}{x_o}} \sum_{n=-\infty}^{\infty} (2n+1-y/h) U(\tau - t'_y(n)) \times \end{aligned} \quad (23)$$

$$\times \left\{ \frac{t_d}{\tau_{yn}} e^{-\frac{\tau}{2t'_r}} I_1 \left(\frac{\tau_{yn}}{2t'_r} \right) + \frac{1}{\varepsilon_r t_r} \int_{t'_y(n)}^{\tau} \frac{t_d}{\tau'_{yn}} e^{-\frac{\tau'}{2t'_r}} I_1 \left(\frac{\tau'_{yn}}{2t'_r} \right) d\tau' \right\}$$

$$\begin{aligned} \left(\sigma + \varepsilon \frac{\partial}{\partial t} \right) E_y \approx \frac{H_z}{x_o} + E_o \frac{\varepsilon_r \varepsilon_o}{\sqrt{\varepsilon_r - 1}} e^{-\frac{x}{x_o}} \sum_{n=-\infty}^{\infty} e^{-\frac{t'_y(n)}{2t'_r}} \delta(\tau - t'_y(n)) \\ + \frac{E_o}{2hZ_o} \left(\frac{t_d}{t'_r} \right)^{\frac{1}{2}} \frac{\varepsilon_r - 2}{\varepsilon_r - 1} e^{-\frac{x}{x_o}} e^{-\frac{\tau}{2t'_r}} \sum_{n=-\infty}^{\infty} U(\tau - t'_y(n)) \times \\ \times \left\{ I_0 \left(\frac{\tau_{yn}}{2t'_r} \right) + \frac{\varepsilon_r}{\varepsilon_r - 2} \frac{\tau}{\tau_{yn}} I_1 \left(\frac{\tau_{yn}}{2t'_r} \right) \right\} \end{aligned}$$

where, as defined in Equation 16, $t'_y(n) = \sqrt{((2n+1)h-y)^2(\varepsilon_r-1)}/c$,
 $\tau_{yn} = \left(\tau^2 - t'^2_{ty}(n) \right)^{\frac{1}{2}}$ and $\tau'_{yn} = \left(\tau'^2 - t'^2_{ty}(n) \right)^{\frac{1}{2}}$.

In the series representation in Equation 23, one can see that every term (i.e., with a specific n) is exactly the same as Equation 19, if h is replaced by $2n+1-y/h$ (i.e., t'_t by $t'_{ty}(n)$, t_d by $t_d(2n+1-y/h)^2$, also). The terms with $n = \pm m$, $m=1,2,3,\dots$, can be considered respectively the m -th reflection from the $y=h$ and $y=0$ planes. That is, the field and current density distributions of the present case can be constructed from the solutions represented by Equation 19. As is obvious from Equation 23, the smaller τ is, the fewer terms are required for the calculations.

At very late times ($10^3 t_d \geq \tau \gg t'_r, t_d$), one can see from Equation 22 that the field and current density distributions approach the following values:

$$H_z : \frac{E_o}{Z_o} e^{-\frac{x}{x_o}} \frac{\tau}{(t_r t_d)^{1/2}}$$

$$\left(\sigma + \epsilon \frac{\partial}{\partial t}\right) E_x : \frac{E_o}{hZ_o} e^{-\frac{x}{x_o}} \left(\frac{t_d}{t_r}\right)^{1/2} \frac{y}{h} \quad (24)$$

$$\left(\sigma + \epsilon \frac{\partial}{\partial t}\right) E_y : \frac{E_o}{hZ_o} e^{-\frac{x}{x_o}}$$

which are the same as those for the case with $\epsilon_r = 1$, as expected. To obtain the late-time behaviors, one can also use Equation 23, especially when $t'_t \gg t'_r$, in which case only a few terms are needed. However, if $t'_t \ll t'_r$, one needs many terms to obtain the late-time behaviors.

REFERENCES

1. Baum, C.E., "EMP Simulators for Various Types of Nuclear EMP Environments: An Interim Categorization," IEEE Trans. on Antenna and Propagation, AP-26, pp. 35 - 53, January 1978, and also Sensor and Simulation Notes, Note 240, Air Force Weapons Laboratory, 1 January 1978.
2. Baum, C.E., "The Planar, Uniform Surface Transmission Line Driven from a Sheet Source," Sensor and Simulation Notes, Note 48, Air Force Weapons Laboratory, August 1967.
3. Baum, C.E., "A Distributed-Source Conducting-Medium Simulator for Structures Near and Below the Ground Surface," Sensor and Simulation Notes, Note 87, Air Force Weapons Laboratory, July 1969.
4. Baum, C.E., "Electromagnetic Pulse Interaction Close to Nuclear Bursts and Associated EMP Environment Specification," Interaction Notes, Note 76, Air Force Weapons Laboratory, July 1971.

$$(2) \quad \epsilon/\epsilon_0 = \epsilon_r > 1.$$

For this case, one finds that the ω -integrals are of the forms of Equation 12, but with $\zeta^2 = \omega^2 \mu_0 \epsilon_0 (1 - \epsilon_r) + j\omega \mu_0 \sigma B - 1/x_0^2$. The integrands have poles at the zeros of $\sinh(\zeta h)$ which are now at $\omega = j\omega_m^\pm = jB(2t'_r)^{-1} \times \left(1 \pm \sqrt{1 - 4t'_r(m^2 \pi^2 - h^2/x_0^2)/(B^2 t_d)} \right)$, $m=0,1,2,\dots$, but no branch points. By deforming the integration path, one gets the following representations for the field and current densities.

$$\begin{aligned}
 H_z &= \frac{2V_0}{hZ_0 B} e^{-\frac{x}{x_0}} \sum_{m=0}^{\infty} \frac{(-1)^m \cos(m\pi y/h) U(\tau - t'_{ty})}{(1 + \delta_{m0}) \sqrt{1 - 4t'_r(m^2 \pi^2 - h^2/x_0^2)/(B^2 t_d)}} \times \\
 &\quad \times \left[e^{-\omega_m^- \tau} \left(1 - \frac{\epsilon_r}{\epsilon_r - 1} \omega_m^- t'_r \right) - e^{-\omega_m^+ \tau} \left(1 - \frac{\epsilon_r}{\epsilon_r - 1} \omega_m^+ t'_r \right) \right] \\
 (\sigma + \epsilon \frac{\partial}{\partial t}) E_x &= \frac{-2V_0}{h^2 Z_0 B} e^{-\frac{x}{x_0}} \sum_{m=1}^{\infty} \frac{(-1)^m m\pi \sin(m\pi y/h) U(\tau - t'_{ty})}{\sqrt{1 - 4t'_r(m^2 \pi^2 - h^2/x_0^2)/(B^2 t_d)}} \times \\
 &\quad \times \left[e^{-\omega_m^- \tau} \left(1 - \frac{\epsilon_r}{\epsilon_r - 1} \omega_m^- t'_r \right) - e^{-\omega_m^+ \tau} \left(1 - \frac{\epsilon_r}{\epsilon_r - 1} \omega_m^+ t'_r \right) \right] \\
 (\sigma + \epsilon \frac{\partial}{\partial t}) E_y &= \frac{-2V_0}{h^2 Z_0 B} e^{-\frac{x}{x_0}} \sum_{m=0}^{\infty} \frac{(-1)^m \cos(m\pi y/h) U(\tau - t'_{ty})}{(1 + \delta_{m0}) \sqrt{1 - 4t'_r(m^2 \pi^2 - h^2/x_0^2)/(B^2 t_d)}} \times \\
 &\quad \times \left[e^{-\omega_m^- \tau} \left(\omega_m^- t_t - \frac{h}{x_0} \right) \left(1 - \frac{\epsilon_r}{\epsilon_r - 1} \omega_m^- t'_r \right) - e^{-\omega_m^+ \tau} \left(\omega_m^+ t_t - \frac{h}{x_0} \right) \left(1 - \frac{\epsilon_r}{\epsilon_r - 1} \omega_m^+ t'_r \right) \right]
 \end{aligned} \tag{15}$$

where $t_t = h/c$, and $t'_{ty} = (h-y)\sqrt{\epsilon_r - 1}/c$.

As in Equation 8, the infinite responses (i.e., δ -functions) at $\tau = t'_{ty}$ in Equation 15 are not included. Equation 15 reduces to Equation 13 when $\epsilon_r \rightarrow 1$, as expected. From Equation 15, one observes that only a couple of terms with smaller $\text{Re}(\omega_m^\pm)$'s are required for good approximations to the field quantities when $\tau \gg 2t'_r, t'_d$. But, when $\tau \leq 2t'_r$, the series representation of Equation 15 does not converge at all and one has to seek for alternative representations.

An alternative representation can be obtained by expressing the hyperbolic functions in Equation 12 in terms of exponential functions, using the Taylor expansions and then applying the techniques used to get Equation 8. The results are given as follows (for $\tau > t'_{ty}$, of course):

$$\begin{aligned}
 H_z &= \frac{V_o}{hZ_o} \left(\frac{t'_d}{t'_r} \right)^{1/2} e^{-\frac{x}{x_o}} e^{-\frac{B\tau}{2t'_r}} \sum_{n=-\infty}^{\infty} U(\tau_{yn}^2) \times \\
 &\times \left\{ \left[1 - \frac{\epsilon_r B}{2(\epsilon_r - 1)} \right] I_o(AA) + \frac{\epsilon_r B}{2(\epsilon_r - 1)} \sqrt{1 + \frac{4t'_r}{B^2 t_{dx_o}} \frac{\tau}{\tau_{yn}}} I_1(AA) \right\} \\
 (\sigma + \epsilon \frac{\partial}{\partial t}) E_x &= \frac{V_o}{h^2 Z_o} \left(\frac{t'_d}{t'_r} \right)^{1/2} \frac{B}{4(\epsilon_r - 1)} \sqrt{1 + \frac{4t'_r}{B^2 t_{dx_o}}} e^{-\frac{x}{x_o}} e^{-\frac{B\tau}{2t'_r}} \sum_{n=-\infty}^{\infty} U(\tau_{yn}^2) \times \\
 &\times \frac{t'_d(2n+1-y/h)}{\tau_{yn}} \left\{ \left[(2-B)\epsilon_r - 2 \right] I_1(AA) + \frac{\epsilon_r B\tau}{\tau_{yn}} \sqrt{1 + \frac{4t'_r}{B^2 t_{dx_o}}} I_2(AA) \right\} \\
 (\sigma + \epsilon \frac{\partial}{\partial t}) E_y &= \frac{H_z}{x_o} - \frac{V_o}{h^2 Z_o} \frac{t'_d}{t'_r} \frac{\epsilon_r B}{4(\epsilon_r - 1)^{3/2}} e^{-\frac{x}{x_o}} e^{-\frac{B\tau}{2t'_r}} \sum_{n=-\infty}^{\infty} U(\tau_{yn}^2) \times \\
 &\times \left\{ \left[\frac{(2-B)\epsilon_r - 2}{\epsilon_r} - \frac{B}{2} \left(1 + \frac{4t'_r}{B^2 t_{dx_o}} \right) \right] I_o(AA) \right\}
 \end{aligned}$$

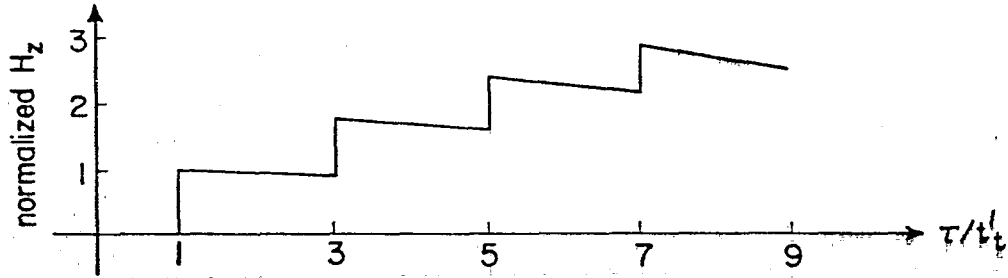
$$\begin{aligned}
& + \frac{(2B-2)\epsilon_r + 2}{\epsilon_r} \sqrt{1 + \frac{4t'_r}{B^2 t_{dx_0}}} \frac{\tau}{\tau_{yn}} I_1(AA) \\
& - \frac{B}{2} \left(1 + \frac{4t'_r}{B^2 t_{dx_0}} \right) \frac{2\tau^2 - \tau_{yn}^2}{\tau_{yn}^2} I_2(AA) \left. \right\} \quad (16)
\end{aligned}$$

where $AA = B\tau_{yn} \sqrt{1 + 4t'_r/(B^2 t_{dx_0})} / (2t'_r)$, $\tau_{yn} = (\tau^2 - t_{ty}'(n)^2)^{1/2}$ and $t_{ty}'(n) = \sqrt{(2n+1)h-y}^2 (\epsilon_r - 1) / c$. From the above equation, one can see that the smaller τ is, the fewer terms are required for the calculations. In Equation 16, the infinite responses at $\tau = t_{ty}'(n)$ (i.e., $\delta(\tau - t_{ty}'(n))$, etc.) are not shown.

To derive Equations 15 and 16, it has been assumed that $R > 2$ (i.e., $B > 0$). The results for the situation with $2 \geq R \geq 0$ are different. However, for most of the practical situations, $R \gg 2$ and the approximations $B \approx 1$, $1 + 4t'_r/(B^2 t_{dx_0}) \approx 1$ can always be made to simplify Equations 15 and 16.

In the series representation of Equation 16, one can see that every term (i.e., with a specific n) is exactly the same as Equation 8, if $t_{ty}'(n)$ is replaced by t'_t . That is, in addition to the diffusion and Cerenkov processes, the field and current density distributions are determined by the bounces between $y=0$ and $y=h$ planes. And, the field and current density distributions of the present case can be easily constructed from the solutions represented by Equation 8. One set of example curves given for $t'_t/t'_r = 0.2$, $\epsilon_r = 10$ and $y=0$ is presented in Figure 13. The t'_t/t'_r value given for this example is relatively small. Thus, as can be seen from Figure 13, one needs several bounces to reach the late-time behaviors of $H_z/H_o \rightarrow 1$, $(\sigma + \epsilon \frac{\partial}{\partial t}) E_x / J_o \rightarrow 0$, $(\sigma + \epsilon \frac{\partial}{\partial t}) E_y / J_o \rightarrow 0$ which can be implied from Equation 15 when $\tau \gg t'_r, t'_d$. However, when t'_t/t'_r is large, one does not need many bounces to reach those late-time values.

(a)



(b)

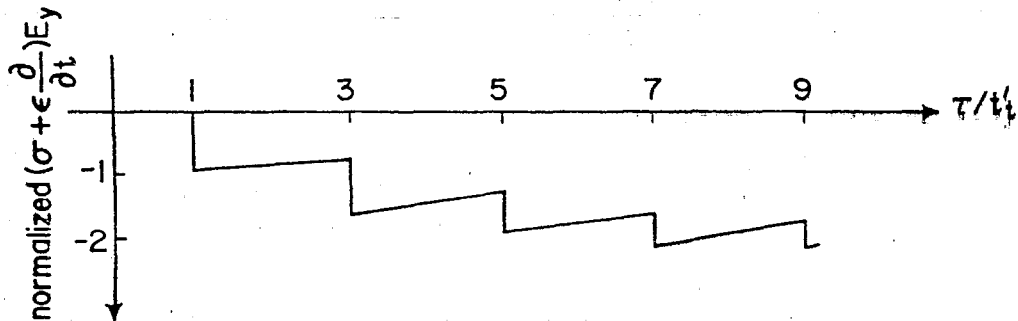


Figure 13. (a) $9(t'_r/t'_t)H_z/(8H_0)$, (b) $18(t'_r/t'_d) \left(\sigma + \epsilon \frac{\partial}{\partial t} \right) E_y/J_0$ at $y=0$ as functions of τ/t'_t for $x_0/h \geq 200$, $\epsilon_r = 10$ and $t'_t/t'_r = 0.2$, for the simulator with $\sigma_2 \rightarrow \infty$, $\sigma_1 = \sigma$, $\epsilon_1 = \epsilon = \epsilon_r \epsilon_0$, $E_x^e = V_0 \delta(ct-x) \exp(-x/x_0)$. Here $H_0 = hJ_0 = V_0 (hZ_0)^{-1} \exp(-x/x_0)$, $Z_0 = (\mu_0/\epsilon_0)^{1/2}$, $t_d = \mu_0 \sigma h^2$, $t'_t = h\sqrt{\epsilon_r - 1}/c$, $t'_r = \epsilon_0(\epsilon_r - 1)/\sigma$, $t'_t/t'_r = t_d/t'_t = (t_d/t'_r)^{1/2}$, $\tau = t - x/c$.

IV. UNIT-STEP SOURCE FIELD

In the last section, the field and current density distributions for two special simulator geometries with a δ -function source field $E_x^e = V_0 \delta(ct - x) \times \exp(-x/x_0)$ have been obtained. In this section, the corresponding distributions for the same special simulator geometries, but with a unit-step source field $E_x^e = E_0 U(t - x/c) \exp(-x/x_0)$, will be sought.

For the simulator with a unit-step source field, one finds that the (ω, k) -domain solutions are still given by Equations 5 and 6, except that \tilde{E}_x^e has a new value $E_0 \delta(k - \omega/c + j/x_0)/(j\omega)$. The (t, x) -domain solutions can then be calculated from the inverse Fourier-transform integrals, the second equation of Equation 1. Due to the presence of the term $\delta(k - \omega/c + j/x_0)$, the k -integral can be easily performed. To calculate the remaining ω -integrals, one can either deform the integration paths as was done in Section III or compute convolution integrals of the form

$$\int_{-\infty}^{\infty} F_1(\tau') U(\tau - \tau') d\tau'$$

where F_1 is the solution with a δ -function source field.

From Section III, it is observed that for the situations of practical interest the approximations $R = \mu_0 \sigma c x_0 \rightarrow \infty$, $B = 1 - 2/R \rightarrow 1$ and $\tau/t_{dx_0} \rightarrow 0$ can always be used. That is, the field and current density distributions in a simulator with a source field containing the factor $\exp(-x/x_0)$ can be approximated with $\exp(-x/x_0)$ times the distributions derived for a source field which does not contain this factor (i.e., $x_0 \rightarrow \infty$). This argument will now be applied throughout this section to simplify the calculations. The approximated solutions are presented as follows.

$$A. \quad \sigma_1 = \sigma_2 = \sigma, \quad \epsilon_1 = \epsilon_2 = \epsilon, \quad E_x^e = E_0 U(t - x/c) \exp(-x/x_0), \quad y \leq h$$

The two cases will be considered depending on whether or not ϵ equals to ϵ_0 .

$$(1) \quad \epsilon = \epsilon_0$$

For this case, the following expressions for the field and current density distributions at $y=0$ are obtained.

$$\begin{aligned}
 H_z &\approx \frac{E_0}{Z_0} \left\{ \left[\left(\frac{t_r}{\pi\tau} \right)^{\frac{1}{2}} + \left(\frac{4\tau}{\pi t_r} \right)^{\frac{1}{2}} \right] e^{-\frac{t_d}{4\tau}} \right. \\
 &\quad \left. - \left(\frac{t_d}{t_r} \right)^{\frac{1}{2}} \left[1 - \operatorname{erf} \left(\sqrt{\frac{t_d}{4\tau}} \right) \right] \right\} e^{-\frac{x}{x_0}} U(\tau) \\
 (\sigma + \epsilon_0 \frac{\partial}{\partial t}) E_x &\approx \frac{E_0}{hZ_0} \left\{ \frac{t_d}{2\tau} \left(\frac{t_r}{\pi\tau} \right)^{\frac{1}{2}} e^{-\frac{t_d}{4\tau}} \right. \\
 &\quad \left. + \left(\frac{t_d}{t_r} \right)^{\frac{1}{2}} \left[1 - \operatorname{erf} \left(\sqrt{\frac{t_d}{4\tau}} \right) \right] \right\} e^{-\frac{x}{x_0}} U(\tau) \\
 (\sigma + \epsilon_0 \frac{\partial}{\partial t}) E_y &\approx \frac{H_z}{x_0} + \frac{E_0}{hZ_0} \left(\frac{t_d}{\pi\tau} \right)^{\frac{1}{2}} e^{-\frac{t_d}{4\tau}} e^{-\frac{x}{x_0}} U(\tau) \times \\
 &\quad \times \left(1 - \frac{t_r}{2\tau} + \frac{t_r t_d}{4\tau^2} \right)
 \end{aligned} \tag{17}$$

where $\operatorname{erf}(z)$ is the error function defined as

$$\operatorname{erf}(z) = \frac{2}{\sqrt{\pi}} \int_0^z e^{-p^2} dp$$

The field and current density distributions at an arbitrary $y < h$ can be calculated by simply replacing h and t_d in Equation 17 with $(h-y)$ and t_{dy} .

Based on Equation 17, several curves are presented in Figures 14 - 16 for various t_r/t_d . At very early and late times (defined respectively by $\tau \ll t_d$ and $\tau \gg t_d$), Equation 17 can be simplified by using the asymptotic approximations for the error function and retaining only one or two terms in the equation. From the simplified equation and the curves in Figures 14 - 16, one can summarize the behaviors of the field and current densities in Table 6.

$$(2) \quad \epsilon/\epsilon_0 = \epsilon_r > 1$$

In section III, it was mentioned that some δ -function responses have to be added to Equation 8 to obtain complete solutions for this simulator geometry with a δ -function source field. These δ -function responses are now given as below.

$$H_z : \quad \frac{V_0}{c} \frac{\epsilon_r}{Z_0 \sqrt{\epsilon_r - 1}} e^{-\frac{t'_t}{2t'_r}} \delta(\tau - t'_t)$$

$$\left(\sigma + \epsilon \frac{\partial}{\partial t}\right) E_x : \quad \frac{V_0}{c} e^{-\frac{t'_t}{2t'_r}} \left[\sigma \delta(\tau - t'_t) + \epsilon_r \epsilon_0 \delta'(\tau - t'_t) \right] \quad (18)$$

$$\left(\sigma + \epsilon \frac{\partial}{\partial t}\right) E_y : \quad \frac{V_0}{c} \frac{1}{\sqrt{\epsilon_r - 1}} e^{-\frac{t'_t}{2t'_r}} \left[\sigma \delta(\tau - t'_t) + \epsilon_r \epsilon_0 \delta'(\tau - t'_t) \right]$$

By using the combination of Equations 8 and 18 for F_1 in the convolution integrals, the following expressions for the field and current density distributions at $y=0$ are obtained:

$$H_z \approx \frac{E_0}{Z_0} \frac{\epsilon_r}{\sqrt{\epsilon_r - 1}} e^{-\frac{x}{x_0}} U(\tau - t'_t) \times \left\{ e^{-\frac{\tau}{2t'_r}} I_0 \left[\frac{1}{2t'_r} \sqrt{\tau^2 - t'^2} \right] + \right.$$

$$\left. + \frac{(\epsilon_r - 1)}{\epsilon_r t'_r} \int_{t'_t}^{\tau} e^{-\frac{\tau'}{2t'_r}} I_0 \left[\frac{1}{2t'_r} \sqrt{\tau'^2 - t'^2} \right] d\tau' \right\}$$

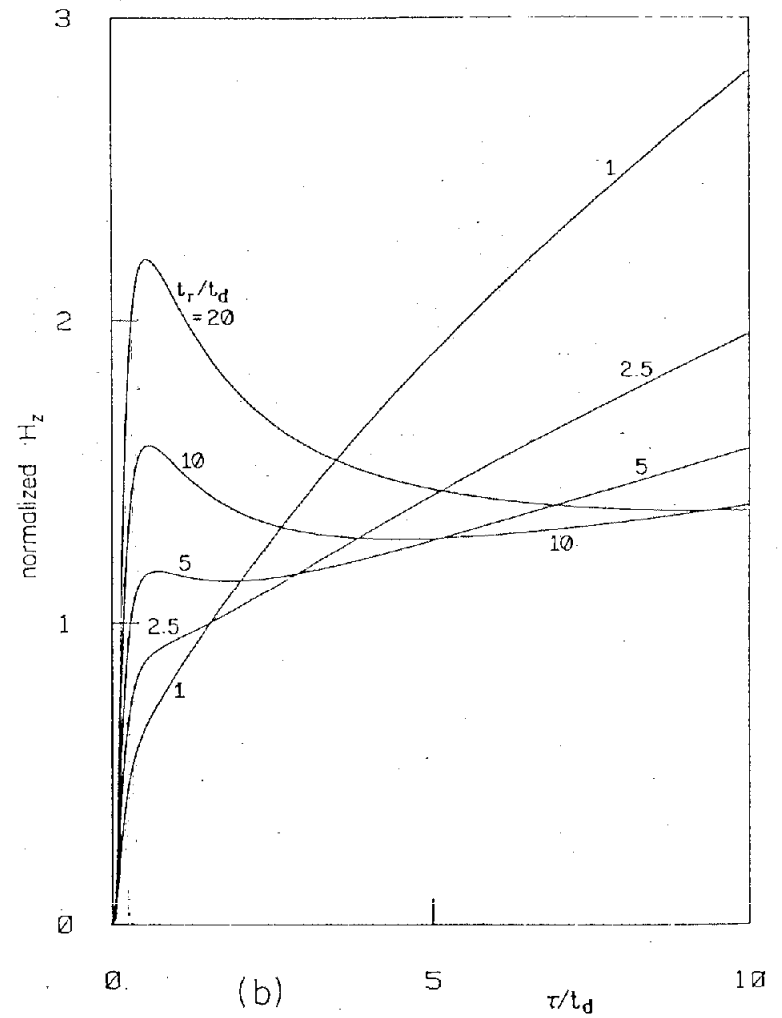
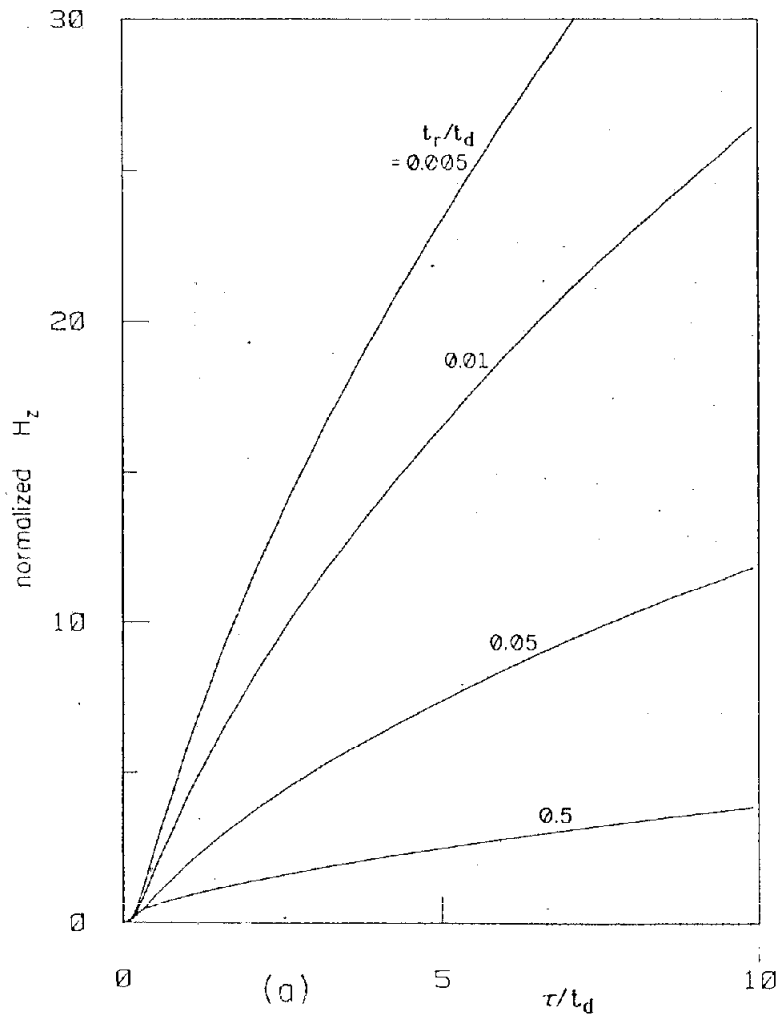


Figure 14. H_z/H'_0 at $y=0$ as a function of τ/t_d for $x_0/h \geq 200$ and various t_r/t_d , for the simulator with $\sigma_1 = \sigma_2 = \sigma$, $\epsilon_1 = \epsilon_2 = \epsilon_0$, $E_x^e = E_0 \exp(-x/x_0)U(t-x/c)$. Here, $H'_0 = E_0 \exp(-x/x_0)Z_0^{-1}$, $Z_0 = (\mu_0/\epsilon_0)^{1/2}$, $t_r = \epsilon_0/\sigma$, $t_d = \mu_0 ch^2$, $\tau = t-x/c$.

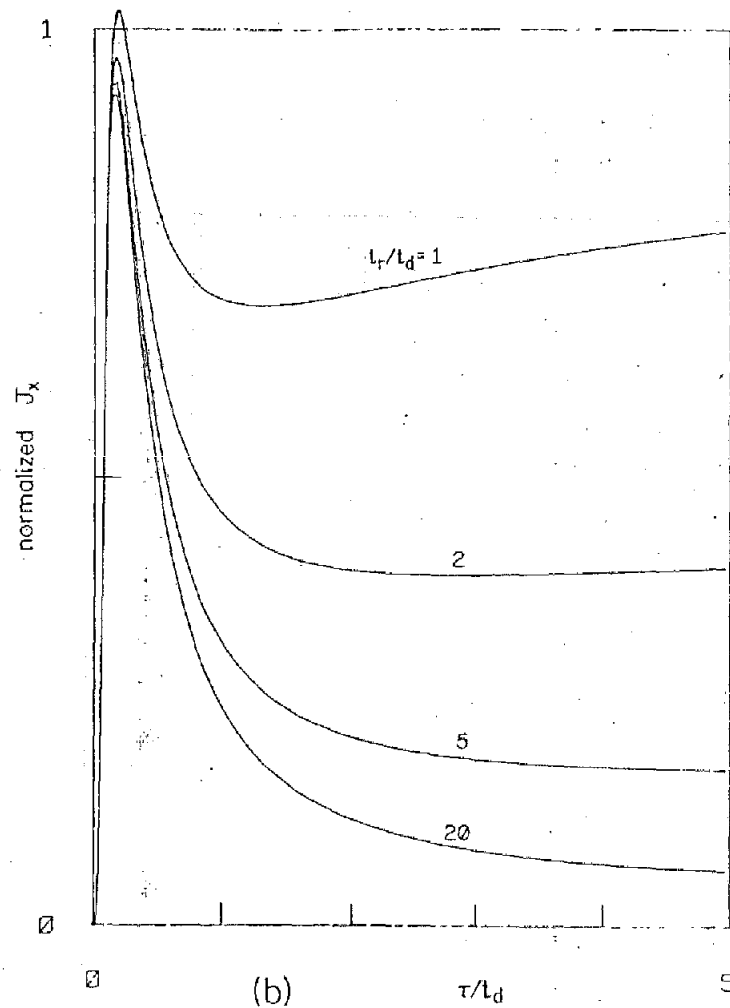
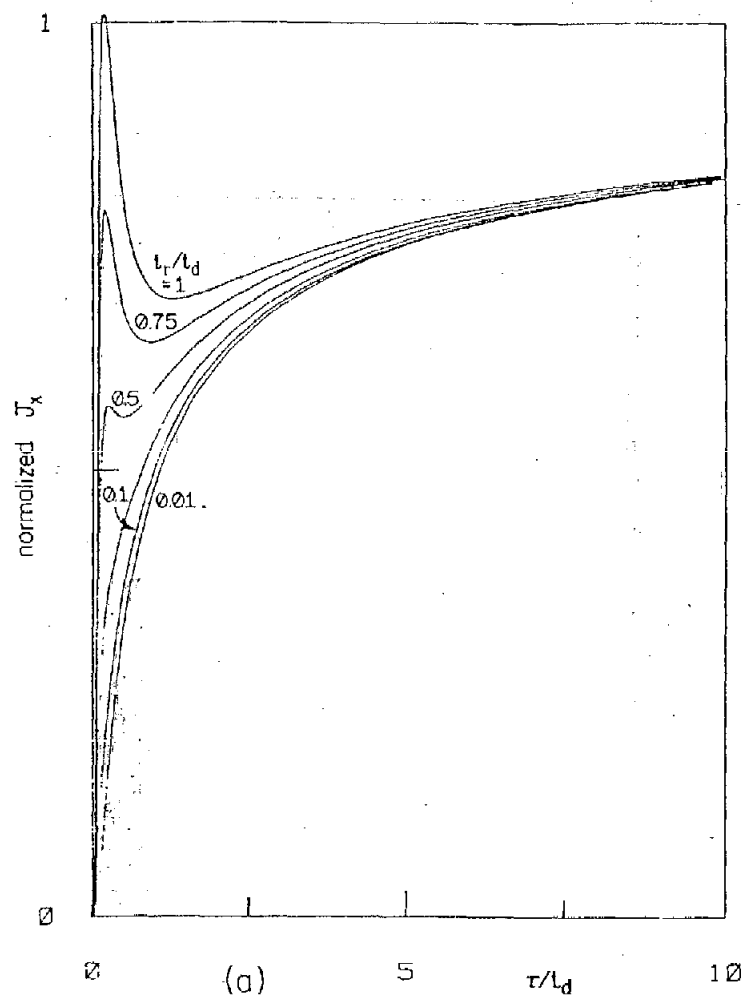


Figure 15. (a) $(t_r/t_d)^{1/2} J_x/J'_0$, (b) $(t_d/t_r)^{1/2} J_x/J'_0$ at $y=0$ as functions of τ/t_d for $x_0/h \geq 200$ and various t_r/t_d , for the simulator with $\sigma_1 = \sigma_2 = \sigma$, $\epsilon_1 = \epsilon_2 = \epsilon_0$, $E_x^e = E_0 \exp(-x/x_0) U(t-x/c)$. Here, $J_x = (\sigma + \epsilon_0 \frac{\partial}{\partial t}) E_x$, $J'_0 = E_0 (hZ_0)^{-1} \exp(-x/x_0)$, $Z_0 = (\mu_0/\epsilon_0)^{1/2}$, $t_r = \epsilon_0/\sigma$, $t_d = \mu_0 \sigma h^2$, $\tau = t - x/c$.

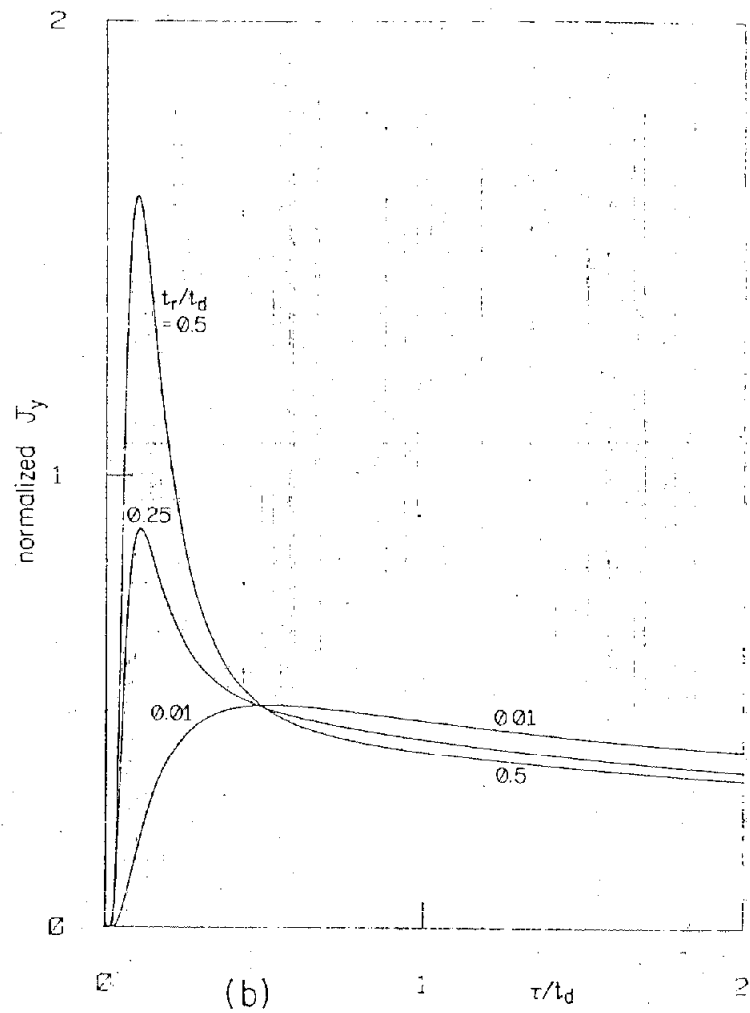
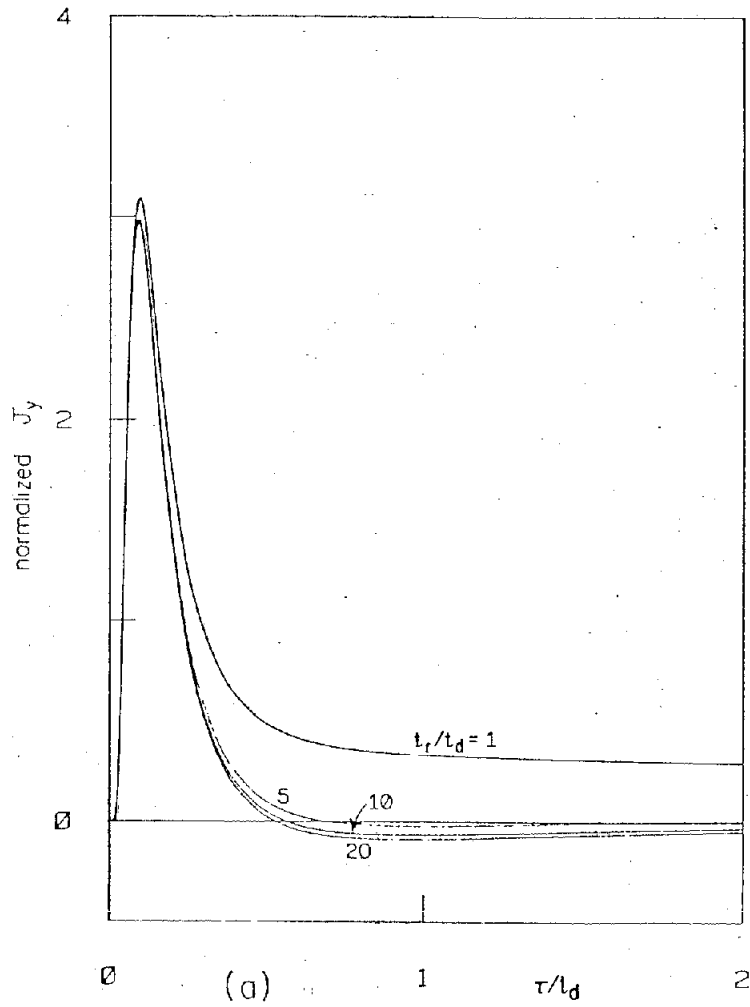


Figure 16. (a) $(t_d/t_r)J_y/J'_0$, (b) J_y/J'_0 at $y=0$ as functions of τ/t_d for $x_0/h \geq 200$ and various t_r/t_d , for the simulator with $\sigma_1 = \sigma_2 = \sigma$, $\epsilon_1 = \epsilon_2 = \epsilon_0$, $E_x^e = E_0 \exp(-x/x_0)U(t-x/c)$. Here, $J_y = (\sigma + \epsilon_0 \frac{\partial}{\partial t})E_y$, $J'_0 = E_0 (hZ_0)^{-1} \exp(-x/x_0)$, $Z_0 = (\mu_0/\epsilon_0)^{1/2}$, $t_r = \epsilon_0/\sigma$, $t_d = \mu_0 \sigma h^2$, $\tau = t - x/c$.

TABLE 6. FIELD AND CURRENT DENSITY FOR UNIT-STEP SOURCE FIELD AT $y=0$ FOR
 $\sigma_1 = \sigma_2 = \sigma$, $\epsilon_1 = \epsilon_2 = \epsilon_0$, $x_0 \geq 200$ m, $\sigma \geq 3 \times 10^{-4}$ mho/m AND $x_0/h \geq 200$ [†]

Quantity	First Maximum*		First Minimum*		Late Time Value $t_{dx_0} > \tau \gg t_r, t_d$	Condition
	τ	Value	τ	Value		
$\frac{H_z}{H'_0}$	$t_d \geq \tau \geq \frac{t_d}{2}$	$0.5 \left(\frac{t_r}{t_d} \right)^{\frac{1}{2}}$	$0.5 t_r$	Less than 1.5	$\left(\frac{4\tau}{\pi t_r} \right)^{\frac{1}{2}}$	$t_r/t_d \geq 4$
	Monotonically increasing					$t_r/t_d < 4$
$\frac{(\sigma + \epsilon_0 \frac{\partial}{\partial t}) E_x}{J'_0}$	$\frac{t_d}{3} \geq \tau \geq \frac{t_d}{6}$	$\left(\frac{t_r}{t_d} \right)^{\frac{1}{2}}$	$1.5 t_r$	$(t_d/t_r)^{\frac{1}{2}} > \text{value}$ $> 0.5(t_d/t_r)^{\frac{1}{2}}$	$\left(\frac{t_d}{t_r} \right)^{\frac{1}{2}}$	$t_r/t_d \geq \frac{4}{9}$
	Monotonically increasing					$t_r/t_d < \frac{4}{9}$
$\frac{(\sigma + \epsilon_0 \frac{\partial}{\partial t}) E_y}{J'_0}$ **	$0.09 t_d$	$3 t_r/t_d$	Fall to 1/e of the maximum at $\tau \sim 0.5 t_d$		0	$t_r/t_d \geq 0.5$
	$0.5 t_d$	0.5	Fall to 1/(2e) at $\tau \sim 9.5 t_d$			$t_r/t_d \leq 0.01$

[†] $t_d = \mu_0 \sigma h^2$, $t_r = \epsilon_0 / \sigma$, $H'_0 = E_0 \exp(-x/x_0) Z_0^{-1}$, $J'_0 = h^{-1} H'_0$, $t_{dx_0} = \mu_0 \sigma x_0^2$

* See Figures 14 - 16, referred to the local maximum and minimum.

** For $0.5 > t_r/t_d > 0.01$, the behaviors are between the tabulated extreme situations.

$$\begin{aligned}
\left(\sigma + \varepsilon \frac{\partial}{\partial t}\right) E_x &\approx E_0 e^{-\frac{x}{x_0}} e^{-\frac{t'_t}{2t'_r}} \left[\varepsilon_r \varepsilon_0 \delta(\tau - t'_t) + \sigma U(\tau - t'_t) \right] \\
&+ \frac{E_0}{2hZ_0} \frac{\varepsilon_r}{\sqrt{\varepsilon_r - 1}} e^{-\frac{x}{x_0}} U(\tau - t'_t) \times \left\{ \frac{t_d}{\sqrt{\tau^2 - t'_t{}^2}} e^{-\frac{\tau}{2t'_r}} I_1 \left[\frac{1}{2t'_r} \sqrt{\tau^2 - t'_t{}^2} \right] + \right. \\
&\left. + \frac{\varepsilon_r - 1}{\varepsilon_r t'_r} \int_{t'_t}^{\tau} \frac{t_d}{\sqrt{\tau'^2 - t'_t{}^2}} e^{-\frac{\tau'}{2t'_r}} I_1 \left[\frac{1}{2t'_r} \sqrt{\tau'^2 - t'_t{}^2} \right] d\tau' \right\}
\end{aligned} \tag{19}$$

$$\begin{aligned}
\left(\sigma + \varepsilon \frac{\partial}{\partial t}\right) E_y &\approx \frac{H_z}{x_0} + \frac{E_0}{2hZ_0} \left(\frac{t_d}{t'_r}\right)^{\frac{1}{2}} \frac{(\varepsilon_r - 2)}{(\varepsilon_r - 1)} e^{-\frac{x}{x_0}} e^{-\frac{\tau}{2t'_r}} U(\tau - t'_t) \times \\
&\times \left\{ I_0 \left[\frac{1}{2t'_r} \sqrt{\tau^2 - t'_t{}^2} \right] + \frac{\varepsilon_r}{\varepsilon_r - 2} \frac{\tau}{\sqrt{\tau^2 - t'_t{}^2}} I_1 \left[\frac{1}{2t'_r} \sqrt{\tau^2 - t'_t{}^2} \right] \right\} \\
&+ \frac{E_0}{\sqrt{\varepsilon_r - 1}} \varepsilon_r \varepsilon_0 e^{-\frac{t'_t}{2t'_r}} \delta(\tau - t'_t)
\end{aligned}$$

The results at an arbitrary $y < h$ can be calculated by replacing h , t_d and t'_t in Equation 19 with $(h - y)$, t_{dy} and $t'_t(1 - y/h)$, respectively.

Equation 19 involves integrals of Bessel's functions which in principle can be evaluated by numerical integrations. However, instead of going through this complicated, time-consuming process, only the asymptotic approximations of Equation 19 at early and late times will be analyzed, from which together with the results for the δ -function source field case (see Table 3 and Figures 5 - 7), the approximate behaviors of the field and current density distributions are summarized in Table 7.

TABLE 7. FIELD AND CURRENT DENSITY FOR UNIT-STEP SOURCE FIELD FOR $\sigma_1 = \sigma_2 = \sigma$, $\epsilon_1 = \epsilon_2 = \epsilon = \epsilon_r \epsilon_0$,
 $40 \geq \epsilon_r \geq 10$, $\sigma \geq 3 \times 10^{-4}$ mho/m, $x_0 \geq 200$ m AND $x_0/h \geq 200$ [†]

Quantity	Initial Value at $\tau = t'_t$	Late Time Value for $t_{dx_0} > \tau \gg t'_r, t'_t, t'_d$	Approximate Behavior Between t'_t and the Late Time.
$\frac{H_z}{H'_0}$	$\sqrt{\epsilon_r} e^{-\frac{t'_t}{2t'_r}}$	$\left(\frac{4\tau}{\pi t'_r}\right)^{1/2}$	Monotonically increasing
$\frac{(\sigma + \epsilon \frac{\partial}{\partial t}) E_x}{J'_0}$	$\left(\frac{t'_d}{t'_r}\right)^{1/2} \left[1 + \frac{1}{8} \left(\frac{t'_d}{t'_r}\right)^{1/2} \right] e^{-t'_t/(2t'_r)}$	$\left(\frac{t'_d}{t'_r}\right)^{1/2}$	Monotonically increasing, reach $\sim (t'_d/t'_r)^{1/2}$ at approximately tens of t'_r or tens of t'_t , whichever is larger
$\frac{(\sigma + \epsilon \frac{\partial}{\partial t}) E_y}{J'_0}$	$\frac{1}{2} \left(\frac{t'_d}{t'_r}\right)^{1/2} \left(1 + \frac{t'_t}{4t'_r} \right) e^{-t'_t/(2t'_r)}$	0	Same as that of H_z/H'_0 of Table 3 (i.e., results due to a δ -function source field)

[†] $t'_r = \epsilon_0/\sigma$, $t'_t = \epsilon_0(\epsilon_r - 1)/\sigma$, $t'_d = \mu_0 \sigma h^2$, $t'^2_t = h^2(\epsilon_r)/c^2 = t'_d t'_r$, $H'_0 = hJ'_0 = E_0 Z_0^{-1} \exp(-x/x_0)$.

And the δ -function responses at t'_t are excluded. $t_{dx_0} = \mu_0 \sigma x_0^2$.

B. $\sigma_2 \rightarrow \infty$, $\sigma_1 = \sigma$, $\epsilon_1 = \epsilon$, $E_x^e = E_0 U(t - x/c) \exp(-x/x_0)$, $0 \leq y < h$

Two cases depending on whether or not ϵ equals ϵ_0 will be considered.

(1) $\epsilon = \epsilon_0$

Two different series representations are obtained for the field and current density distributions. The one to be used for late times ($t_{dx_0} > \tau > t_d$) is given by (for $y \neq h$)

$$\begin{aligned}
 H_z \approx & \frac{E_0}{Z_0} \left(\frac{t_r}{t_d} \right)^{\frac{1}{2}} e^{-\frac{x}{x_0}} U(\tau) \left\{ \frac{\tau}{t_r} - \frac{t_d}{6t_r} \left(1 - \frac{3y^2}{h^2} \right) + 1 + \right. \\
 & \left. + 2 \sum_{m=1}^{\infty} (-1)^m \cos \left(\frac{m\pi y}{h} \right) e^{-\frac{m^2 \pi^2 \tau}{t_d}} \left(1 - \frac{t_d}{m^2 \pi^2 t_r} \right) \right\} \\
 \left(\sigma + \epsilon_0 \frac{\partial}{\partial t} \right) E_x \approx & \frac{E_0}{hZ_0} \left(\frac{t_r}{t_d} \right)^{\frac{1}{2}} e^{-\frac{x}{x_0}} U(\tau) \left\{ \frac{t_d y}{t_r h} - \right. \\
 & \left. - 2 \sum_{m=1}^{\infty} (-1)^m \sin \left(\frac{m\pi y}{h} \right) e^{-\frac{m^2 \pi^2 \tau}{t_d}} \left(1 - \frac{t_d}{m^2 \pi^2 t_r} \right) \right\} \quad (20) \\
 \left(\sigma + \epsilon_0 \frac{\partial}{\partial t} \right) E_y \approx & \frac{H_z}{x_0} + \frac{2E_0}{hZ_0} e^{-\frac{x}{x_0}} U(\tau) \sum_{m=0}^{\infty} \frac{(-1)^m \cos(m\pi y/h)}{1 + \delta_{m0}} \times \\
 & \times \left(1 - \frac{m^2 \pi^2 t_r}{t_d} \right) e^{-\frac{m^2 \pi^2 \tau}{t_d}}
 \end{aligned}$$

The representation appropriate for early times ($\tau \ll t_d$) is given by

$$H_z \approx \frac{E_o}{Z_o} e^{-\frac{x}{x_o}} U(\tau) \sum_{n=-\infty}^{\infty} \left\{ \left[\left(\frac{t_r}{\pi\tau} \right)^{\frac{1}{2}} + \left(\frac{4\tau}{\pi t_r} \right)^{\frac{1}{2}} \right] e^{-\frac{t_{dy}^{(n)}}{4\tau}} - \left(\frac{t_{dy}^{(n)}}{t_r} \right)^{\frac{1}{2}} \left[1 - \operatorname{erf} \left(\sqrt{\frac{t_{dy}^{(n)}}{4\tau}} \right) \right] \right\}$$

$$\left(\sigma + \epsilon_o \frac{\partial}{\partial t} \right) E_x \approx \frac{E_o}{hZ_o} \left(\frac{t_d}{t_r} \right)^{\frac{1}{2}} e^{-\frac{x}{x_o}} U(\tau) \times \sum_{n=-\infty}^{\infty} (2n + 1 - y/h) \times \quad (21)$$

$$\times \left\{ \frac{t_r}{2\tau} \left(\frac{t_d}{\pi\tau} \right)^{\frac{1}{2}} e^{-\frac{t_{dy}^{(n)}}{4\tau}} + \left[1 - \operatorname{erf} \left(\sqrt{\frac{t_{dy}^{(n)}}{4\tau}} \right) \right] |2n + 1 - y/h|^{-1} \right\}$$

$$\left(\sigma + \epsilon_o \frac{\partial}{\partial t} \right) E_y \approx \frac{H_z}{x_o} + \frac{E_o}{hZ_o} \left(\frac{t_d}{\pi\tau} \right)^{\frac{1}{2}} e^{-\frac{x}{x_o}} U(\tau) \times \sum_{n=-\infty}^{\infty} \left(1 - \frac{t_r}{2\tau} + \frac{t_r t_{dy}^{(n)}}{4\tau^2} \right) e^{-\frac{t_{dy}^{(n)}}{4\tau}}$$

Based on Equations 20 and 21 several curves are presented in Figures 17-21, for $y=0, 0.5h$, and various t_r/t_d . At very early ($\tau \ll t_d$) and late ($\tau \gg t_d$) times, Equations 20 and 21 can be approximated with only one or two terms corresponding to small m 's and n 's. With this approximation and the curves in Figures 17-21, the analytical behaviors of the field and current densities can be obtained and are summarized in Table 8.

$$(2) \epsilon/\epsilon_o = \epsilon_r > 1$$

Two different series representations are obtained for the field and current density distributions. The one to be used for late times ($t_{dx_o} > \tau \gg t_r, t_d$) is given by (for $y \neq h$)

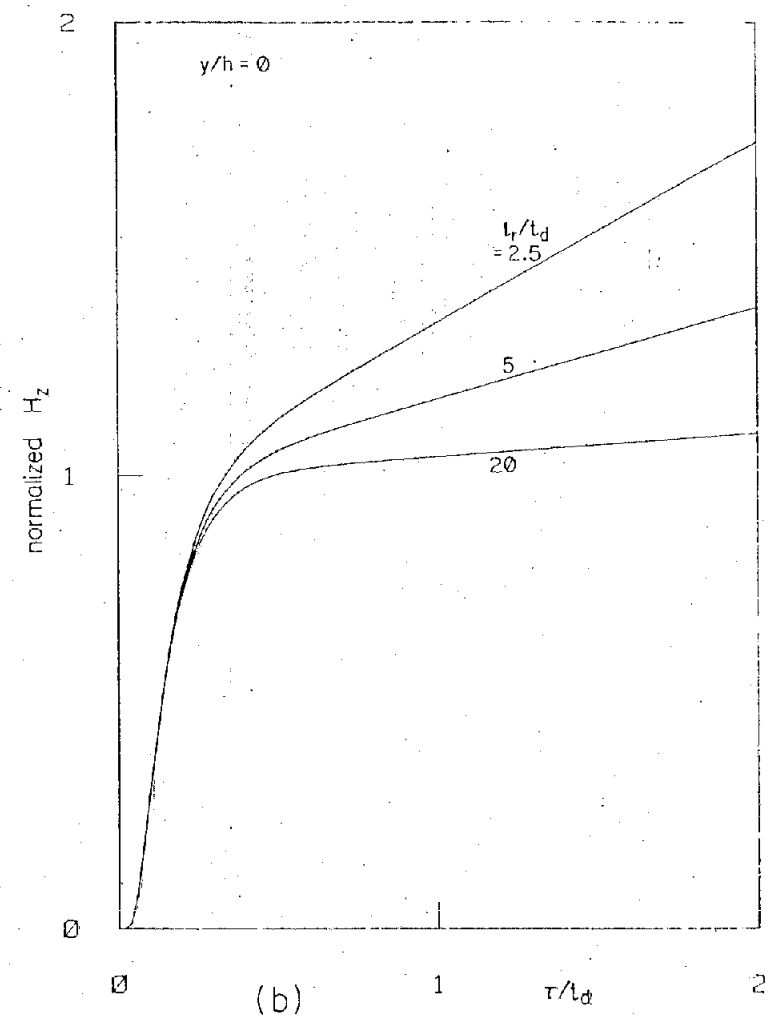
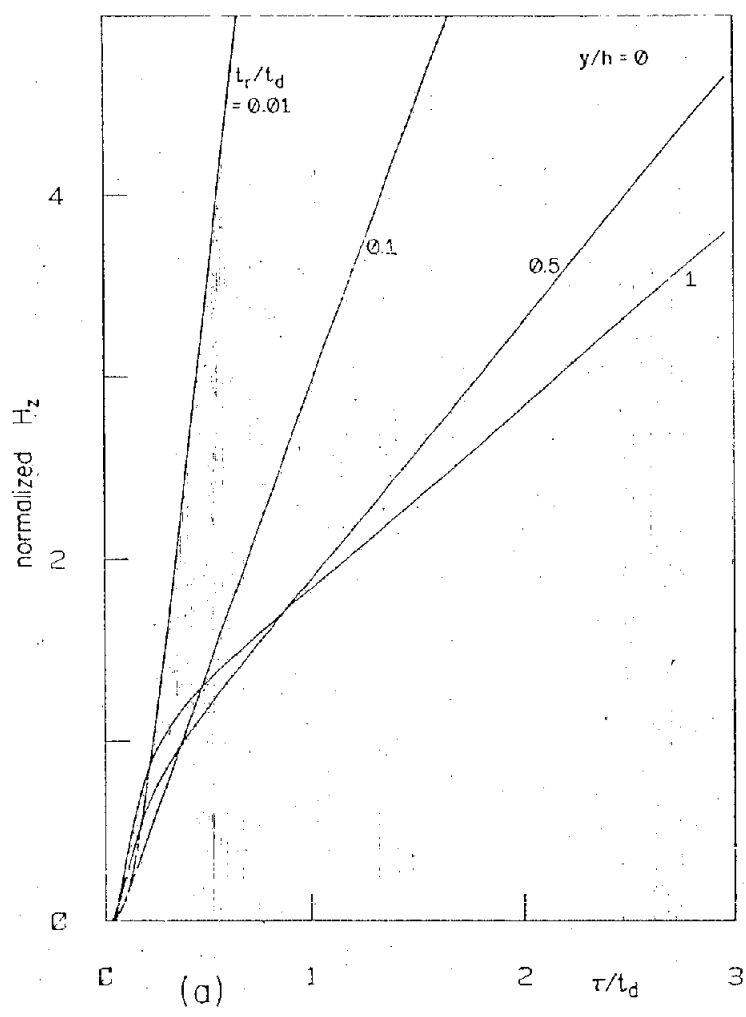


Figure 17. (a) H_z/H'_0 , (b) $(t_d/t_r)^{1/2} H_z/H'_0$ at $y=0$ as functions of τ/t_d for $x_0/h \geq 200$ and various t_r/t_d , for the simulator with $\sigma_2 \rightarrow \infty$, $\sigma_1 = \sigma$, $\epsilon_1 = \epsilon_0$, $E_x^e = E_0 \exp(-x/x_0) U(t-x/c)$. Here, $H'_0 = E_0 Z_0^{-1} \exp(-x/x_0)$, $Z_0 = (\mu_0/\epsilon_0)^{1/2}$, $t_r = \epsilon_0/\sigma$, $t_d = \mu_0 \sigma h^2$, $\tau = t-x/c$.

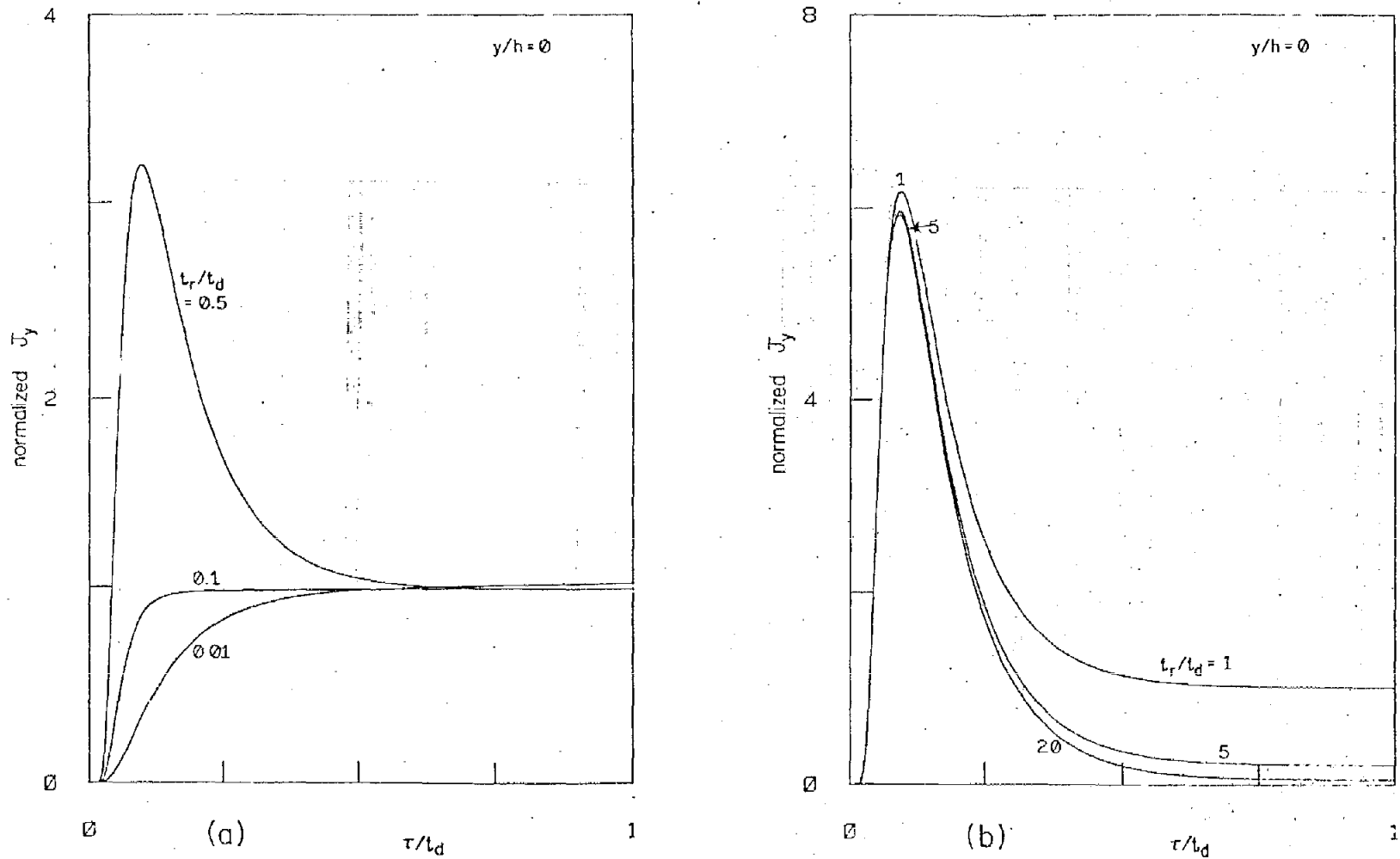


Figure 18. (a) J_y/J'_0 , (b) $(t_d/t_r)J_y/J'_0$ at $y=0$ as functions of τ/t_d for $x_0/h \geq 200$ and various t_r/t_d , for the simulator with $\sigma_2 \rightarrow \infty$, $\sigma_1 = \sigma$, $\epsilon_1 = \epsilon_0$, $E_x^e = E_0 \exp(-x/x_0)U(t-x/c)$. Here, $J_y = (\sigma + \epsilon_0 \frac{\partial}{\partial t})E_y$, $J'_0 = E_0(hZ_0)^{-1} \exp(-x/x_0)$, $Z_0 = (\mu_0/\epsilon_0)^{1/2}$, $t_r = \epsilon_0/\sigma$, $t_d = \mu_0 \sigma h^2$, $\tau = t - x/c$.

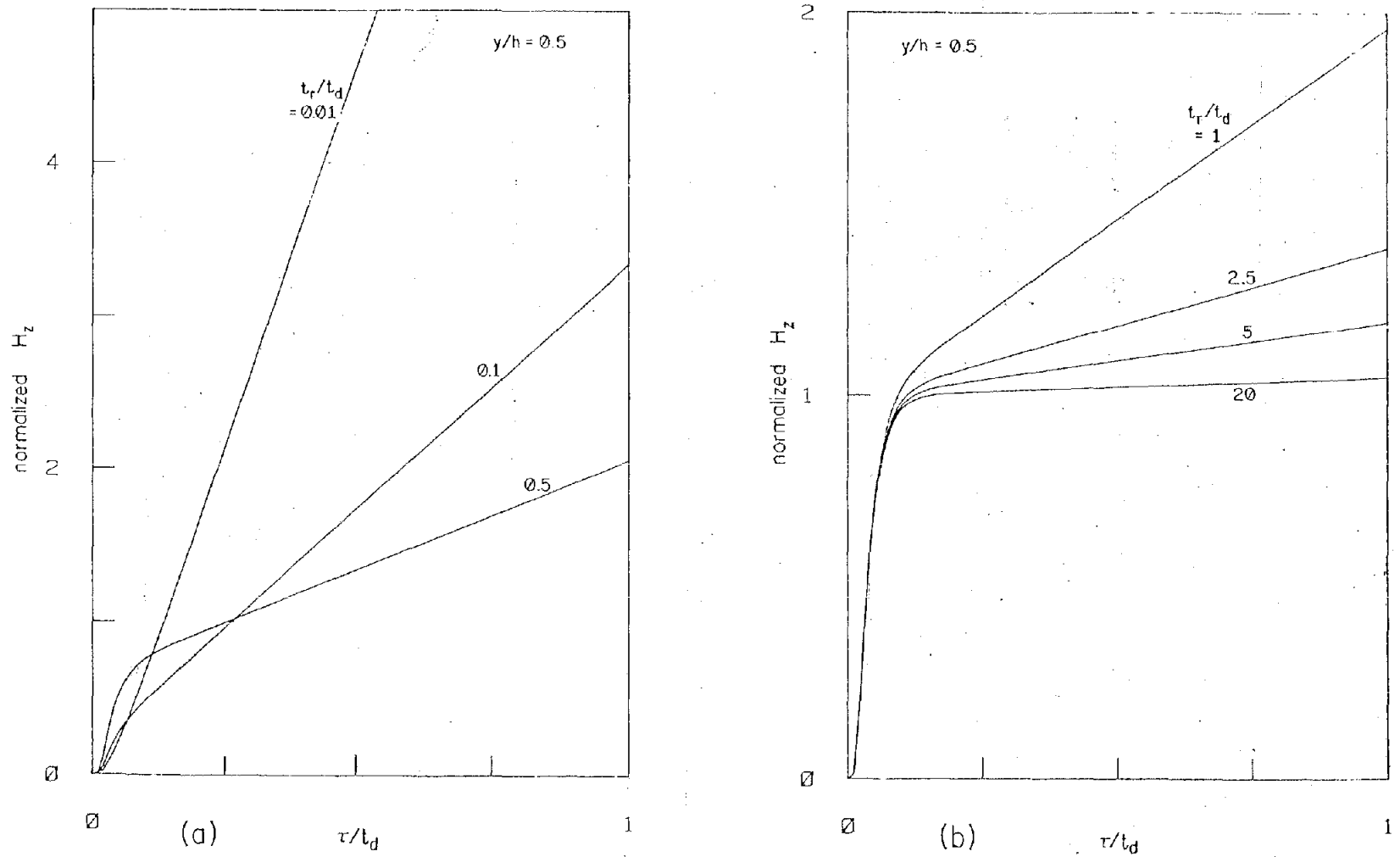


Figure 19. (a) H_z/H'_0 , (b) $(t_d/t_r)^{1/2} H_z/H'_0$ at $y/h = 0.5$ as functions of τ/t_d for $x_0/h \geq 200$ and various t_r/t_d , for the simulator with $\sigma_2 \rightarrow \infty$, $\sigma_1 = \sigma$, $\epsilon_1 = \epsilon_0$, $E_x^e = E_0 \exp(-x/x_0) U(t - x/c)$. Here, $H'_0 = E_0 Z_0^{-1} \times \exp(-x/x_0)$, $Z_0 = (\mu_0/\epsilon_0)^{1/2}$, $t_r = \epsilon_0/\sigma$, $t_d = \mu_0 \sigma h^2$, $\tau = t - x/c$.

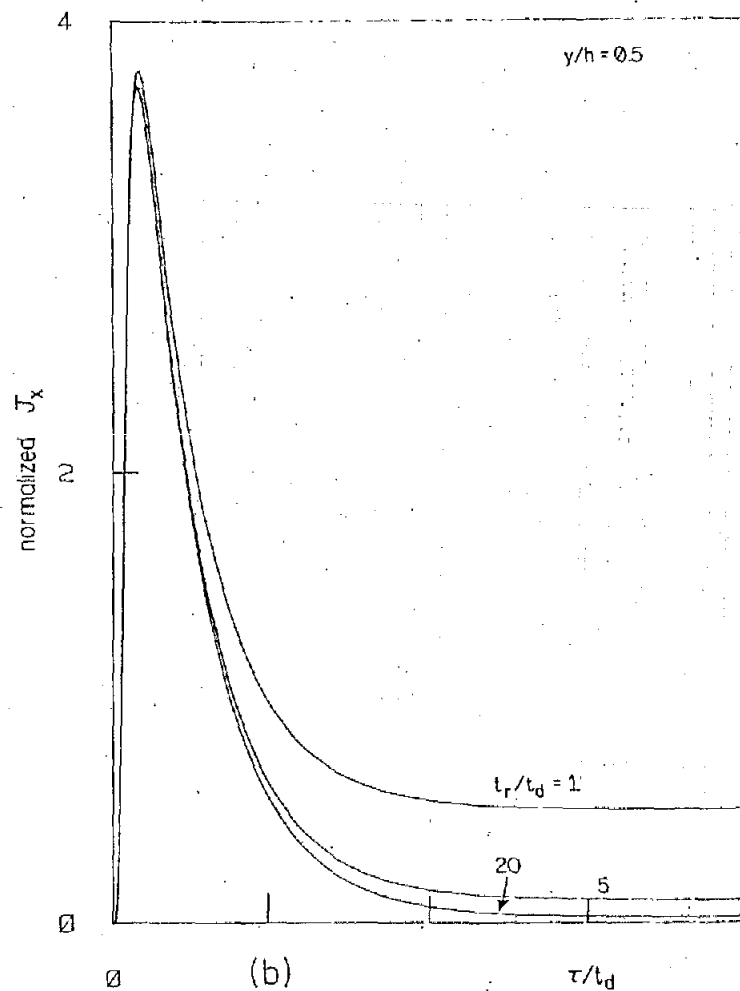
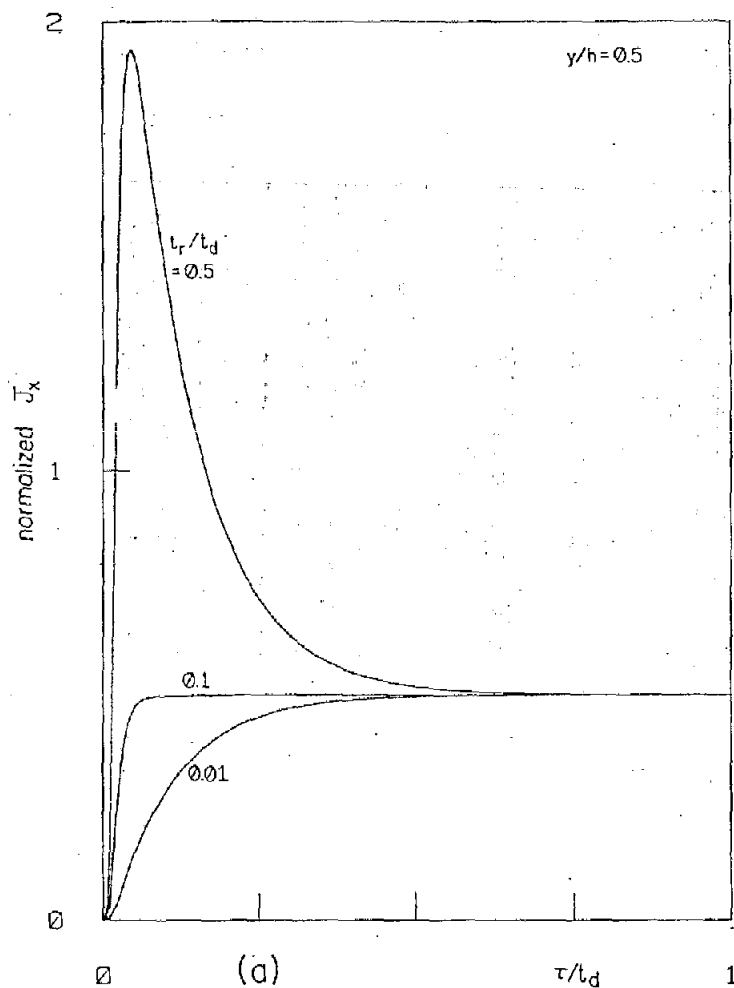


Figure 20. (a) $(t_r/t_d)^{1/2} J_x/J'_0$, (b) $(t_d/t_r)^{1/2} J_x/J'_0$ at $y/h = 0.5$ as functions of τ/t_d for $x_0/h \geq 200$ and various t_r/t_d , for the simulator with $\sigma_2 \rightarrow \infty$, $\sigma_1 = \sigma$, $\epsilon_1 = \epsilon_0$, $E_x^e = E_0 \exp(-x/x_0) U(t - x/c)$. Here, $J_x = (\sigma + \epsilon_0 \frac{\partial}{\partial t}) E_x$, $J'_0 = E_0 (hZ_0)^{-1} \exp(-x/x_0)$, $Z_0 = (\mu_0/\epsilon_0)^{1/2}$, $t_r = \epsilon_0/\sigma$, $t_d = \mu_0 \sigma h^2$, $\tau = t - x/c$.

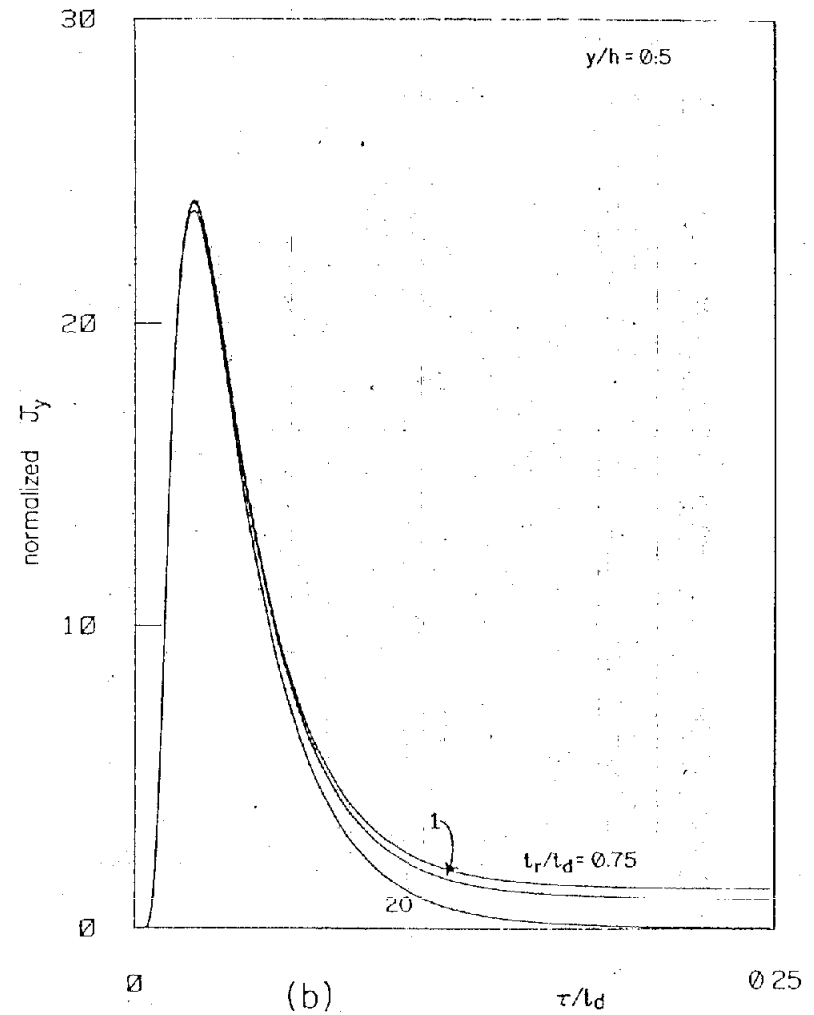
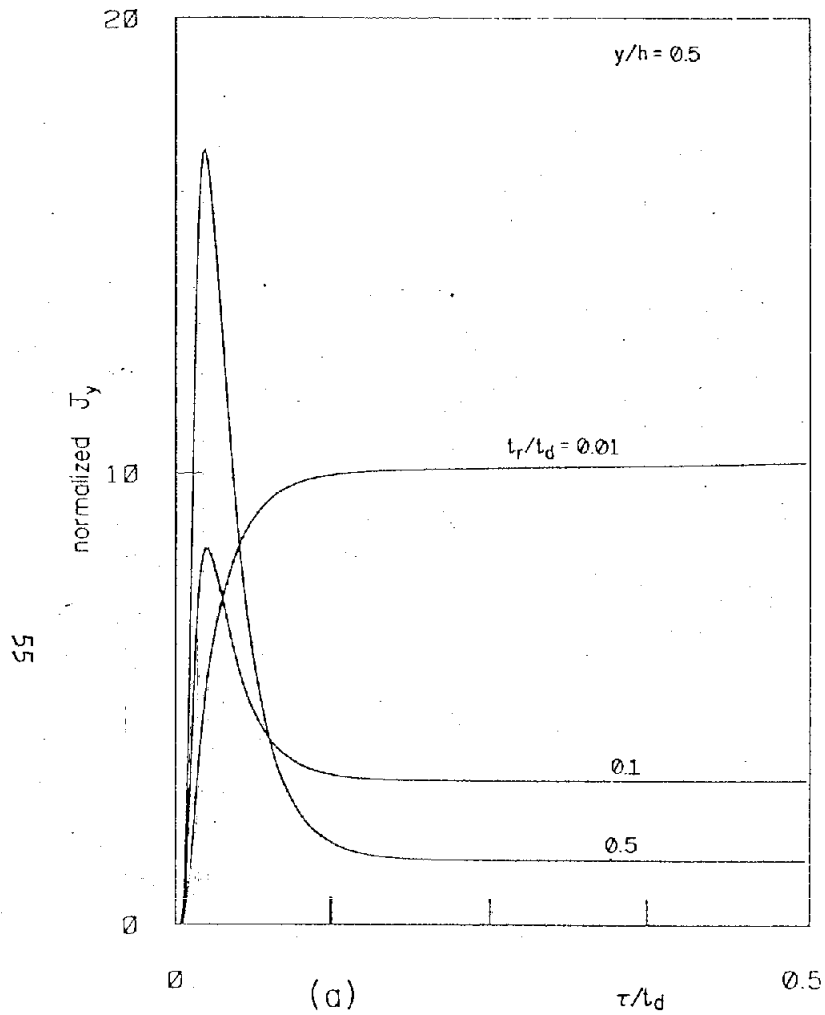


Figure 21. (a) $(t_d/t_r)^{1/2} J_y/J'_0$, (b) $(t_d/t_r) J_y/J'_0$ at $y/h = 0.5$, as functions of τ/t_d for $x_0/h \geq 200$ and various t_r/t_d , for the simulator with $\sigma_2 \rightarrow \infty$, $\sigma_1 = \sigma$, $\epsilon_1 = \epsilon_0$, $E_x^e = E_0 \exp(-x/x_0) U(t-x/c)$. Here, $J_y = (\sigma + \epsilon_0 \frac{\partial}{\partial t}) E_y$, $J'_0 = E_0 (hZ_0)^{-1} \exp(-x/x_0)$, $Z_0 = (\mu_0/\epsilon_0)^{1/2}$, $t_r = \epsilon_0/\sigma$, $t_d = \mu_0 \sigma h^2$, $\tau = t - x/c$.

TABLE 8. FIELD AND CURRENT DENSITY FOR UNIT-STEP SOURCE FIELD FOR $\sigma_2 \rightarrow \infty$, $\sigma_1 = \sigma$, $\epsilon_1 = \epsilon_0$,
 $\sigma \geq 3 \times 10^{-4}$ mho/m, $x_0 \geq 200$ m, AND $x_0/h \geq 100^\dagger$

Quantity	Location y/h	Local Maximum		Late Time Value ($t_{dx_0} > \tau \gg t_r, t_d$)	Condition
		Value	Time to Reach Maximum (τ)		
$\frac{H_z}{H'_0}$	$1 > \frac{y}{h} \geq 0$	Monotonically increasing. At early time, the larger y/h is, the faster it increases.		$\frac{\tau}{(t_r t_d)^{1/2}}$	any t_r/t_d
$\frac{(\sigma + \epsilon_0 \frac{\partial}{\partial t}) E_x}{J'_0}$	y/h = 0	= 0		$\left(\frac{t_d}{t_r}\right)^{1/2} \frac{y}{h}$	None
	$1 > \frac{y}{h} \geq \frac{1}{2}$	Monotonically increasing			$t_r/t_{dy} \leq 4/9$
$\left(\frac{t_r}{t_d}\right)^{1/2} \left(1 - \frac{y}{h}\right)^{-2}$		$\frac{t_{dy}}{3} \geq \tau \geq \frac{t_{dy}}{6}$			$\frac{t_r}{t_{dy}} \geq \frac{4}{9}$
$\frac{(\sigma + \epsilon_0 \frac{\partial}{\partial t}) E_y}{J'_0}$	$\frac{y}{h} = 0$	Monotonically increasing, reach ~ 1 at or before $0.5 t_d$		1	$t_r/t_d \leq 0.1$
		$6(t_r/t_d)$	$0.09 t_d$		$t_r/t_d \geq 0.5$
	$1 > \frac{y}{h} \geq \frac{1}{2}$	Monotonically increasing, reach ~ 1 at or before $0.5 t_{dy}$			$t_r/t_{dy} \leq 0.1$
		$3 \frac{t_r}{t_d} \left(1 - \frac{y}{h}\right)^{-3}$	$0.09 t_{dy}$		$\frac{t_r}{t_{dy}} \geq 0.5$

56

$^\dagger t_{dy} = t_d(1-y/h)^2 = \mu_0 \sigma h^2 (1-y/h)^2$, $H'_0 = hJ'_0 = E_0 Z_0^{-1} \exp(-x/x_0)$, $t_{dx_0} = \mu_0 \sigma x_0^2$.

* Same as H_z/H_0 of Tables 4 and 5.

$$\begin{aligned}
H_z \approx & \frac{E_0}{Z_0} \left(\frac{t_r}{t_d} \right)^{\frac{1}{2}} e^{-\frac{x}{x_0}} U(\tau - t'_{ty}) \left\{ \frac{\tau}{t_r} - \frac{t_d}{6t_r} \left(1 - \frac{3y^2}{h^2} \right) + 1 - e^{-\frac{\tau}{t'_r}} \right. \\
& + 2 \sum_{m=1}^{\infty} \frac{(-1)^m \cos(m\pi y/h)}{\sqrt{1 - 4t'_m{}^2 \pi^2 / t_d}} \left(\frac{\epsilon_r \omega_m^- t_r - 1}{\omega_m^- t_r} e^{-\omega_m^- \tau} - \frac{\epsilon_r \omega_m^+ t_r - 1}{\omega_m^+ t_r} e^{-\omega_m^+ \tau} \right) \left. \right\} \\
(\sigma + \epsilon \frac{\partial}{\partial t}) E_x \approx & \frac{E_0}{hZ_0} \left(\frac{t_r}{t_d} \right)^{\frac{1}{2}} e^{-\frac{x}{x_0}} U(\tau - t'_{ty}) \left\{ \frac{t_d}{t_r} \frac{y}{h} - \right. \\
& \left. - 2 \sum_{m=1}^{\infty} \frac{(-1)^m m\pi \sin(m\pi y/h)}{\sqrt{1 - 4t'_m{}^2 \pi^2 / t_d}} \left(\frac{\epsilon_r \omega_m^- t_r - 1}{\omega_m^- t_r} e^{-\omega_m^- \tau} - \frac{\epsilon_r \omega_m^+ t_r - 1}{\omega_m^+ t_r} e^{-\omega_m^+ \tau} \right) \right\}
\end{aligned} \tag{22}$$

$$\begin{aligned}
(\sigma + \epsilon \frac{\partial}{\partial t}) E_y \approx & \frac{E_0}{hZ_0} e^{-\frac{x}{x_0}} U(\tau - t'_{ty}) \left\{ 1 + \frac{1}{\epsilon_r - 1} e^{-\frac{\tau}{t'_r}} \right. \\
& + 2 \sum_{m=1}^{\infty} \frac{(-1)^m \cos(m\pi y/h)}{\sqrt{1 - 4t'_m{}^2 \pi^2 / t_d}} \left((1 - \epsilon_r \omega_m^- t_r) e^{-\omega_m^- \tau} - (1 - \epsilon_r \omega_m^+ t_r) e^{-\omega_m^+ \tau} \right) \left. \right\} + \frac{H_z}{x_0}
\end{aligned}$$

$$\text{where } \omega_m^{\pm} = \left(1 \pm \sqrt{1 - 4t'_m{}^2 \pi^2 / t_d} \right) / (2t'_r).$$

The representation appropriate for early times (i.e., for τ up to several t'_t) is given by

$$\begin{aligned}
H_z \approx & \frac{E_0}{Z_0} \frac{\epsilon_r}{\sqrt{\epsilon_r - 1}} e^{-\frac{x}{x_0}} \sum_{n=-\infty}^{\infty} U(\tau - t'_{ty}^{(n)}) \times \left\{ e^{-\frac{\tau}{2t'_r}} I_0 \left(\frac{\tau y_n}{2t'_r} \right) + \right. \\
& \left. + \frac{1}{\epsilon_r t_r} \int_{t'_{ty}^{(n)}}^{\tau} e^{-\frac{\tau'}{2t'_r}} I_0 \left(\frac{\tau' y_n}{2t'_r} \right) d\tau' \right\}
\end{aligned} \tag{23}$$

$$\begin{aligned} \left(\sigma + \varepsilon \frac{\partial}{\partial t} \right) E_x \approx E_o e^{-\frac{x}{x_o}} \sum_{n=-\infty}^{\infty} \frac{(2n+1-y/h)}{|2n+1-y/h|} e^{-\frac{t'_y(n)}{2t'_r}} \left[\varepsilon_r \varepsilon_o \delta(\tau - t'_{ty}(n)) + \sigma U(\tau - t'_{ty}(n)) \right] \\ + \frac{E_o}{2hZ_o} \frac{\varepsilon_r}{\sqrt{\varepsilon_r - 1}} e^{-\frac{x}{x_o}} \sum_{n=-\infty}^{\infty} (2n+1-y/h) U(\tau - t'_{ty}(n)) \times \end{aligned} \quad (23)$$

$$\times \left\{ \frac{t_d}{\tau_{yn}} e^{-\frac{\tau}{2t'_r}} I_1 \left(\frac{\tau_{yn}}{2t'_r} \right) + \frac{1}{\varepsilon_r t_r} \int_{t'_{ty}}^{\tau} \frac{t_d}{\tau'_{yn}} e^{-\frac{\tau'}{2t'_r}} I_1 \left(\frac{\tau'_{yn}}{2t'_r} \right) d\tau' \right\}$$

$$\begin{aligned} \left(\sigma + \varepsilon \frac{\partial}{\partial t} \right) E_y \approx \frac{H_z}{x_o} + E_o \frac{\varepsilon_r \varepsilon_o}{\sqrt{\varepsilon_r - 1}} e^{-\frac{x}{x_o}} \sum_{n=-\infty}^{\infty} e^{-\frac{t'_y(n)}{2t'_r}} \delta(\tau - t'_{ty}(n)) \\ + \frac{E_o}{2hZ_o} \left(\frac{t_d}{t'_r} \right)^{\frac{1}{2}} \frac{\varepsilon_r - 2}{\varepsilon_r - 1} e^{-\frac{x}{x_o}} e^{-\frac{\tau}{2t'_r}} \sum_{n=-\infty}^{\infty} U(\tau - t'_{ty}(n)) \times \\ \times \left\{ I_0 \left(\frac{\tau_{yn}}{2t'_r} \right) + \frac{\varepsilon_r}{\varepsilon_r - 2} \frac{\tau}{\tau_{yn}} I_1 \left(\frac{\tau_{yn}}{2t'_r} \right) \right\} \end{aligned}$$

where, as defined in Equation 16, $t'_y(n) = \sqrt{((2n+1)h-y)^2(\varepsilon_r-1)}/c$,
 $\tau_{yn} = \left(\tau^2 - t'_{ty}(n)^2 \right)^{\frac{1}{2}}$ and $\tau'_{yn} = \left(\tau'^2 - t'_{ty}(n)^2 \right)^{\frac{1}{2}}$.

In the series representation in Equation 23, one can see that every term (i.e., with a specific n) is exactly the same as Equation 19, if h is replaced by $2n+1-y/h$ (i.e., t'_t by $t'_{ty}(n)$, t_d by $t_d(2n+1-y/h)^2$, also). The terms with $n = \pm m$, $m=1,2,3,\dots$, can be considered respectively the m -th reflection from the $y=h$ and $y=0$ planes. That is, the field and current density distributions of the present case can be constructed from the solutions represented by Equation 19. As is obvious from Equation 23, the smaller τ is, the fewer terms are required for the calculations.

At very late times ($10^3 t_d \geq \tau \gg t'_r, t_d$), one can see from Equation 22 that the field and current density distributions approach the following values:

$$H_z : \frac{E_o}{Z_o} e^{-\frac{x}{x_o}} \frac{\tau}{(t_r t_d)^{1/2}}$$

$$\left(\sigma + \epsilon \frac{\partial}{\partial t}\right) E_x : \frac{E_o}{hZ_o} e^{-\frac{x}{x_o}} \left(\frac{t_d}{t_r}\right)^{1/2} \frac{y}{h} \quad (24)$$

$$\left(\sigma + \epsilon \frac{\partial}{\partial t}\right) E_y : \frac{E_o}{hZ_o} e^{-\frac{x}{x_o}}$$

which are the same as those for the case with $\epsilon_r = 1$, as expected. To obtain the late-time behaviors, one can also use Equation 23, especially when $t'_t \gg t'_r$, in which case only a few terms are needed. However, if $t'_t \ll t'_r$, one needs many terms to obtain the late-time behaviors.

REFERENCES

1. Baum, C.E., "EMP Simulators for Various Types of Nuclear EMP Environments: An Interim Categorization," IEEE Trans. on Antenna and Propagation, AP-26, pp. 35 - 53, January 1978, and also Sensor and Simulation Notes, Note 240, Air Force Weapons Laboratory, 1 January 1978.
2. Baum, C.E., "The Planar, Uniform Surface Transmission Line Driven from a Sheet Source," Sensor and Simulation Notes, Note 48, Air Force Weapons Laboratory, August 1967.
3. Baum, C.E., "A Distributed-Source Conducting-Medium Simulator for Structures Near and Below the Ground Surface," Sensor and Simulation Notes, Note 87, Air Force Weapons Laboratory, July 1969.
4. Baum, C.E., "Electromagnetic Pulse Interaction Close to Nuclear Bursts and Associated EMP Environment Specification," Interaction Notes, Note 76, Air Force Weapons Laboratory, July 1971.